The Macroscopic Transport Equations of Phonons in Solids

by
Michael Fryer
B.Eng., University of Victoria, 2010

A Thesis Submitted in Partial Fulfillment of the Requirements for the Degree of

MASTER OF APPLIED SCIENCE

in the Department of Mechanical Engineering

The Macroscopic Transport Equations of Phonons in Solids

by
Michael Fryer
B.Eng., University of Victoria, 2010

Supervisory Committee

Dr. Henning Struchtrup - Supervisor
(Department of Mechanical Engineering)

Dr. Rustom Bhiladvala - Departmental Member
(Department of Mechanical Engineering)

Supervisory Committee

Dr. Henning Struchtrup - Supervisor
(Department of Mechanical Engineering)

Dr. Rustom Bhiladvala - Departmental Member
(Department of Mechanical Engineering)

Abstract

There has been an increasing focus on using nanoscale devices for various applications ranging from computer components to biomechanical sensors. In order to effectively design devices of this size, it is important to understand the properties of materials at this length scale and their relevant transport equations. At everyday length scales, heat transport is governed by Fourier's law, but at the nanoscale, it becomes increasingly inaccurate. Phonon kinetic theory can be used to develop more accurate governing equations. We present the moment method, which takes integral moments of the phonon Boltzmann kinetic equation to develop a set of equations based on macroscopic properties such as energy and heat flux. The advantage of using this method is that transport properties in nanodevices can be approximated analytically and efficiently. A number of simplifying assumptions are used in order to linearize the equations. Boundary conditions for the moment method are derived based on a microscopic model of phonons interacting with a surface by scattering, reflection or thermalization. Several simple, one dimensional problems are solved using the moment method equation. The results show the effects of phonon surface interactions and how they affect overal properties of a nanoscale device. Some of these effects were observed in a recent experiment and are replicated by other modeling techniques. Although the moment method has described some effects of nanoscale heat transfer, the model is limited by some of its simplifying assumptions. Several of these simplifying assumptions could be removed for greater accuracy, but it would introduce non-linearity into the moment method.

Contents

List of Figures

Acknowledgments

In 2010 I had a conversation with my supervisor, Dr. Henning Struchtrup, that convinced me to do my master's degree with him. The journey since then has been one where I have learned a lot about myself, research and teaching. As always, there is a significant cost to graduate school and I appreciate the generous support of both the University of Victoria and the Natural Sciences and Engineering Research Council of Canada (NSERC). A lot of people have shaped my experience as a graduate student, from professors to the undergraduates who come to my TA office hours and I would like to thank some of those who stand out. At the top of the list is Dr. Struchtrup, for his patience, intellect and vision for my project. I always appreciated his open door policy and the many times he guided me through the challenging areas of my work. Another influential person in my research was my office mate Anirudh Rana. He was always open to bounce ideas off of and his optimistic personality pervaded our office. I appreciate the countless hours he spent helping me with math, computer programming and all of the little problems that can come up in any research project. I would like to thank Dr. Ingenuin Gasser of the University of Hamburg for allowing me to work at his institution for several months and gain valuable time working abroad (funded by the NSERC Michael Smith Foreign Study Supplement). I would also like to express my appreciation to all of my roommates, for allowing me to ceaselessly babble on about any obscure problem I had with my work whether they understood it or not. I want to acknowledge my parents, who taught me to think analytically early and often and have always supported and loved me. Finally, thank you Jesus Christ, for making me, loving me and saving me.

Nomenclature

$A_{\alpha\beta}$, $\mathcal{A}$	Coefficient matrix for the x derivative of the system of moment equations
a	Crystal lattice vector
α	Proportion of phonons that scatter and reflect at a surface
$B_{\alpha\beta}$, $\mathcal{B}$	Coefficient matrix for the y derivative of the system of moment equations
β	Proportion of phonons that thermalize at a surface
c	The speed of sound in a solid
c_v	Heat capacity
E	$\frac{e}{c}$
E_s	Surface energy, i.e. $\frac{e_s}{c}$
e	Energy density
ε_r^n	$\lvert\sigma_r^n\rvert$
f	Phonon particle distribution function
γ	Phonon specular reflection parameter
H	$\frac{c^5\hbar^4}{16\pi y(k_B T)^5}$
$\hbar$	Reduced Plank's constant $\approx 1.054 \times 10^{-34}$J·s
J_n	$\frac{15\prod_{j=0}^{n}(2j+1)}{\pi^4 n!}$
K	Interatomic force - modelled as an ideal spring constant
$\bar{K}$	Wavenumber of the laser induced diffraction grating in the periodic initial condition experiment
Kn	$\frac{\lambda}{L}$, the resistive Knudsen number, $Kn_R = \frac{\lambda_R}{L}$
k_i	Phonon wave vector
k_B	Boltzmann constant $\approx 1.381 \times 10^{-23} m^2 kg \cdot s \cdot K^{-1}$
κ	Heat conductivity
L	Length scale of a problem domain
λ	Mean free path (λ_R is resistive MFP, λ_N is normal MFP, λ is total MFP)
M	Particle Mass, total number of nodes in y direction for numerical model
$M_{\langle ijk\rangle}$	The third moment (flux of $N_{\langle ij\rangle}$)

N	Total number of Particles, total number of nodes in x direction for the numerical model
$N_{\langle ij \rangle}$	The second moment (momentum flux)
ν	The wall normal
$P, \mathcal{P}$	collision matrix for a system of moment equations
p_i	Phonon momentum density
q_k	Heat flux per unit rarea
ρ	Phonon scattering parameter
ρ_{mat}	Material density
S	Boltzmann Equation Collision Term
σ_r^n	$\frac{(-1)^{n-r}\left(\frac{n-r}{2}\right)!\left(\frac{r}{2}\right)!}{r!!\left(1+\frac{n}{2}\right)!}$ for even r and 0 for odd r
T	Temperature
τ	Mean free time (τ_R is resistive MFT, τ_N is normal MFT, τ is total MFT)
τ_A	The wall tangential vector
u	Specific internal energy
$u_{\langle i_1 \ldots i_n \rangle}$	Generalized Moment tensor
v_g	Group Velocity
v_p	Phase Velocity
ω	Frequency
$\mathcal{X}^{\pm}$	Coefficient Matrix for the x-wall boundary condition in the numerical scheme
$\mathcal{X}^{d\pm}$	Inhomogenous coefficient matrix for the x-wall boundary condition in the numerical scheme
$\mathcal{X}_r^n$	$\frac{n!}{r!(n-r)!}$
y	The density of states
$\mathcal{Y}^{\pm}$	Coefficient Matrix for the y-wall boundary condition in the numerical scheme
$\mathcal{Y}^{d\pm}$	Inhomogenous coefficient matrix for the y-wall boundary condition in the numerical scheme

1 Introduction

In the latter half of the twentieth century, there has been an increasing focus on the miniturization of devices by scientists and engineers. Microtechnology, followed by nanotechnology has become a major research topic in universities and in private industry, as people try to make technology cheaper, more efficient, faster, more accurate, more sensitive and less of a burden on the environment. One of the most striking examples of miniaturization is the phenomenom known as "Moore's Law," where the number of transistors in an integrated circuit doubles every two years [1]. Moore's Law has been roughly correct since 1965. Aside from the miniturization of computers, Micro-Electrical Mechanical Systems (MEMS) is a rapidly growing area of engineering where new tools are developed for achieving tasks at small scales. Another growing area is microfluidics, especially in biotechnology, where micro and nano sensors are used to manipulate cells, bacteria, viruses and DNA [2].

For effective design and fabrication of nanodevices, a quantitative physical understanding is necessary. Effects that can be ignored at macro scales can dominate at micro and nano scales, and vice versa. As length scale decreases, the surface properties of a given substance become more important and the bulk properties become less [3]. As a result, the classical laws of continuum mechanics necessarily break down.

One important area of research in nanotechnology is the study of temperature and heat transport. Temperature plays an important role in nanotechnology because it can affect virtually any other property, such as viscosity, electrical conductivity, elasticity, and ductility. Furthermore, small size of a device (resulting in a tiny thermal mass), combined with high energy sources (such as lasers) has the potential to cause extreme changes in temperature. Understanding temperature and heat transport at the nanoscale will improve design and sensitivity of sensors and increase the effectiveness of thermal management of heat sources, such as transistors on computer chips.

In order to determine and describe the macroscopic properties of nanodevices (i.e. temperature, heat flux, etc.) and their related thermodynamic processes, a microscopic analysis of materials can be used to develop relevant constitutive equations. That is, an analysis based on the microscopic interactions and phenomena of particles (atoms, molecules, photons, phonons, etc.) can be used to determine macroscopic properties of a nanodevice.

Heat in a solid is caused by microscopic vibrations of particles in a crystal lattice with respect to their mean position. These vibrations can be quantized into particles known as phonons [4] [5]. Macroscopic properties, such as heat flux, internal energy, and temperature can be determined by analyzing the microscopic properties of phonons, such as phonon frequency, and phonon crystal momentum.

Approaches that track all phonons (a branch of molecular dynamics) can be computationally expensive when there are a large number of particles. Another method, known as Direct Simulation Monte Carlo (DSMC) is to use the kinetic theory of particles and do a statistical analysis of groups of particles acting together [6]. This allows for larger domains than molecular dynamics, but still can be computationally expensive, although there are efforts to make it more efficient [7].

The method presented in this report uses microscopic properties of phonons to develop extended macroscopic transport equations. Boundary conditions are derived in the same way by analyzing and approximating phonon-boundary interactions and devoloping corresponding macroscopic boundary equations. A benefit of this method is that instead of numerically solving a specific problem, general equations are developed. These equations can be analyzed and manipulated to gain a better understanding of nanoscale heat transport. This also leads to increased computational efficiency. In certain geometries, the equations can even be solved analytically.

The phonon-Boltzmann equation, discovered by Peierls [8], governs the kinetic transport of phonons at the microscale. Macroscale transport equations were derived by taking integral moments of the phonon-Boltzmann equation [9] in a similar way to Grad's macroscopic moment derivation of the original Boltzmann equation for gas kinetics [10].

This report presents a brief introduction to classical heat conduction and phonons followed by a more detailed description of the phonon-Boltzmann equation and the macroscopic moment equations. General boundary conditions in three dimensions are derived from a model of phonon-boundary interactions. Several simple one dimensional problems are solved analytically and compared to classical Fourier heat transfer and a simple two dimensional numerical model is developed and presented.

1.1 Classical Heat Conduction

Heat conduction in classical solid bodies follows Fourier's law

$$q_k = -\kappa(T)\frac{dT}{dx_k}\,, \tag{1.1}$$

where q_k is the heat flux per unit area, the subscript k denotes the three dimensions, $\kappa(T)$ is the heat conductivity and T is the temperature. This is a phenomenological equation that requires experimentation to determine the heat conductivity of the material being analyzed. Fourier's law leads directly to the heat equation, which governs the diffusion (i.e. conduction) of energy in a rigid solid

$$\frac{\partial u}{\partial t} - \frac{\kappa\left(T\right)}{c_v\left(T\right)\rho}\frac{\partial^2 u}{\partial x_k \partial x_k} = 0\,, \tag{1.2}$$

where u is the internal energy, ρ is the density and $c_v\left(T\right)$ is the specific heat of the material. Although Fourier's law often correctly predicts heat flow, at very high temperature gradients, small length scales and in high purity crystals the equation breaks down for reasons that will be explained in the following sections.

2 Phonons and the Microscale Description of Conduction

In order to understand heat transfer from a non-Fourier perspective, microscopic effects must be taken into account. To understand the classical law and to develop extended equations, the mechanism of energy transport needs to be analyzed microscopically.

In a solid, atoms are fixed in a lattice and held in place by the attractive and repulsive electromagnetic forces. These forces could be the Lennard-Jones potential, ionic bonds, covalent bonds or metalic bonds [11]. Heat is transferred through a solid by vibrations of atoms around their mean position in the solid's lattice where adjacent particles exchange energy. Phonons are a particle representation of these vibrations [4]. They have energy and momentum, can interact with other particles, such as electrons and photons, and also interact with material boundaries. Macroscopic properties, such as temperature, heat capacity and heat flux in solids are obtained by averaging over the microscopic properties of phonons. There are two ways of describing phonons, from a classical perspective and a quantum perspective. Both are outlined in the next two sections.

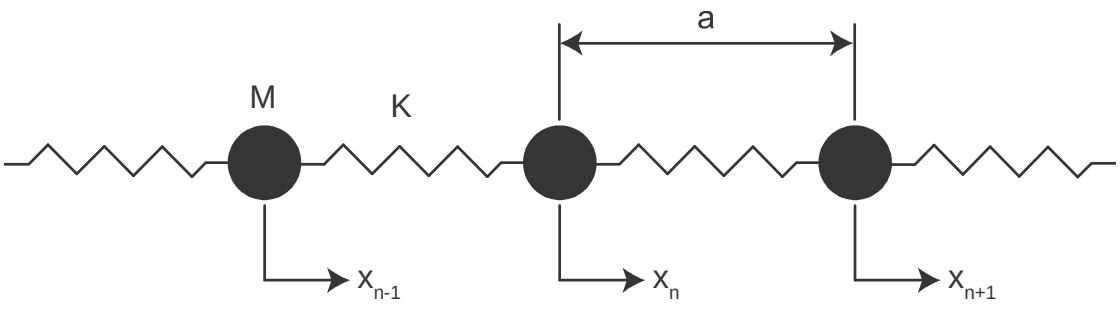

Figure 2.1: A linear chain of atoms connected by ideal springs

2.1 Classical Phonons

To understand a one-dimensional classical phonon model, consider a linear chain of N particles connected to each other by ideal springs such as in Figure 2.1. This roughly approximates atoms in a one dimensional crystal. Although the Lennard-Jones potential is not parabolic, for small displacements from the mean lattice position, and if effects from non-neighbouring atoms are ignored, it can be approximated as such [12]. Using Hooke's law, we can derive the equations of motion for the masses in the system:

$$M\ddot{x}_n = K\left(x_{n+1} + x_{n-1} - 2x_n\right); n = 1...N \tag{2.1}$$

Here M is the mass of one particle, K is the spring constant between the atoms and x_n is the displacement of the nth particle in the chain from its mean position. Note that there are N coupled equations that need to be solved. We also assume a periodic boundary condition at the ends of the chain, which is equivalent to a chain where both ends are linked. This is not a necessary assumption; however, it is a constraint that simplifies the solution. The periodic assumption results in the boundary condition

$$x_{n+dN} = x_n \ , \ \ d \in \mathbb{Z} \ . \tag{2.2}$$

In order to decouple the equations, we take the discrete Fourier transform in space, which is defined as

$$\mathcal{F}(x_n) = X_s = \frac{1}{N}\sum_{n=1}^{N} x_n e^{i\frac{2\pi s}{N}n} \ \ , \tag{2.3}$$

with inverse[1]

$$\mathcal{F}^{-1}(X_s) = x_n = \sum_{s=-\frac{N-1}{2}}^{s=\frac{N-1}{2}} X_s e^{-i\frac{2\pi s}{N}n} \quad . \tag{2.4}$$

The Fourier transform relates the displacement of adjacent particles by exponentials. For example, if we substitute $x_{n\pm1}$ for x_n in equation (2.3) it yields

$$\mathcal{F}(x_{n\pm1}) = \frac{1}{N}\sum_{n=1}^{N} x_{n\pm1} e^{i\frac{2\pi s}{N}n} = e^{\mp i\frac{2\pi s}{N}} \frac{1}{N}\sum_{n=1}^{N} x_{n\pm1} e^{i\frac{2\pi s}{N}(n\pm1)} \quad . \tag{2.5}$$

Equation (2.5) is simplified using the periodic property of equation (2.2) such that

$$e^{\mp i\frac{2\pi s}{N}} \frac{1}{N}\sum_{n=1}^{N} x_{n\pm1} e^{i\frac{2\pi s}{N}(n\pm1)} = e^{\mp i\frac{2\pi s}{N}} \frac{1}{N}\sum_{n=1}^{N} x_n e^{i\frac{2\pi s}{N}n}$$

Therefore the exponential relation of the Fourier transform is

$$\mathcal{F}(x_{n\pm1}) = e^{\mp i\frac{2\pi s}{N}} \mathcal{F}(x_n) \quad . \tag{2.6}$$

This property is also the same for the inverse Fourier transform with opposite signs,

$$\mathcal{F}^{-1}(X_{s\pm1}) = e^{\pm i\frac{2\pi s}{N}} \mathcal{F}^{-1}(X_s) \quad . \tag{2.7}$$

Taking the Fourier transform of equation (2.1) results in

$$M\ddot{X}_s = K(e^{\frac{-i2s\pi}{N}} + e^{\frac{i2s\pi}{N}} - 2)X_s \ , \tag{2.8}$$

which can be rearranged using Euler's equation and trigonometry to become

$$\ddot{X}_s = -4\frac{K}{M}\sin^2\left(\frac{\pi s}{N}\right) X_s \quad . \tag{2.9}$$

This differential equation has the well known form

$$\ddot{X}_s = -\omega_s^2 X_s \quad , \tag{2.10}$$

where ω_s is the angular frequency; in the single atom chain,

$$\omega_s = 2\sqrt{\frac{K}{M}}\left|\sin\left(\frac{\pi s}{N}\right)\right| \quad . \tag{2.11}$$

[1]It is convenient to use an odd number of N so that a symmetric summation around 0 can be done, however this is not strictly necessary.

The solution of equation 2.10 must be an exponential function. First we apply two initial conditions to fully define the solution:

$$\begin{aligned} \dot{X}_s(0) &= \dot{X}_s^0 \\ X_s(0) &= X_s^0 \ ., \end{aligned} \tag{2.12}$$

where X_s^0 and $\dot{X}_s^0$ are the Fourier transforms of the initial conditions.

The solution in Fourier space is

$$X_s(t) = A_{-s}e^{i\omega_s t} + A_s^* e^{-i\omega_s t} \quad , \tag{2.13}$$

where A_{-s} is a constant related to the initial conditions as

$$A_{-s} = \frac{1}{2}\left(X_s^0 + \frac{1}{i\omega_s}\dot{X}_s^0\right) \quad , \tag{2.14}$$

and A_s^* is the complex conjugate of A_s.

With the full solution in the frequency domain, the solution in the time domain can be found by taking the inverse discrete Fourier transform by substituting equation (2.13) into equation (2.4). Since the terms in the equation can be added in any order, it is easier to interpret the equation if the first term is switched around so that A_{-s} becomes A_s and $e^{i\frac{2s\pi}{N}n}$ becomes $e^{-i\frac{2s\pi}{N}n}$. If this is done, the final form of the equation is

$$x_n(t) = \sum_{s=-\frac{N-1}{2}}^{s=\frac{N-1}{2}} \left\{A_s e^{-i\left(\frac{2s\pi}{N}n - \omega_s t\right)} + A_s^* e^{i\left(\frac{2s\pi}{N}n - \omega_s t\right)}\right\} \quad . \tag{2.15}$$

Equation (2.15) is the general solution of the single particle linear chain model.

In the chain, there are N particles spaced a apart from each other, so the total length is

$$L = Na \quad . \tag{2.16}$$

The wavenumber is defined as

$$k_s = \frac{2\pi s}{L} \quad . \tag{2.17}$$

This simplifies equation (2.15) to

$$x_n(t) = \sum_{s=-\frac{N-1}{2}}^{s=\frac{N-1}{2}} \left\{A_s e^{-i(k_s an - \omega_s t)} + A_s^* e^{i(k_s an - \omega_s t)}\right\} \quad . \tag{2.18}$$

This general solution is a superposition of plane harmonic wave in complex notation. The two terms represent forwards and backwards propagating waves with amplitudes A_s, frequency ω_s and wavenumber k_s. Since the two terms are complex conjugates of each other, the wave equation always has a purely real answer.

2.1.1 Phase Velocity and Group Velocity

The classical derivation of lattice vibration yields a plane harmonic wave solution; however, it is necessary to describe phonons as particles. Waves, in general, are everywhere in a domain, while particles are localized in space. To describe phonons, it is therefore necessary to localize these waves, which was first done by Peierls in 1929 [8]. Peierls described phonons as "packets" of waves. These packets can be made by summing together a small number of waves with nearly the same wave number. Summing waves with nearly the same frequency causes "beating" which creates localized spikes due to constructive and destructive interference. These localizations are, in the classical frame, the phonons. While a single wave travels with the phase velocity,

$$v_p = \frac{\omega}{k} \quad , \tag{2.19}$$

the energy or signal of a number of superimposed waves travels with the group velocity,

$$v_g = \frac{\partial \omega}{\partial k} \quad , \tag{2.20}$$

where $k = |\mathbf{k}|$. Therefore a classical phonon is basically a wave packet that travels at the group velocity. The reason why energy travels with the group velocity and not the phase velocity is explained in Appendix A.

2.1.2 The Dispersion Relation and the Brioullin Zone

The wavenumber and the frequency of the solution are not independent of one another. Using the definition of k_s and substituting into equation (2.11) gives

$$\omega_s = 2\sqrt{\frac{K}{M}} \left| \sin\left(\frac{k_s a}{2}\right) \right| \quad . \tag{2.21}$$

This equation is known as the dispersion relation and is a periodic sine function which is shown in Figure 2.2. Since the relation is periodic with $\frac{2\pi}{a}$, it is only necessary to know the dispersion relation for k in the

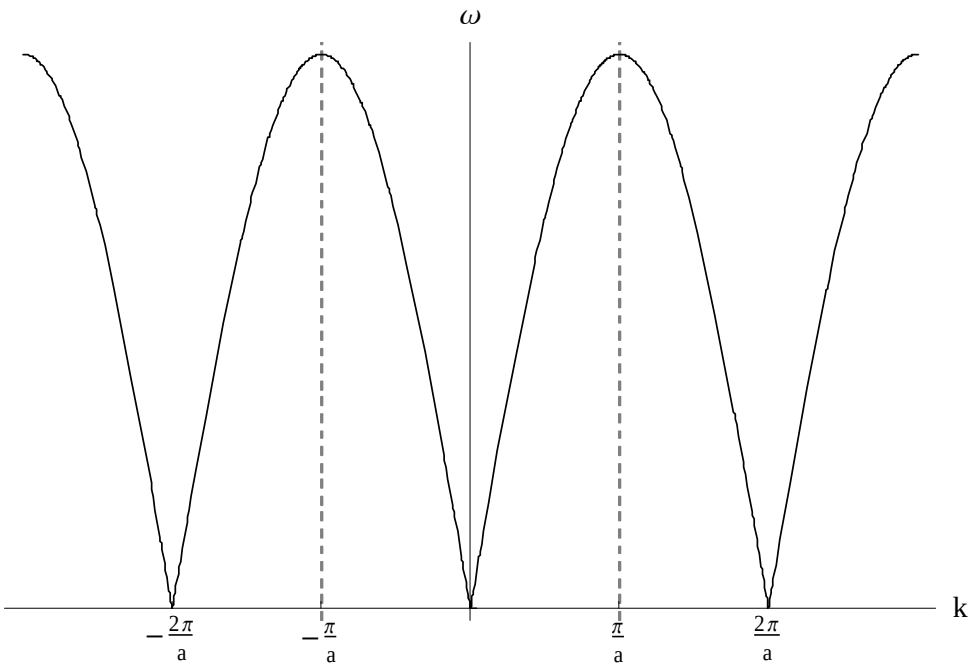

Figure 2.2: The classical dispersion relation for a linear chain of particles. The Brillouin zone is between the two dashed lines.

domain $\left(\frac{-\pi}{a}, \frac{\pi}{a}\right)$. This region is known as the Brioullin zone, and it completely describes the dispersion relation. If there is ever a wavenumber that is outside of the Brioullin zone, it can be expressed as a wavenumber in the Brioullin zone added to an integer multiple of $\frac{2\pi}{a}$,

$$k_s = k_b + \frac{2\pi}{a}m, \;\; m \in \mathbb{Z} \;\; , \tag{2.22}$$

where $\frac{2\pi}{a}m$ is the reciprocal lattice vector. The Brioullin zone is very important for determining macroscopic properties because it fully describes all k vectors. Therefore to integrate over all k requires a summation over the domain of just the Brioullin zone.

2.1.3 Optical Phonons

Optical phonons occur when there is more than one particle in the basis of a unit cell [13]. They are called optical phonons because they are often created by interaction with photons. A unit cell is the smallest repeating element in a lattice. That is, a lattice can be constructed simply by placing unit cells side by side in all directions that the lattice is defined. Therefore non-trivial unit cells occur when there are different

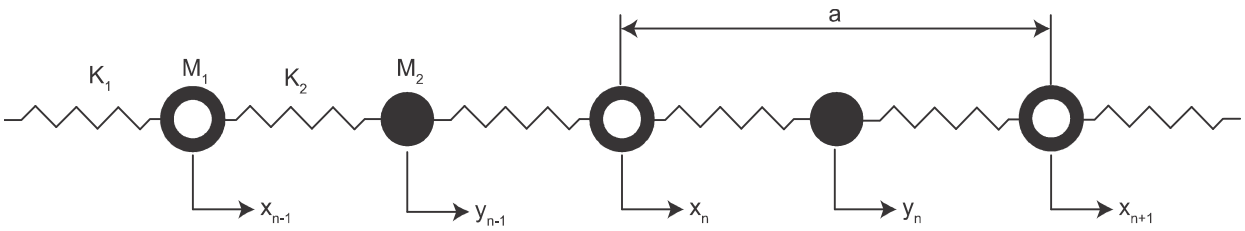

Figure 2.3: A linear chain with a two atom basis.

particles in a lattice, or in lattices with more than one dimension (where a crystal would have a unit cell such as body centered cubic, face centered cubic, etc.). In the beginning of section 2.1 the unit cell had only one particle.

To understand optical phonons consider a linear chain such as at the beginning of section 2.1, except that now there are two atoms of different types with alternating masses and spring constants between them, such as in Figure 2.3. Note that the unit cell of the chain must now contain two atoms instead of one. Using Hooke's law, we derive the equations of motion for the two masses,

$$\begin{aligned} M_1\ddot{x}_n &= K_2(y_n - x_n) - K_1(x_n - y_{n-1}) \\ M_2\ddot{y}_n &= K_1(x_{n+1} - y_n) - K_2(y_n - x_n) \quad , \end{aligned} \tag{2.23}$$

wher x_n and y_n denote the location of particles of type 1 and 2 respectively. Extending our analysis in section 2.1, we assume a wave solution,

$$\begin{aligned} x_n(t) &= x_0 e^{i(kan-\omega t)} \\ y_n(t) &= y_0 e^{i(kan-\omega t)} \quad . \end{aligned} \tag{2.24}$$

This ansatz does not include any summations, because it is a specific solution not a general set of solutions such as in equation (2.15).

If we substitute equation (2.24) into equation (2.23) and rearrange, it yields

$$\begin{bmatrix} -\frac{K_1+K_2}{M_1} & \frac{K_1 e^{-ika}+K_2}{M_1} \\ \frac{K_1 e^{ika}+K_2}{M_2} & -\frac{K_1+K_2}{M2} \end{bmatrix} \begin{pmatrix} x_0 \\ y_0 \end{pmatrix} = -\omega^2 \begin{pmatrix} x_0 \\ y_0 \end{pmatrix} \tag{2.25}$$

In order to find non-trivial solutions to the problem $-\omega^2$ must be an eigenvalue of equation (2.25). By taking

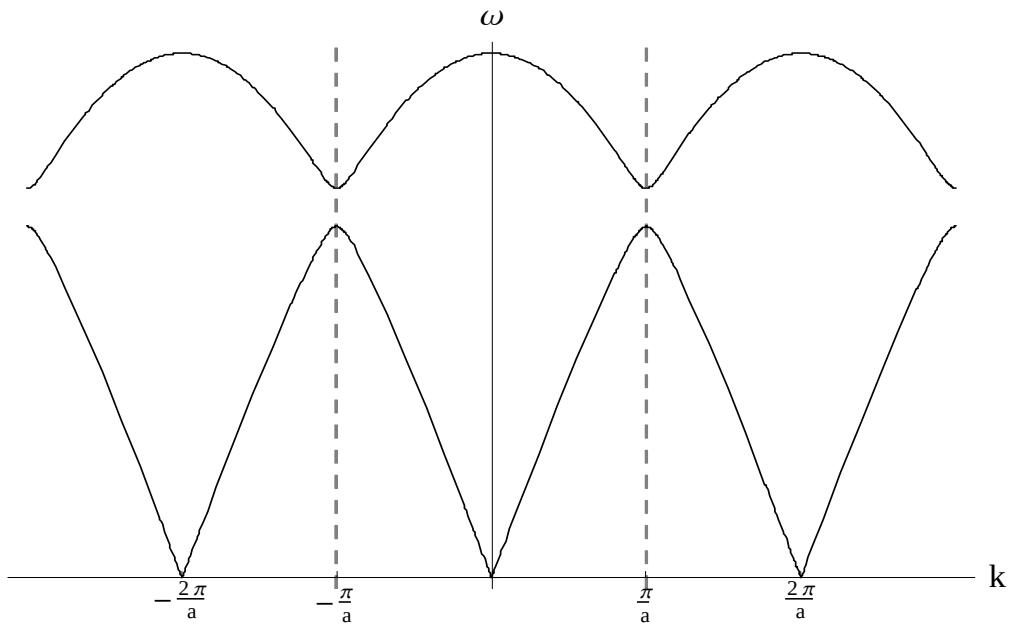

Figure 2.4: The dispersion relation for acoustic and optical phonons. Acoustic phonons approach zero frequency as k goes to zero, while optical phonons always have high frequencies, regardless of k.

the determinant of the equation we find that

$$-(K_1 + K_2)(M_1 + M_2)\omega^2 + M_1 M_2 \omega^4 + 2K_1 K_2 - 2K_1 K_2 \cos ka = 0 \tag{2.26}$$

The relation between ω and k gives rise to optical and acoustic phonons. Optical phonons are waves that occur when atoms within a unit cell move relative to each other. This means that they must have a very short wavelength and high frequency. Acoustic phonons are vibrations of the unit cell itself relative to the other unit cells. Acoustic phonons are phonons where ω linearly approaches zero as k goes to zero. The slope is the speed of sound in the chain. Optical phonons only have high values of ω (high frequency) and strongly interact with the electromagnetic field. Since they always require high energy, they can sometimes be ignored, especially if the temperature is low. Figure 2.4 shows the dispersion relation over two Brillioun zones for a typical linear chain with two different masses and spring constants. The upper wave is for optical phonons and the lower is for acoustic. As can be seen in the graph the optical phonons must have a very high frequencies even at low wavenumber.

2.2 Phonons in 3 Dimensions

Phonon theory can be extended to higher dimensions, however this report will not examine this in detail. For three dimensional phonons consider, instead of a linear chain, a lattice of particles in three dimensions where all particles that are adjacent to each other are connected by springs. An analysis similar to Section 2.1 can be done, except with three dimensional vectors. As a result the wavenumber, k, becomes the wave vector, $\mathbf{k}$, and the Brillouin zone also becomes three dimensional and significantly more complex. There are three polarizations of waves in the solution: two transverse modes and one longitdudinal mode. In transverse waves lattice particles move perpendicular to the direction of the $\mathbf{k}$ vector and in longitududinal waves they move parallel to $\mathbf{k}$. Note that the one dimensional wave analysis done above is for a longitudinal wave. Generally, transverse waves have a lower phase velocity than longitudinal waves [14]. It is also possible to determine the group velocity, using a three dimensional derivation similar to Appendix A. From this it is possible to show that the group velocity is not necessarily in the same direction as the phase velocity [14].

2.3 Quantum Mechanical Phonons

A quantum analysis of phonons is beyond the scope of this report. However, there are some important properties from quantum mechanics that allow phonons to be localized as particles instead of waves. A derivation of phonon quantum behavior can be found in many introductory solid state physics textbooks such as in Snoke [4].

Consider the linear chain of 2.1. Instead of using Newton's Laws for the analysis, the Schrödinger equation (the quantum mechanical equivalent of Newton's laws) is used. After decoupling the equation in a similar way to Section 2.1, the equation can be turned into a sum of independent quantum harmonic oscillators. Solutions to the Schrödinger equation for a harmonic oscillator must have an energy of $\hbar\omega$

In his landmark paper on phonons [8], Rudolf Peierls determined that phonons could be treated as particles with an energy of $\hbar\omega$ and a momentum of $\hbar\mathbf{k}$. However, there are some important differences from regular particles:

- Phonons are created and destroyed, therefore the number of phonons is not conserved.

- Phonon energy is always conserved in an interaction, but momentum is not always. For this reason, phonon momentum is sometimes called quasimomentum or crystal momentum [15].

If particles in a crystal acted linearly (i.e. the interatomic potential was quadratic and therefore the interatomic forces were linear), there would be no phonon-phonon interaction at all, much like classical waves passing through each other without any disturbance. However Peierls showed that non-harmonic cubic terms in the interatomic potential allows for creation and destruction of phonons in three phonon interactions [9]. Either two phonons combine to form one phonon or one phonon decays into two. Since energy is conserved

$$\hbar\omega' + \hbar\omega'' = \hbar\omega''' \text{ or } \hbar\omega' = \hbar\omega'' + \hbar\omega''' \ . \tag{2.27}$$

Phonon momentum, however, is not always conserved. It obeys the rule

$$\hbar\mathbf{k}' + \hbar\mathbf{k}'' = \hbar\mathbf{k}''' + \hbar\mathbf{G} \text{ or } \hbar\mathbf{k}' = \hbar\mathbf{k}'' + \hbar\mathbf{k}''' + \hbar\mathbf{G} \ . \tag{2.28}$$

Here $\mathbf{G}$ is the reciprocal lattice vector. In the one dimensional case shown in equation (2.22), $\mathbf{G}$ would be $\frac{2\pi}{a}m$.

If G is 0, the phonon momentum is conserved, which is equivalent to an interaction where all of the phonons (on the left and right of the equation) always remain in the Brioullin zone. These processes are normal or N processes. If G is non-zero, momentum is not conserved, which is equivalent to one or more of the phonons having a momentum outside of the Brioullin zone and then being projected back into the Brioullin zone using the reciprocal lattice vector. These interactions are called Umklapp processes or U processes [15]. Phonon interactions with lattice imperfections and walls generally do not conserve momentum but do conserve energy. These processes combined with Umklapp processes are together called resistive or R processes [9].

3 The Phonon Gas

3.1 The Particle Distribution Function

Using the classical and quantum derivations of phonons allows us to analyze heat conduction by considering a gas of phonons. This gas has different properties than a real gas, but the same basic approach to the kinetic theory of gases can be applied to phonons as well. The kinetic theory of phonons begins with defining the particle properties of a phonon [8], [16]:

- Phonons have an energy of $\hbar\omega$ and a momentum[2] of $\hbar k_i$.
- Phonons can be created and destroyed.
- Phonons travel with the group velocity $\frac{\partial\omega}{\partial k_i}$.
- Phonon interaction involves momentum conserving N processes and non-conserving R processes.

With the properties of the phonons defined, their kinetic equation can be derived. We first define the particle distribution function f, by defining the number of particles in a the differential volume $d\mathbf{x}$ and with a certain differential wavevector $d\mathbf{k}$ to be

$$dN = f\left(x, k_i, t\right) d\mathbf{x} d\mathbf{k} \quad . \tag{3.1}$$

The six dimensions of space and wavevector combined are called the phase space. It follows that the total number of particles in a volume, V, is f integrated by $\mathbf{x}$ and $\mathbf{k}$,

$$N = \int_{BZ} \int_{V} f\left(x, k_i, t\right) d\mathbf{x} d\mathbf{k} \quad , \tag{3.2}$$

where BZ denotes the Brillouin zone of the phonon's dispersion relation. Removing the spatial integral results in the number density,

$$n\left(x, t\right) = \int_{BZ} f\left(x, k_i, t\right) d\mathbf{k} \quad . \tag{3.3}$$

[2]For the rest of this paper, lower case english letters will be used to denote Einstein index notation. Therefore vector $\mathbf{k}$ is equivalent to k_i.

f is a function that describes how many particles there are for a given wave vector at a given time in a given space. It is therefore the essential building block for determining macroscopic properties by integrating over its domain. For example, since the energy of a single particle is $\hbar\omega$, the energy density is

$$e = \int_{BZ} \hbar\omega f d\mathbf{k} \quad . \tag{3.4}$$

Following the same argument, the quasimomentum of the system is

$$p_i = \int_{BZ} \hbar k_i f d\mathbf{k} \quad . \tag{3.5}$$

3.2 Phonon Entropy and Equilibrium Distribution

Another important macroscopic property we can determine is the entropy of a system. From statistical thermodynamics, we start from Boltzmann's formulation of entropy [17]

$$\mathcal{S} = k_B \ln \Omega \quad , \tag{3.6}$$

where k_B is Boltzmann's constant and Ω is the number of possible microscopic states that a system can be in while retaining the same macroscopic properties. From quantum mechanics, theory shows that phonons are indistinguishable from one another, and they can all exist in the same energy state, so they are bosons [19]. It can be shown by applying equation (3.6) that bosons have an entropy density of

$$s = -k_B \int \left(f \ln \frac{f}{y} - (y+f) \ln \left(1 + \frac{f}{y} \right) \right) d\mathbf{k} \quad , \tag{3.7}$$

where f is the distribution function, k_B is the Boltzmann constant and y is the density of states [18]. The density of states is a property derived from quantum mechanics that is dependent on the Brillouin zone of a crystal lattice. For a detailed derivation of the density of states see [19].

Since entropy always remains the same or increases during a process in an isolated system, equilibrium occurs when entropy is at a maximum. Therefore, to find the distribution function in equilibrium, f_{eq}, equation (3.7) should be maximized under the constraint of given energy. Note that in general derivations of the Bose distribution (such as for photons), the maximization is also constrained by number conservation, but this does not apply to phonons as discussed in Section 2.3. We use a Lagrange multiplier, β, to consider the energy constraint,

$$\phi = -k_B \int \left(f \ln \frac{f}{y} - (y+f) \ln \left(1 + \frac{f}{y} \right) \right) d\mathbf{x} d\mathbf{k} + \beta \left(\int \hbar\omega f d\mathbf{x} d\mathbf{k} - E \right) \quad . \tag{3.8}$$

The equilibrium distribution occurs at maximum ϕ and is given by

$$f_{eq} = \frac{y}{e^{\beta\hbar\omega} - 1} \quad , \tag{3.9}$$

which is commonly known as the Bose-Einstein (or simply Bose) distribution [19].

The Lagrange multiplier, β, follows from the Gibbs equation, which relates entropy to energy, pressure and volume at equilibrium

$$T d\mathcal{S} = dE + P dV \quad , \tag{3.10}$$

where $\mathcal{S} = sV$. By using equation (3.7) and taking its differential at equilibrium, we obtain

$$ds = k_B \int d \left(\left(\beta\hbar\omega f_{eq} + y \ln \left(1 + \frac{f}{y} \right) \right) d\mathbf{k} \right) \quad . \tag{3.11}$$

We are free to substitue f with equation (3.9) at any point because we are taking the differential at equilibrium. In the above equation we do it only when it is convenient to cancel out terms. Note that the first term in the integral is the energy multiplied by β, that is

$$ds = k_B d(e\beta) + k_B \int d \left(y \ln \left(1 + \frac{f}{y} \right) \right) d\mathbf{k} \quad . \tag{3.12}$$

Using the product rule for differentiation and by substituting the equilibrium distribution into the remaining f term causes all but one term to cancel and yields

$$ds = k_B \beta de \quad . \tag{3.13}$$

From the Gibbs equation, we can determine that

$$\beta = \frac{1}{k_B T} \quad . \tag{3.14}$$

We can also determine the pressure by multiplying ds by the volume

$$V ds = V \frac{de}{T} \quad . \tag{3.15}$$

Rearranging the equation by bringing the volume into the differential yields

$$T d\mathcal{S} = dE + (Ts - e) dV \quad , \tag{3.16}$$

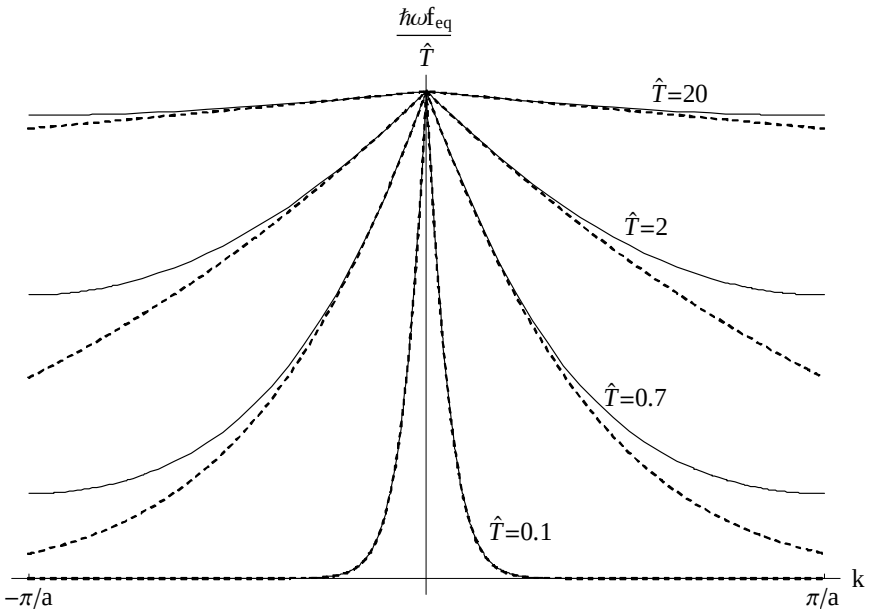

Figure 3.1: The energy distribution function of the linear chain of atoms for various temperatures. Real dispersion is solid and linear dispersion is dashed.

where $E = eV$. Comparing equation 3.16 with equation 3.10 yields the phonon gas pressure

$$P = Ts - e \quad . \tag{3.17}$$

3.3 Debye Temperature

The equilibrium properties of a phonon gas can be computed by integrating the equilibrium distribution function, f_{eq}, which was explicitly determined in Section 3.2. For the linear chain of atoms, the dispersion relation in equation (2.21) is used for ω. This dispersion relation makes analytical integration very difficult. In order to avoid this, the dispersion relation may be approximated by a linear relation between ω and k

$$\omega = ck \quad , \tag{3.18}$$

where c is the speed of sound. For the linear chain of atoms, the speed of sound is the group velocity at the limit as k goes to zero,

$$c = \lim_{k \to 0} \frac{d\omega}{dk} = a\sqrt{\frac{K}{M}} \quad . \tag{3.19}$$

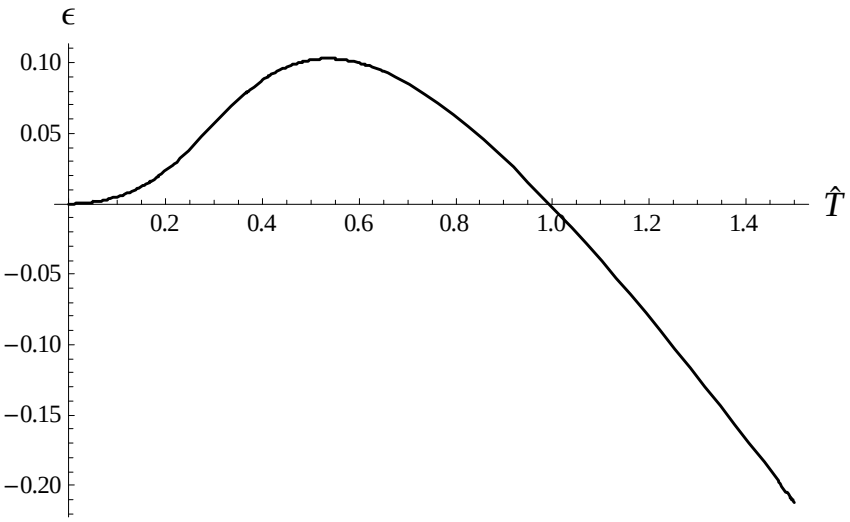

Figure 3.2: The relative error between real dispersion and linear dispersion with an infinite Brillioun zone as a function of temperature.

To non-dimensionalize the temperature in the Bose distribution, we first define the Debye temperature as [28]

$$T_D = \frac{\hbar}{k_B}\sqrt{\frac{K}{M}} \quad . \tag{3.20}$$

We then define $\hat{T}$ as

$$\hat{T} = \frac{T}{T_D} \tag{3.21}$$

so that

$$f_{eq} = \frac{y}{\exp\left[\frac{ak}{\hat{T}}\right] - 1} \tag{3.22}$$

The linear dispersion relation's accuracy can be compared to non linear dispersion using the energy distribution function (i.e. $\hbar\omega f_{eq}$). The energy distribution function is shown in Figure 3.1 for a variety of $\hat{T}$ ranging from 0.1 to 20. The linear dispersion approximation of the energy distribution function is shown as dashed lines. The graph was normalized by dividing the energy distribution function by the Debye temperature. By inspecting the graph, the distribution for linear dispersion seems to closely approximates the actual dispersion relation with the largest errors at $\hat{T}$ equals 0.7.

Another difficulty in performing analytical integrations of the distribution function is the finite size of the Brillioun zone. Bose distribution integrals are much simpler to integrate from negative to positive inifinity

as opposed to between two finite points. However notice that if the Debye temperature is much less than unity in Figure 3.1, the function drops to approximately zero before it reaches the Brillioun zone boundary. Therefore, for low temperatures, the Brillioun zone can be expanded to positive and negative infinity without any ramifications, for example energy density can be approximated as

$$e = \int_{BZ} \hbar\omega f dk \approx \int_{-\infty}^{\infty} \hbar\omega f dk \quad \text{for} \quad \hat{T} \ll 1 \quad . \tag{3.23}$$

A plot showing the relative error between linear dispersion integrated over an infinite Brillioun zone and one dimensional real dispersion is shown in Figure 3.2. The plot shows a less than ten percent error for a Debye temperature up to about 1.2. After 1.2, the error gets progressively larger to the point that the approximation is useless. The reason the error gets so large is because at higher $\hat{T}$, the linear dispersion approximation is non-zero outside the Brillioun zone.

The Debye temperature is a useful value that can be used to determine how accurate the linear phonon dispersion approximation is and how far theory can be pushed with these approximations. Unfortunately, for many materials the Debye temperature is well below room temperature so these approximations can cause significant errors. The table below shows the Debye temperature for some materials that are encountered in nano-devices [5]. It is important to note that copper, silver and gold are not usually in single crystal form so the assumptions in this work may not necessarily apply to them.

Element	**Debye Temperature (K)**
Carbon	2230
Silicon	645
Copper	343
Silver	225
Gold	165

One possible way to extend the model further is to sacrifice the simplicity of infinite Brillioun zones and use finite ones instead while still keeping linear dispersion. Figure 3.3 shows the relative error between real dispersion and linear dispersion integrated over a finite Brillioun zone. The error goes up to twelve percent at Debye temperatures below unity and then approaches zero as the Debye temperature gets larger. The

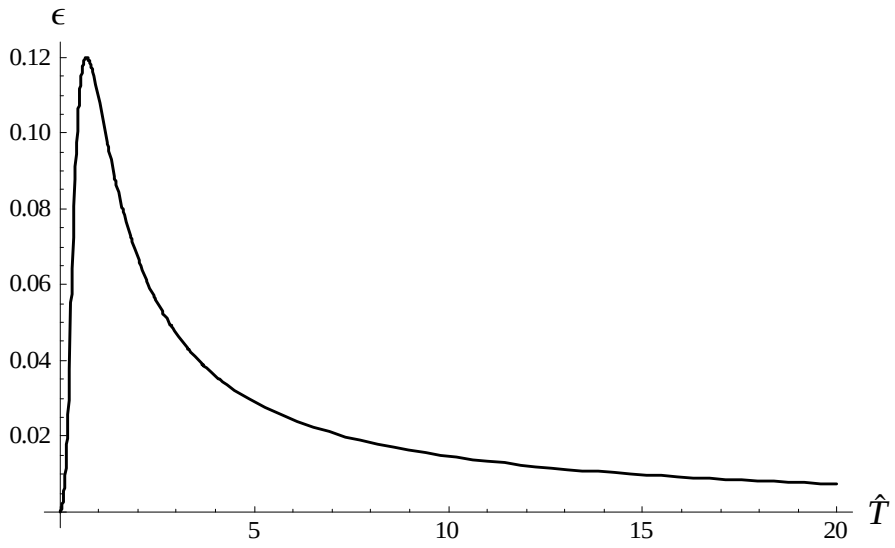

Figure 3.3: The relative error between real dispersion and linear dispersion in a finite Brillioun zone for the linear chain of atoms.

reason for this is that the Bose distribution approaches a flat line as $\hat{T}$ approaches infinity, much like the linear dispersion approximation.

3.4 Phonon Energy Distribution

The equilibrium energy distribution of three dimensional phonons can be determined by integrating equation (3.4) in three dimensions. As explained briefly in Section 2.2, the distribution function must now be integrated over the wavevector $\mathbf{k}$. For simplicity, we define k to be the magnitude of $\mathbf{k}$ and k_1, k_2 and k_3 are the components of $\mathbf{k}$. With the linear dispersion approximation, $\omega = ck$, this yields

$$e = \iiint_{-\infty}^{\infty} \hbar\omega f d\mathbf{k} = \iiint_{-\infty}^{\infty} \frac{\hbar cky}{e^{\frac{\hbar ck}{k_B T}} - 1} d\mathbf{k} \quad . \tag{3.24}$$

Converting to spherical coordinates and integrating over the solid angle gives

$$e = 4\pi \int_0^{\infty} \frac{\hbar cky}{e^{\frac{\hbar ck}{k_B T}} - 1} k^2 dk \quad . \tag{3.25}$$

To move all of the constants outside the integral, we do the coordinate transformation

$$x = \frac{\hbar ck}{k_B T} \tag{3.26}$$

to get

$$e = \frac{4\pi k_B^4 T^4}{\hbar^3 c^3} y \int_0^\infty \frac{x^3}{e^x - 1} dx \tag{3.27}$$

which yields

$$e = \frac{4\pi k_B^4 y}{\hbar^3} \frac{T^4}{c^3} \quad . \tag{3.28}$$

This relation shows that the energy of a solid in equilibrium is a quartic function of temperature and is also dependent on the speed of sound in the solid.

3.5 Wave modes and the Debye velocity

The linear chain model presented above only has one dimension, and therefore only one type of wave. In three dimensions, there are three different types of waves. Consider the linear chain in Figure 2.1 except that now the particles can move in three dimensions. The particles can move to the left and right, such as in the pure one dimensional case, but they can also move up and down as well as in and out of the page. Notice that up and down is equivalent to in and out by the symmetry of the system. The side to side motion is known as a longitudinal wave, while the other two types of motion are transverse waves. Therefore there are two transverse and one longitudinal mode for any linear chain. Now suppose that instead of a linear chain there was actually a three dimensional lattice of particles[3]. This lattice could be described by three linearly independent basis vectors. Each basis vector would each have one longitudinal and two transverse waves associated with it, making nine waves. This means there are six independent dispersion relations (since the two transverse waves would have the same properties) to fully describe a wave in a three dimensional lattice.

The linear dispersion approximation can be used to simplify ω, but there would still be three independent velocities, c_{t_1}, c_{t_2} and c_l where t and l represent the transverse and longitudinal modes respectively. The transverse modes have the same velocity, so although they are treated separatly for most of this section, in general $c_{t_1} = c_{t_2}$. This leads to three separate distribution functions that are superimposed on each other.

[3]In three dimensions, the Brillouin Zone may be quite complex and anisotropic. One way to simplify a three dimensional Brillouin Zone is to assume it is a sphere with the same volume as the actual Brillouin Zone.

In equilibrium with linear dispersion they are

$$\begin{aligned} f_{t_1} &= \frac{y}{\exp\left[\frac{\hbar c_{t_1} k}{k_B T}\right] - 1} \quad , \\ f_{t_2} &= \frac{y}{\exp\left[\frac{\hbar c_{t_2} k}{k_B T}\right] - 1} \quad , \\ f_l &= \frac{y}{\exp\left[\frac{\hbar c_l k}{k_B T}\right] - 1} \quad . \end{aligned} \tag{3.29}$$

As a result, the total distribution function is

$$f = f_{t_1} + f_{t_2} + f_l \quad . \tag{3.30}$$

In order to simplify the description of the phonon gas, we will not distinguish between phonons of different modes. For the following model we replace each mode's velocity with the Debye velocity, c_D, such that in equilibrium [28]

$$f = f_{t_1} + f_{t_2} + f_l = \frac{3y}{\exp\left[\frac{\hbar c_D k}{k_B T}\right] - 1} \quad . \tag{3.31}$$

The Debye velocity should be chosen such that the energy of the three modes is the same as the simplified case. An expression for the Debye velocity is found by determining the energy distribution

$$e = e_{t_1} + e_{t_2} + e_l \quad , \tag{3.32}$$

and using the energy expression in equation (3.28),

$$3\alpha \frac{T^4}{c_D^3} = \alpha \frac{T^4}{c_{t_1}^3} + \alpha \frac{T^4}{c_{t_2}^3} + \alpha \frac{T^4}{c_l^3} \quad . \tag{3.33}$$

This yields an expression for the Debye velocity in terms of the transverse and longitudinal velocities:

$$\frac{1}{c_D^3} = \frac{1}{3c_{t_1}^3} + \frac{1}{3c_{t2}^3} + \frac{1}{3c_l^3} = \frac{2}{3c_t^3} + \frac{1}{3c_l^3} \quad . \tag{3.34}$$

The Debye Velocity is an elegant simplification of a three dimensional lattice, however we should summarize the approximations that it requires and their cumulative effects. First of all, the Debye velocity requires linear dispersion and that the Brillioun zone can be extended to infinity. This is only a good approximation when the temperature of the domain is much lower than the Debye temperature. The second approximation is that the velocities in the different lattice directions are all the same. This makes the model purely isotropic and has the effect of making the Brillioun zone spherical. Any anisotropic studies would have to somehow

take these different velocities into account. Finally the Debye velocity does not distinguish between the modes of the vibrations.

4 The Boltzmann Equation and Moment Method

4.1 The Phonon-Boltzmann Equation

Since phonons can be described as particles, complete with a stochastic distribution function, we can now describe phonon processes through the change of the distribution function over time. Changes to f are caused by transport of phonons and phonon collisions (R and N processes). Hence it is possible to write a phonon-Boltzmann equation

$$\frac{\partial f}{\partial t} + \frac{\partial \omega}{\partial k_k}\frac{\partial f}{\partial x_k} = S(f) \quad , \tag{4.1}$$

where f is the particle distribution function and $S(f)$ is the collision term. The equation was first written by Peierls [8]. The collision term is a non-linear integral over the distribution function and requires quantum theory for it to be explicitly described. The transport term describes free flight of phonons with the group velocity, $\frac{\partial \omega}{\partial k_k}$. The group velocity of the phonons can be approximated by the Debye velocity.

The collision term can be broken into two parts, one representing normal processes and the other representing resistive processes,

$$S\left(f\right) = S_N\left(f\right) + S_R\left(f\right) \tag{4.2}$$

By inspection, it is apparent that the collision term must go to zero at equilibrium. This is simply because in equilibrium there can be no temporal variations in f and there can be no transport of f either, that is the two terms on the left of the equation must vanish. Furthermore, the collision term must also bring f towards equilibrium. Finally, since we know that in equilibrium f is the Bose distribution we have that $S\left(f_{Bose}\right)$ must be zero.

4.2 Macroscopic Moment Equations (Conservation laws)

The phonon Boltzmann equation can be solved using direct numerical simulation or by direct simulation Monte Carlo (DSMC) [6] and [7]. These produce accurate results (dispersion relations, Brillouin zones and

other properties can be implemented explicitly) but they carry a very high computational cost. Another method is to approximate the Boltzmann equation by develpping macroscopic equations by integration. We assume linear dispersion and use the 3-D Debye velocity which we now denote as the vector

$$c_i = cn_i \quad , \tag{4.3}$$

where n_k is the phonon direction, and c is the Debye speed. Furthermore we can represent the vector k_i as

$$k_i = kn_i \quad , \tag{4.4}$$

For the energy balance equation, we multiply phonon Boltzmann equation by $\hbar\omega$ and integrate,

$$\int \frac{\partial f}{\partial t}\hbar\omega d\mathbf{k} + \int c_i \frac{\partial f}{\partial x_i}\hbar\omega d\mathbf{k} = \int S(f)\hbar\omega d\mathbf{k} \quad . \tag{4.5}$$

The first term is simple because t is independent of k,

$$\int \frac{\partial f}{\partial t}\hbar\omega d\mathbf{k} = \frac{\partial}{\partial t}\int \hbar\omega f d\mathbf{k} = \frac{\partial e}{\partial t} \quad . \tag{4.6}$$

The second term can be simplified by substituting ck for ω,

$$\int c_i \frac{\partial f}{\partial x_i}\hbar\omega d\mathbf{k} = \int c_i \frac{\partial f}{\partial x_i}\hbar ck d\mathbf{k} \quad . \tag{4.7}$$

Furthermore, c and the x derivative can be moved out of the integral because they are independent of $\mathbf{k}$. Thus equation (4.7) becomes

$$\int c_i \frac{\partial f}{\partial x_i}\hbar ck d\mathbf{k} = c^2 \frac{\partial}{\partial x_i}\int \hbar k n_i f d\mathbf{k} = c^2 \frac{\partial}{\partial x_i}\int \hbar k_i f d\mathbf{k} = c^2 \frac{\partial p_i}{\partial x_i} \quad . \tag{4.8}$$

Finally, the collision term must also be integrated. Since the collision term consists only of N and R processes, which both conserve energy, the integration of the collision term must be zero. Therefore the energy conservation equation is

$$\frac{\partial e}{\partial t} + c^2 \frac{\partial p_i}{\partial x_i} = 0 \; . \tag{4.9}$$

The same process can be used for the momentum conservation equation. The phonon-Boltzmann equation is multiplied by hk_j and integrated,

$$\int \frac{\partial f}{\partial t}\hbar k_j d\mathbf{k} + \int c_i \frac{\partial f}{\partial x_i}\hbar k_j d\mathbf{k} = \int S(f)\hbar k_j d\mathbf{k} \; . \tag{4.10}$$

The first term is the momentum rate of change,

$$\int \frac{\partial f}{\partial t} \hbar k_j d\mathbf{k} = \frac{\partial p_j}{\partial t} \quad . \tag{4.11}$$

The second term can be rearranged such that

$$\int c_i \frac{\partial f}{\partial x_i} \hbar k_j d\mathbf{k} = \frac{\partial}{\partial x_i} \int \hbar c \frac{k_j k_i}{k} f d\mathbf{k} = c \frac{\partial N_{ij}}{\partial x_i} \quad . \tag{4.12}$$

Here, N_{ij} has been defined as a rank two tensor that is analgous to the stress tensor in continuum fluid mechanics. On careful inspection, it is helpful to decouple the stress tensor from energy by splitting it into its trace and trace-free parts (a trace-free matrix is indicated by angled brackets around its indices),

$$N_{ij} = \frac{1}{3} N_{kk} \delta_{ij} + N_{\langle ij \rangle} = \frac{1}{3} \int \hbar \frac{k_k k_k}{k} f d\mathbf{k} \delta_{ij} + N_{\langle ij \rangle} = \frac{1}{3c} \int \hbar \omega f d\mathbf{k} \delta_{ij} + N_{\langle ij \rangle} = \frac{e}{3c} \delta_{ij} + N_{\langle ij \rangle} \quad . \tag{4.13}$$

The integration of the collision term will be 0 for N processes because they conserve momentum, but there will be a non-zero contribution from the R processes. We define S_R as the collision term for only R processes, which gives

$$\int S(f) \hbar k_i d\mathbf{k} = \int S_R(f) \hbar k_i d\mathbf{k} = P_i \quad , \tag{4.14}$$

Where P_i is the integrated collision term in the momentum equation. Finally, the momentum equation is

$$\frac{\partial p_j}{\partial t} + \frac{1}{3} \frac{\partial e}{\partial x_j} + c \frac{\partial N_{\langle ij \rangle}}{\partial x_i} = P_j \tag{4.15}$$

The momentum equation, like the energy equation, has a term that includes a higher order moment, $N_{\langle ij \rangle}$. Another equation can be made for $N_{\langle ij \rangle}$ that will similarly have a higher order moment, $M_{\langle ij \rangle k}$ and so on. In theory, an infinite set of moment equations can be generated which would fully describe the distribution function. In other words, the hierarchy of inifinitely many moment balance equations is equivalent to the Boltzmann equation. In practice, it is necessary to consider only a finite number of moments, which leads to the so-called closure problem: For example, consider only the moments e and p_i for which the moment equations are the balances of energy (equation 4.9) and momentum (equation 4.15). These contain the additional quantities $N_{\langle ij \rangle}$ and P_i, and thus are not a closed system of equations for e and p_i. The closure problem is to find constitutive relations for N_{ij} and P_i (or higher order moments if you want more equations) as functions of the lower order moments e, p_i, etc. (and possibly their derivatives).

4.3 Approximating the Collision Term - The Callaway Model

The highly non-linear collision term in kinetic theory is extremely difficult to handle in computational models or anlytical treatment, so an approximation is often used. In gas kinetics, one of the most well known approximations is the Bhatnagar-Gross-Krook or BGK model [20]. An equivalent model for phonons was introduced by Callaway five years later [21]. First, the Callaway model separates the collision term into two contributions for normal collisions and resistive collisions, respectively, as explained in Section 2.3

$$S = S_N + S_R \quad . \tag{4.16}$$

For both normal and resistive collisions, Callaway uses an approach similar to the BGK model where S is determined by the deviation of f from a respective *local* equilibrium distribution f_N or f_R,

$$S = -\frac{1}{\tau_N(k)}(f - f_N) - \frac{1}{\tau_R(k)}(f - f_R) \quad . \tag{4.17}$$

Here, $\tau_{N,R}$ is the frequency of N or R collisions between phonons which depends on wave vector. In the Callaway model, the absolute value of $S_{N,R}$ is large when the actual distribution function, f, is far from the local equilibrium distribution function $f_{N,R}$.

We determine the local equilibrium distribution f_R from maximizing entropy under the constraint of prescribed local energy; recall that resistive interactions conserve energy but not momentum. Therefore, the distribution is determined using the same process as in Section 3.2 and the function for entropy must be maximized,

$$\phi = -k_B \int \left(f \ln \frac{f}{y} - (y+f)\ln\left(1+\frac{f}{y}\right)\right) d\mathbf{k} + \beta\left(\int h\omega f d\mathbf{k} - E\right) \quad . \tag{4.18}$$

This equation is similar to equation (3.8) except that it is for a *local* distribution so there is no integration over $\mathbf{x}$ and it is in three dimensions instead of one. The equation yields the Bose distribution at maximum entropy,

$$f_R = \frac{y}{e^{\beta_R \hbar\omega} - 1} \quad . \tag{4.19}$$

The Langrange multiplier, β_R, is determined by recalling that, since energy is conserved in R-processes, the integration of the resistive collision term in the energy equation must be 0 (see equation (4.9)),

$$\int \hbar\omega S_R d\mathbf{k} = -\int \frac{\hbar\omega}{\tau_R(k)}(f - f_R)\, d\mathbf{k} = 0 \quad . \tag{4.20}$$

Equation (4.20) is another non-linear integration since, in general, τ_R is a function of k. The gray matter approximation greatly simplifies the equation by assuming that τ_R is constant. This allows it to be removed from the equation and the integration becomes the difference in energy between f and f_R,

$$\int \hbar\omega f d\mathbf{k} = \int \hbar\omega f_R d\mathbf{k} \quad . \tag{4.21}$$

Therefore f_R is actually a function dependent on f. It can be described as the target distribution function for R processes. That is, any R process brings f closer to f_R; however, after each resistive interaction, f_R itself is changed (since it is a function of f), until both f and f_R both reach global equilibrium and S_R becomes zero.

The same process is used to determine f_N, except that energy and momentum are conserved in normal processes, so that f_N follows from maximizing entropy under the constraints of prescribed local energy and momentum. The momentum constraint adds three additional Lagrange multipliers γ_i, one for each dimension, so that now one needs to maximize

$$\phi = -k_B \int \left(f \ln \frac{f}{y} - (y+f) \ln \left(1 + \frac{f}{y} \right) \right) d\mathbf{k} + \beta \left(\int h\omega f d\mathbf{k} - e \right) + \gamma_i \left(\int \hbar k_i f d\mathbf{k} - p_i \right) \quad . \tag{4.22}$$

Maximization yields the drifting Bose distribution,

$$f_N = \frac{y}{e^{\beta_N \hbar\omega + \gamma_i \hbar k_i} - 1} \quad . \tag{4.23}$$

The Lagrange multipliers are found by using the constraints that f and f_N must conserve energy and momentum during N processes,

$$\begin{aligned} e &= \int \hbar\omega f d\mathbf{k} = \int \hbar\omega f_N d\mathbf{k} \ , \\ p_i &= \int \hbar k_i f d\mathbf{k} = \int \hbar k_i f_N d\mathbf{k} \ . \end{aligned} \tag{4.24}$$

The Callaway model for grey matter can then be incorporated into the macroscopic moment equations. For the energy equation, we already know the collision term is zero. For the momentum equation, we determine P_i by integrating the R and N collision terms,

$$P_i = \int S_R(f) \hbar k_j d\mathbf{k} + \int S_N(f) \hbar k_j d\mathbf{k} = -\frac{1}{\tau_R} \int (f - f_R) \hbar k_j d\mathbf{k} + 0 \tag{4.25}$$

$$= -\frac{1}{\tau_R} \int f \hbar k_j d\mathbf{k} + \frac{1}{\tau_R} \int f_R \hbar k_j d\mathbf{k} = -\frac{1}{\tau_R} p_i \quad . \tag{4.26}$$

Note that the collision term for the normal processes conserves momentum, so it must be zero by the same argument used in the energy equation. The integration over f_R is also zero because it is the Bose distribution, which is isotropic.

4.4 Closure for Local Equilibrium and Fourier's law

A simple closure method can be used to produce Fourier's law of heat conduction. To do this, we take the first four moment equations for energy and momentum,

$$\frac{\partial e}{\partial t} + c^2 \frac{\partial p_i}{\partial x_i} = 0 \tag{4.27}$$

$$\frac{\partial p_j}{\partial t} + \frac{1}{3}\frac{\partial e}{\partial x_j} + c\frac{\partial N_{\langle ij \rangle}}{\partial x_i} = -\frac{1}{\tau_R} p_j \quad . \tag{4.28}$$

We then need a constitutive equation for the stress tensor, $N_{\langle ij \rangle}$. Fourier's law requires a continuum assumption which means that the local distribution must be the Bose distribution, which gives

$$N_{\langle ij \rangle} = \int \hbar \frac{k_{<i} k_{j>}}{k} f_B d\mathbf{k} = 0 \quad , \tag{4.29}$$

where $k_{<i}k_{j>}$is the trace free part of the tensor $k_i k_j$. The integral is zero because the bose distribution is fully isotropic, and it is multiplied by the fully anisotropic trace free tensor. Rearranging equation (4.28) for a steady process and multiplying by c^2 yields Fourier's law,

$$c^2 p_i = -\frac{\tau_R c^2}{3}\frac{\partial e}{\partial x_i} = -\frac{\tau_R c^2}{3}\rho_{mat} c_v \frac{\partial T}{\partial x_i} = -\kappa \frac{\partial T}{\partial x_i} \quad , \tag{4.30}$$

Where $c^2 p_i$ is the heat flux per unit area, q. This derivation of Fourier's law shows that the microscopic R collision frequency is related to the heat conductivity, κ, the density, ρ_{mat} and the specific heat, c_v of a material,

$$\tau_R = \frac{3\kappa}{c^2 \rho_{mat} c_v} \quad . \tag{4.31}$$

This is a powerful relation because now the R process frequency can be easily measured using a basic macroscopic experiment.

4.5 The Generalized Moment Equations

By inspection of equations 4.27 and 4.28, it is apparent that each equation contains a moment and a flux (a higher order moment). As a result an infinite number of moment equations can be generated each containing

a moment and the flux of a higher order moment. The more moment equations used in a calculation would produce a more accurate calculation of f [9]. We define the general moment density, $u_{\langle i_1 \ldots i_n \rangle}$,

$$u_{\langle i_1 \ldots i_n \rangle} = \left\{ ..., \hbar \int \left(\frac{1}{k} \right)^{n-1} k_{<i_1} k_{i_2} \ldots k_{i_n>} f d\mathbf{k}, ... \right\}, \quad n \in 1, 2, 3, ... \quad , \tag{4.32}$$

and the general flux, $f_{\langle i_1 \ldots i_n \rangle k}$,

$$f_{\langle i_1 \ldots i_n \rangle k} = \left\{ ..., \hbar \int \left(\frac{1}{k} \right)^{n} k_{<i_1} k_{i_2} \ldots k_{i_n>} k_k f d\mathbf{k}, ... \right\} \quad . \tag{4.33}$$

It can be shown [9] that the flux relates to the moment densities by the formula

$$f_{\langle i_1 \ldots i_n \rangle k} = \frac{n}{2n+1} u_{<<i_1 \ldots i_{n-1}>} \delta_{i_n>k} + u_{\langle i_1 \ldots i_n k \rangle} \quad . \tag{4.34}$$

This relationship combined with applying the approach shown in Section 4.2 to arbitrary moments yields the general balance equation

$$\frac{\partial u_{\langle i_1 \ldots i_n \rangle}}{\partial t} + c \frac{\partial f_{\langle i_1 \ldots i_n \rangle k}}{\partial x_k} = P_{\langle i_1 \ldots i_n \rangle} \quad . \tag{4.35}$$

The flux can be removed using equation 4.34,

$$\frac{\partial u_{\langle i_1 \ldots i_n \rangle}}{\partial t} + c \frac{n}{2n+1} \frac{\partial u_{<<i_1 \ldots i_{n-1}>}}{\partial x_{i_n>}} + c \frac{\partial u_{\langle i_1 \ldots i_n k \rangle}}{\partial x_k} = P_{\langle i_1 \ldots i_n \rangle} \quad . \tag{4.36}$$

Thus an infinitely large set of moment equations can be generated by using this generic balance equation. For practical computing, this must be limited, but a higher order set of equations gives a better accuracy at the expense of more equations. A future research topic would be to determine how many moment equations are needed for an accurate solution to a given problem. The number of equations needed should be related to the Knudsen number of the problem, with higher Knudsen numbers needing more moment equations [29].

4.6 Grad's Closure Method

For a practical computation, only a finite number of moment equations can be used. In the highest equation that is used, there is always a flux that is a higher order moment. This results in an ill posed problem because there is one more variable than the number of equations.

In order to deal with this moment, we use Grad's moment method [10] adapted to phonon kinetic theory [9]. The premise of Grad's moment method is to construct the distribution function, f, so that it is a

function of the moments (with the exception of the highest one), i.e. $f = f\left(k, u_{\langle i_1\rangle}, ...u_{\langle i_1...i_n\rangle}\right)$. This way, the highest moment, $u_{\langle i_1...i_{n+1}\rangle}$, can be determined by integrating f and it becomes a function of the lower order moments. This reduces the number of variables to the number of equations and allows the system to be solved.

To construct f, we consider the entropy of the system in a similar way to equation (3.8), except this time we define our entropy so that all moments are used [16],

$$\begin{aligned}\phi = -k_B \int \left(f \ln \frac{f}{y} - (y+f)\ln\left(1+\frac{f}{y}\right)\right) dxdk \\ + \beta\left(\int \hbar\omega f dxdk - E\right) + \sum_{n=1}^{N}\left\{\Delta_{\langle i_1...i_n\rangle}\left(\hbar\left(\frac{1}{k}\right)^{n-1} k_{<i_1}k_{i_2}...k_{i_n>} f dxdk - u_{\langle i_1...i_n\rangle}\right)\right\} \quad , \end{aligned} \tag{4.37}$$

where $\Delta_{\langle i_1...i_n\rangle}$ is the general Lagrange multiplier.

Maximizing equation (4.37) and using equation (3.14) to substitute β for $\frac{1}{k_B T}$ yields

$$f = \frac{y}{\exp\left[\frac{\hbar c k}{k_B T} + \sum_{n=1}^{N}\left\{\Delta_{\langle i_1...i_n\rangle}\hbar\left(\frac{1}{k}\right)^{n-1} k_{<i_1}k_{i_2}...k_{i_n>}\right\}\right] - 1} \quad . \tag{4.38}$$

We assume that the distribution function is only a small distance from local equilibrium, which allows f to be linearized by taking a multidimensional first order Taylor series in all moments [9] (except for the zeroeth moment, energy),

$$f = f_{Bose} + \frac{k_B T}{\hbar c}\frac{\partial f_{Bose}}{\partial k}\left(\sum_{n=1}^{N}\left\{\Delta_{\langle i_1...i_n\rangle}\hbar\left(\frac{1}{k}\right)^{n-1} k_{<i_1}k_{i_2}...k_{i_n>}\right\}\right) \quad . \tag{4.39}$$

The Lagrange multipliers are determined in terms of their corresponding moment equations by substituting equation (4.39) into equation (4.32). Note that due to the linear construction of this closure method, the lagrange multipliers are only dependent on their corresponding moments and not on any others, which is a major benefit of Grad's closure method at the cost of only being able to model small deviations from the Bose distribution. The final distribution function has the generalized form

$$f(k, T, u_{i_1}, u_{\langle i_1 i_2\rangle}, ..., u_{\langle i_1...i_N\rangle}) = f_{Bose} + \frac{k_B T}{\hbar c}\frac{\partial f_{Bose}}{\partial k}\left(\sum_{n=1}^{N}\frac{15\prod_{j=0}^{n}(2j+1)}{16n!}\frac{c^5\hbar^4}{y\left(\pi k_B T\right)^5}u_{\langle i_1...i_n\rangle}\frac{k_{<i_1}...k_{i_n>}}{k^{n-1}}\right) \quad . \tag{4.40}$$

We can now explicitly determine the higher order moment $u_{\langle i_1...i_{n+1}\rangle}$ by using equation (4.40) in the moment

equation

$$u_{\langle i_1 \ldots i_{N+1} \rangle} = \hbar \int \left(\frac{1}{k}\right)^{n-1} k_{<i_1} k_{i_2} \ldots k_{i_n>} f(k, T, u_{i_1}, u_{\langle i_1 i_2 \rangle}, \ldots, u_{\langle i_1 \ldots i_n \rangle}) d\mathbf{k} \quad . \tag{4.41}$$

We use the property that over all space (i.e. negative to positive infinity) the integral of a product of two trace free tensors is non-zero if and only if the tensors are of the same length, therefore

$$u_{\langle i_1 \ldots i_{N+1} \rangle} = 0 \quad . \tag{4.42}$$

This reduces the number of state variables to the number of equations and closes the system.

Equation (4.40) can also be used to simplify the Callaway model for high moments. Applying the Callaway model to $P_{\langle i_1 \ldots i_n \rangle}$ yields

$$\begin{aligned} P_{\langle i_1 \ldots i_n \rangle} &= -\frac{1}{\tau_R} \int \hbar \left(\frac{1}{k}\right)^{n-1} k_{<i_1} k_{i_2} \ldots k_{i_n>} \left(f - f_R\right) d\mathbf{k} - \frac{1}{\tau_N} \int S_N(f) \hbar \left(\frac{1}{k}\right)^{n-1} k_{<i_1} k_{i_2} \ldots k_{i_n>} \left(f - f_N\right) d\mathbf{k} \\ &= -\frac{1}{\tau_R} u_{\langle i_1 \ldots i_n \rangle} - \frac{1}{\tau_N} u_{\langle i_1 \ldots i_n \rangle} - \frac{1}{\tau_N} \int f_N \hbar \left(\frac{1}{k}\right)^{n-1} k_{<i_1} k_{i_2} \ldots k_{i_n>} d\mathbf{k} \quad . \end{aligned} \tag{4.43}$$

Note that the f_R term will always be zero since it is a Bose distribution which is fully isotropic. Since the moments are trace free, the integral is zero over an isotropic domain. f_N is the drifting Bose distribution and requires further expansion

$$\frac{1}{\tau_N} \int f_N \hbar \left(\frac{1}{k}\right)^{n-1} k_{<i_1} k_{i_2} \ldots k_{i_n>} d\mathbf{k} = \frac{1}{\tau_N} \int \frac{y}{e^{\beta_N \hbar \omega + \gamma_i \hbar k_i} - 1} \hbar \left(\frac{1}{k}\right)^{n-1} k_{<i_1} k_{i_2} \ldots k_{i_n>} d\mathbf{k} \quad . \tag{4.44}$$

This term introduces a non-linearity into the equation, however, by linearizing f_N in the same way we linearize the Grad distribution, equation (4.38) reduces the term to zero for all moments of higher order than p_i, leading to our linearized form of the Callaway model

$$P_{\langle i_1 \ldots i_n \rangle} = -\frac{1}{\tau_R} u_{\langle i_1 \ldots i_n \rangle} - \frac{1}{\tau_N} u_{\langle i_1 \ldots i_n \rangle} = -\frac{1}{\tau} u_{\langle i_1 \ldots i_n \rangle} \quad \text{, for } n > 1, \tag{4.45}$$

where $\frac{1}{\tau}$ is the combined collision frequency of N and R processes. This results in the general balance equation

$$\frac{\partial u_{\langle i_1 \ldots i_n \rangle}}{\partial t} + c \frac{n}{2n+1} \frac{\partial u_{<\langle i_1 \ldots i_{n-1} \rangle>}}{\partial x_{i_n>}} + c \frac{\partial u_{\langle i_1 \ldots i_n k \rangle}}{\partial x_k} = -\frac{1}{\tau} u_{\langle i_1 \ldots i_n \rangle} \quad \text{for } n > 1. \tag{4.46}$$

For $n = N$, the equation simplifies to

$$\frac{\partial u_{\langle i_1 \ldots i_N \rangle}}{\partial t} + c \frac{N}{2N+1} \frac{\partial u_{<\langle i_1 \ldots i_{n-1} \rangle>}}{\partial x_{i_n>}} = -\frac{1}{\tau} u_{\langle i_1 \ldots i_N \rangle} \quad . \tag{4.47}$$

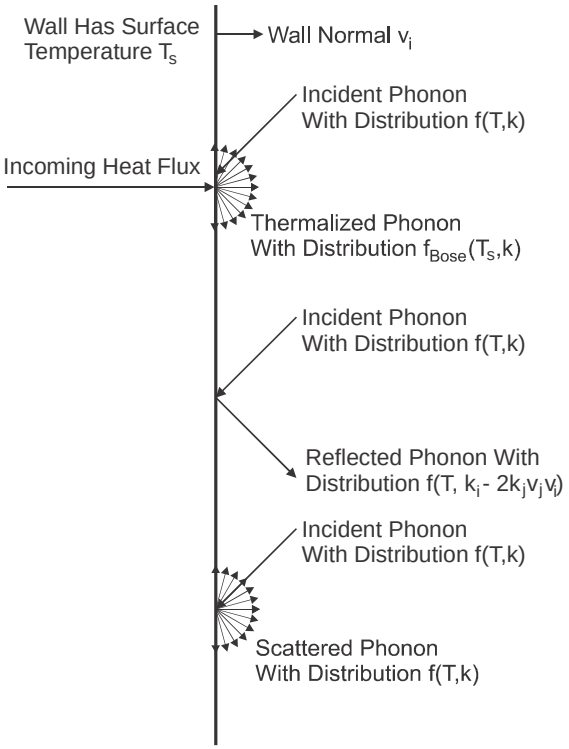

Figure 5.1: The microscopic model used for the phonon interaction with the boundary

5 Boundary Condition for the Phonon Moment Equations

5.1 Microscopic Model of Phonon-Surface Interactions

Boundary conditions are required to determine particular solutions of the moment equations. Just like the moment equations, the boundary conditions are derived from microscopic analysis of the phonon Boltzmann equation. In order to create a sufficient number of boundary conditions, we propose a simple model of phonon interactions with a surface at the microscopic level and then integrate over it to create macroscopic conditions for each state variable.

We assume that there are three possible interactions the phonon can have with the wall as shown in Figure 5.1. The general idea behind this assumption is that the possible interactions that a phonon can have with the wall can be modeled both in a general and mathematically simple way. By varying the amounts of phonons that interact in each of the three ways, actual phonon interactions can be modelled well.

The first process, thermalization, is when a phonon hits the wall and then comes to equilibrium with the

wall before being scattered into the bulk phonon gas. All of the phonons that have thermalized would form a Bose distribution centered on the surface temperature, T_s. It is important to note that thermalization can also create and destroy phonons, since the number of phonons do not need to be conserved. This also allows an energy flux through the surface.

The second type of interaction occurs when a phonon simply bounces off the surface while retaining its energy but changing direction. We split this into two types: isotropic scattering and specular reflection. These two types of reflections are a simple way to approximate directional scattering, where the direction of the scattered phonon is related to its incident angle.

We define $\bar{f}$ as the distribution function of the particles that have interacted with the wall but have not yet interacted with the rest of the bulk phonon gas, f. $\bar{f}$ must then be some function of the incident distribution function before it interacts with the wall (the bulk phonon gas) and some coefficients that account for how many phonons thermalize, scatter and reflect. We define α as the total fraction of phonons that are not thermalized and β as the fraction of phonons that are. Of the α phonons that are reflected and scattered we define γ as the fraction that are scattered, and therefore $(1-\gamma)$ are reflected. This yields the function

$$\bar{f} = \beta f_{Bose}\left(T_s, k\right) + \gamma\alpha f\left(k_i - 2k_k\nu_k\nu_i\right)\sigma\varpi\nu + \frac{\rho}{c}\int\limits_{k_i\nu_i<0} c\left(-n_k\nu_k\right) f\left(k_k\right) d\Omega \quad , \tag{5.1}$$

where T_s is the surface temperature, c is the speed of the phonon, n_k is the direction of the k vector, ν_k is the wall normal and ρ is a constant related to α and γ such that the number of particles reflected and scattered (but not thermalized) are conserved. The first term of the equation is the thermalization term, followed by the reflection term and then the isotropic scattering term.

Note that the argument $k_i - 2k_k\nu_k\nu_i$ simply switches the sign of any component in the direction of the wall normal. For example if the wall normal was $(0, 0, 1)$ and k_i was $(1, 2, 3)$ then the argument would be $(1, 2, -3)$. The scattering term has a half space integral which represents phonons coming towards the surface. This is because the $\bar{f}$ can only be related to phonons that actually strike the surface, so they must be moving towards the surface beforehand.

5.1.1 ρ Relation to α and γ

ρ is related to α and γ by using the fact that the number of phonons that are reflected and scattered are conserved. We equate the number of phonons about to strike the surface that will not reflect and scatter with the number of phonons that have just left the surface that were reflected or scattered. Therefore the conservation of particles can be written as a flux entering and exiting the surface,

$$-\int\limits_{n_k\nu_k<0} \alpha c n_k\nu_k f\left(k_i\right) d\Omega = \int\limits_{n_k\nu_k>0} \gamma\alpha c n_k\nu_k f\left(k_i - 2k_k\nu_k\nu_i\right) d\Omega + \int\limits_{n_k\nu_k>0} c n_k\nu_k \frac{\rho}{c}\left[\int\limits_{n_k\nu_k<0} c\left(-n_k'\nu_k\right) f(k_i')d\Omega'\right] d\Omega \quad . \tag{5.2}$$

An important simplification involves breaking f up into its even and odd parts with respect to $n_k\nu_k$, such that

$$f_{Even}\left(k_i - 2k_k\nu_k\nu_i\right) = f_{Even}\left(k_i\right) \text{ and} \tag{5.3a}$$

$$f_{Odd}\left(k_i - 2k_k\nu_k\nu_i\right) = -f_{Odd}\left(k_i\right) \quad . \tag{5.3b}$$

When multiplied by $n_k\nu_k$ and integrated over all space, the even and odd functions have the following property[4]

$$\int\limits_{n_k\nu_k} n_k\nu_k f_{even}\left(k_i\right) d\Omega = 0 \text{ and} \tag{5.4a}$$

$$\int\limits_{n_k\nu_k} n_k\nu_k f_{odd}\left(k_i\right) d\Omega = \frac{1}{2}\int\limits_{n_k\nu_k>0} n_k\nu_k f_{odd}\left(k_i\right) d\Omega = \frac{1}{2}\int\limits_{n_k\nu_k<0} n_k\nu_k f_{odd}\left(k_i\right) d\Omega \quad , \tag{5.4b}$$

where $\int\limits_{n_k\nu_k}$ denotes an integral bound over all values of $n_k\nu_k$.

Breaking equation (5.2) into even and odd parts yields

$$\begin{aligned} &-\int\limits_{n_k\nu_k<0} \alpha c n_k\nu_k f_{Odd}\left(k_i\right) d\Omega - \int\limits_{n_k\nu_k<0} \alpha c n_k\nu_k f_{Even}\left(k_i\right) d\Omega = \\ &\qquad \int\limits_{n_k\nu_k>0} \gamma\alpha c n_k\nu_k f_{Odd}\left(k_i - 2k_k\nu_k\nu_i\right) d\Omega + \int\limits_{n_k\nu_k>0} \gamma\alpha c n_k\nu_k f_{Even}\left(k_i - 2k_k\nu_k\nu_i\right) d\Omega \\ &+ \int\limits_{n_k\nu_k>0} c n_k\nu_k \frac{\rho}{c}\left[\int\limits_{n_k\nu_k<0} c\left(-n_k'\nu_k\right) f_{Odd}\left(k_i'\right) d\Omega'\right] d\Omega + \int\limits_{n_k\nu_k>0} c n_k\nu_k \frac{\rho}{c}\left[\int\limits_{n_k\nu_k<0} c\left(-n_k'\nu_k\right) f_{Even}\left(k_i'\right) d\Omega'\right] d\Omega \quad . \end{aligned} \tag{5.5}$$

[4] It is important to realize that since $n_k\nu_k$ is itself an odd function $n_k\nu_k f_{Even}$ is an odd function and $n_k\nu_k f_{Odd}$ is an even function.

Using the properties of equation (5.4) we simplify equation (5.5) to,

$$-\alpha\left(\frac{1}{2}\int\limits_{n_k\nu_k} cn_k\nu_k f_{Odd}\left(k_i\right)d\Omega + \int\limits_{n_k\nu_k<0} cn_k\nu_k f_{Even}\left(k_i\right)d\Omega\right) =$$
$$-\gamma\alpha\left(\frac{1}{2}\int\limits_{n_k\nu_k} cn_k\nu_k f_{Odd}\left(k_i\right)d\Omega + \int\limits_{n_k\nu_k<0} cn_k\nu_k f_{Even}\left(k_i\right)d\Omega\right) -$$
$$\rho\pi\left(\frac{1}{2}\int\limits_{n_k\nu_k} cn_k\nu_k f_{Odd}\left(k_i\right)d\Omega + \int\limits_{n_k\nu_k<0} cn_k\nu_k f_{Even}\left(k_i\right)d\Omega\right) \quad . \tag{5.6}$$

The integral terms are now all the same, so they can be factored out, yielding the identity

$$\rho = \frac{\alpha\left(1-\gamma\right)}{\pi} \quad . \tag{5.7}$$

5.1.2 β Relation to α

The relation between β and α is determined by considering the case when the boundary is in equilibrium with the bulk phonon gas (i.e. $T = T_s$). We evaluate β by replacing all distribution functions in equation (5.1) with Bose distributions centered on T_s,

$$f_{Bose}\left(T_s,k\right) = \beta f_{Bose}\left(T_s,k\right) + \gamma\alpha f_{Bose}\left(T_s,k\right) + \frac{\rho}{c}\int\limits_{k_i\vartheta_i<0} c(-n_k\nu_k) f_{Bose}\left(T_s,k\right)d\Omega \quad , \tag{5.8}$$

which when combined with equation (5.7) reduces to

$$\beta = 1-\alpha \quad . \tag{5.9}$$

Equations (5.7) and (5.9) reduce the four parameters to two independent ones. With this information, it is now possible to fully define the distribution function $\bar{f}$.

5.2 Explicit Form of the Linearized Distribution Function for $\bar{f}$

The Grad closure method for the moment equations yields a linearized distribution function that is constructed from the state variables, namely $f = f(T, u_{i_1}...u_{\langle i_1....i_n\rangle})$ in equation (4.40). Therefore an explicit form of $\bar{f}$ can be determined by integrating the scattering term

$$\rho\pi\bar{f}_{scatter} = \frac{\rho}{c}\int\limits_{k_i\nu_i<0} c\left(-n_k\nu_k\right) f\left(k_k\right)d\Omega \quad . \tag{5.10}$$

We start by substituting in equation (4.40) and make some trivial simplifications

$$\rho\pi\bar{f}_{scatter} =$$

$$-\rho \int\limits_{n_k\nu_k<0} n_k\nu_k \left(f_{Bose} + \frac{k_B T}{\hbar c}\frac{\partial f_{Bose}}{\partial k}\left(\sum_{n=1}^{\infty} \frac{15\prod_{j=0}^{n}(2j+1)}{16n!}\frac{c^5\hbar^4}{y\left(\pi k_B T\right)^5} u_{\langle i_1\ldots i_n\rangle}\frac{k_{<i_1}\ldots k_{i_n>}}{k^{n-1}} \right) \right) d\Omega \quad . \tag{5.11}$$

For simplification we define a term, J_n

$$J_n = \frac{15\prod_{j=0}^{n}(2j+1)}{\pi^4 n!} \quad , \tag{5.12}$$

and the term H

$$H = \frac{c^5\hbar^4}{16\pi y\left(k_B T\right)^5} \tag{5.13}$$

We replace k_i with its magnitude, k, and direction vector, n_i, where in polar coordinates

$$n_i = \{\sin\theta\cos\phi, \sin\theta\sin\phi, \cos\theta\ \} \quad . \tag{5.14}$$

Since the integral is only over direction, we can remove all isotropic functions (such as f_{Bose}) from the integral and move k outside the integral as well.

$$\rho\pi\bar{f}_{scatter} = -\rho f_{Bose} \int\limits_{n_k\nu_k<0} n_k\nu_k d\Omega + \rho\pi\frac{k_B T}{\hbar c}\frac{\partial f_{Bose}}{\partial k} k \sum_{n=1}^{\infty}\left(H J_n \left(\frac{-1}{\pi}\right) \int\limits_{n_k\nu_k<0} u_{\langle i_1\ldots i_n\rangle} n_{\langle i_1\ldots i_n\rangle} n_k\nu_k d\Omega \right) \quad , \tag{5.15}$$

where $n_{\langle i_1\ldots i_n\rangle}$ is simply the trace free part of $n_{i_1}n_{i_2}\ldots n_{i_n}$. The factor $\frac{-1}{\pi}$ is inserted to simplify future constants. Another important simplification is that $n_{\langle i_1\ldots i_n\rangle}$ which we will call the trace free direction tensor can actually be simplified to $n_{i_1}n_{i_2}\ldots n_{i_n}$, which we will denote $n_{i_1\ldots i_n}$, because of the property

$$u_{\langle i_1\ldots i_n\rangle} n_{\langle i_1\ldots i_n\rangle} = u_{\langle i_1\ldots i_n\rangle} n_{i_1\ldots i_n} \quad , \tag{5.16}$$

which is true for any product of trace free tensors.

We can now focus on a general pattern for determining the scattering term integral over the direction tensor. This can be simplified by splitting up the direction tensor into its normal (to the wall) and tangential parts. With the wall normal already defined as ν_i, we simplify our problem by assuming ν_i points in the z direction,

$$v_i = \{0, 0, 1\} \quad . \tag{5.17}$$

This allows us to define the normal scaler as

$$\nu = n_i \nu_i = \cos\theta \quad . \tag{5.18}$$

We also define the tangential vector as a two dimensional vector, which is denoted with a capitalized subscript

$$\tau_A = \{\sin\theta\cos\phi, \sin\theta\sin\phi\} \quad . \tag{5.19}$$

Finally this allows us to break up the scalar product $u_{\langle i_1 \ldots i_n \rangle} n_{i_1 \ldots i_n}$ into tangential and normal parts of $u_{\langle i_1 \ldots i_n \rangle}$. For simplicity, $u_{\langle i_1 \ldots i_n \rangle}$ is broken up into several submatrices by using a mixture of capitalized subscipts and v subscripts. In the rank 2 case

$$u_{\langle\, ij \rangle} = \begin{bmatrix} u_{\langle AB \rangle} & u_{\langle \nu A \rangle} \\ u_{\langle A \nu \rangle} & u_{\langle \nu\nu \rangle} \end{bmatrix}$$

such that $u_{\langle AB \rangle}$ is the fully normal part of $u_{\langle ij \rangle}$ and would hence be a two by two tensor. The other parts of $u_{\langle\, ij \rangle}$ are $u_{\langle A\nu \rangle}$ and $u_{\langle \nu A \rangle}$ which are the tangential normal and normal tangential parts respectively (and each two dimensional vectors). The last component is the fully normal part $u_{\langle \nu\nu \rangle}$ which would be a scalar. This can be generalized to higher rank tensors such that $u_{\langle AB\nu \rangle}$ is the "tangential tangential normal" part of $u_{\langle ijk \rangle}$, etc. Note that the trace free brackets indicate that u is trace free in all three indices. It is not trace free in two indices. For example

$$u_{\langle AA \rangle} \neq 0 \text{ but} \tag{5.20a}$$

$$u_{\langle AA \rangle} + u_{\langle \nu\nu \rangle} = 0 \quad . \tag{5.20b}$$

Using these definitions and the symmetry of u and n,

$$u_{\langle ij \rangle} n_{ij} = u_{\langle AB \rangle} \tau_A \tau_B + 2 u_{\langle A\nu \rangle} \tau_A \nu + u_{\langle \nu\nu \rangle} \nu\nu \quad . \tag{5.21}$$

This can be generalized for any order of u with the equation

$$u_{\langle i_1 \ldots i_n \rangle} n_{i_1 \ldots i_n} = \sum_{r=0}^{n} \chi_r^n u_{\langle A_1 \ldots A_r \nu_1 \ldots \nu_{n-r} \rangle} \tau_{A_1} \ldots \tau_{A_r} \nu^{n-r} \quad . \tag{5.22}$$

where χ_r^n are the components of Pascal's triangle,

$$\chi_r^n = \frac{n!}{r!(n-r)!} \quad . \tag{5.23}$$

The integral in equation (5.15) can now be analyzed. Since $u_{\langle A_1 \ldots A_r v_1 \ldots \nu_{n-r} \rangle}$ and χ_r^n are both independent of direction, they can be moved outside the integral, which leaves

$$\left(\frac{-1}{\pi}\right) \int\limits_{n_k \nu_k < 0} u_{\langle i_1 \ldots i_n \rangle} n_{\langle i_1 \ldots i_n \rangle} n_k \nu_k d\Omega = \sum_{r=0}^{n} \chi_r^n u_{\langle A_1 \ldots A_r v_1 \ldots \nu_{n-r} \rangle} \left(\frac{-1}{\pi}\right) \int\limits_{\nu<0} \tau_{A_1} \ldots \tau_{A_r} \nu^{n-r+1} d\Omega \ . \tag{5.24}$$

Note that $n_k \nu_k$ is simply ν and was incorporated into the equation above. We compute this new integral by using the property that the normal tensor is symmetric in all indices, which means that the integral must be a scalar multiplied by a fully symmetric set of two dimensional Kronecker delta functions

$$\frac{-1}{\pi} \int\limits_{\nu<0} \tau_{A_1} \ldots \tau_{A_r} \nu^{n-r+1} d\Omega = \begin{cases} \sigma_r^n \delta_{\{A_1 \ldots A_r\}} & \text{, r even} \\ 0 & \text{, r odd} \end{cases} \tag{5.25}$$

where $\delta_{\{A_1 \ldots A_r\}}$ is the sum of all combinations of Kronecker deltas in a fully symmetric tensor. For example

$$\begin{aligned} \delta_{\{AB\}} &= \delta_{AB} \\ \delta_{\{ABCD\}} &= \delta_{AB}\delta_{CD} + \delta_{AC}\delta_{BD} + \delta_{AD}\delta_{BC} \end{aligned} \tag{5.26}$$

In equation (5.26) if any two indices are switched the answer remains the same, so they are fully symmetric. For any $\delta_{\{A_1 \ldots A_r\}}$, there are $(r-1)!!$ terms. Note that r is always even. Indeed, σ_r^n must be zero if r is odd because there would be an integration of an odd number of sine or cosine functions over the domain 2π in the ϕ direction.

σ_r^n can be determined by taking the full trace (i.e. contracting all 2-D indices) of both sides of equation (5.25). We determine the full trace of a set of fully symmetric delta functions by first taking the trace over two indices and determining

$$\delta_{\{A_1 \ldots A_{r-1} A_r\}} \delta_{A_{r-1} A_r} = \delta_{\{A_1 \ldots A_{r-1} A_{r-1}\}} = (r - 2 + \delta_{AA})\, \delta_{\{A_1 \ldots A_{r-2}\}} = r \delta_{\{A_1 \ldots A_{r-2}\}} \quad , \tag{5.27}$$

since the trace of a two dimensional delta function is 2. By continously applying equation (5.27) until all indices are contracted we find that

$$\text{full trace} \left(\delta_{\{A_1 \ldots A_r\}}\right) = r!! \quad , \tag{5.28}$$

where !! denotes the double factorial, defined by

$$r!! = \begin{cases} \prod_{i=1}^{r} 2i & \text{, r even} \\ \prod_{i=1}^{r} (2i-1) & \text{, r odd} \\ 1 & \text{, 0} \end{cases} \tag{5.29}$$

The full trace of the other side is computed by first determining $\tau_A \tau_A$,

$$\tau_A \tau_A = \sin^2\theta \cos^2\phi + \sin^2\theta \sin^2\phi = \sin^2\theta \quad . \tag{5.30}$$

Thus the full trace is simply $\sin^r\theta$. σ_r^n is determined by solving the full trace of equation (5.25)

$$\sigma_r^n = \begin{cases} \frac{-1}{\pi r!!} \int\limits_{\cos\theta<0} \sin^r\theta \cos^{n-r+1}\theta d\Omega & \text{, r even} \\ 0 & \text{, r odd} \end{cases} , \tag{5.31}$$

which can be simplified to

$$\sigma_r^n = \begin{cases} \frac{(-1)^{n-r}\left(\frac{n-r}{2}\right)!\left(\frac{r}{2}\right)!}{r!!\left(1+\frac{n}{2}\right)!} & \text{, r even} \\ 0 & \text{, r odd} \end{cases} . \tag{5.32}$$

A solution for σ_r^n allows equation (5.24) to be solved

$$\sum_{r=0}^{n} \chi_r^n u_{\langle A_1 \ldots A_r \nu_1 \ldots \nu_{n-r}\rangle} \left(\frac{-1}{\pi}\right) \int\limits_{\nu<0} \tau_{A_1} \ldots \tau_{A_r} \nu^{n-r+1} d\Omega = \sum_{r=0}^{n} \chi_r^n u_{\langle A_1 \ldots A_r \nu_1 \ldots \nu_{n-r}\rangle} \sigma_r^n \delta_{\{A_1 \ldots A_r\}} \quad . \tag{5.33}$$

We contract the fully symmetric delta function with $u_{\langle A_1 \ldots A_r \nu_1 \ldots \nu_{n-r}\rangle}$ using the properties that there are $(r-1)!!$ terms in the delta function and that u is fully symmetric

$$u_{\langle A_1 \ldots A_r \nu_1 \ldots \nu_{n-r}\rangle} \delta_{(A_1 \ldots A_r)} = Z_r u_{\left\langle A_1 A_1 A_2 A_2 \ldots A_{\frac{r}{2}} A_{\frac{r}{2}} \nu_1 \ldots \nu_{n-r}\right\rangle} \tag{5.34}$$

where $Z_r = (r-1)!!$. Since u is trace free in all directions in three dimensions $u_{\left\langle A_1 A_1 A_2 A_2 \ldots A_{\frac{r}{2}} A_{\frac{r}{2}} \nu_1 \ldots \nu_{n-r}\right\rangle}$ can be simplified by equating its trace in any direction to zero. For example for $u_{\langle ij\rangle}$ we know that

$$u_{\langle ii\rangle} = 0 = u_{\langle AA\rangle} + u_{\langle \nu\nu\rangle} \Rightarrow u_{\langle AA\rangle} = -u_{\langle \nu\nu\rangle} \quad . \tag{5.35}$$

This is true for any two indices so that in general

$$u_{\left\langle A_1 A_1 A_2 A_2 \ldots A_{\frac{r}{2}} A_{\frac{r}{2}} \nu_1 \ldots \nu_{n-r}\right\rangle} = (-1)^{\frac{r}{2}} u_{\langle \nu_1 \ldots \nu_n\rangle} \quad . \tag{5.36}$$

It is important to remember that $u_{\langle\nu_1\ldots\nu_n\rangle}$ is a scalar and is the fully normal component of $u_{\langle i_1\ldots i_n\rangle}$. The result from equations (5.36) and (5.33) can be combined with equation (5.15) to determine an explicit form for $f_{scatter}$

$$\bar{f}_{scatter} = f_{Bose} + \frac{k_B T}{\hbar c}\frac{\partial f_{Bose}}{\partial k} k \sum_{n=1}^{\infty}\left(HJ_n \sum_{r=0}^{n}\left((-1)^{\frac{r}{2}}\chi_r^n \sigma_r^n Z_r u_{\langle\nu_1\ldots\nu_n\rangle}\right)\right) \quad . \tag{5.37}$$

For consistency we define

$$\bar{f}_{specular} = f\left(k_i - 2k_k\nu_k\nu_i\right) \tag{5.38}$$

and

$$\bar{f}_{thermalized} = f_{Bose}\left(T_s, k\right) \quad . \tag{5.39}$$

Finally we can express $\bar{f}$ as

$$\bar{f} = \beta\bar{f}_{thermalized} + \alpha\gamma\bar{f}_{specular} + \rho\pi\bar{f}_{scatter} \quad . \tag{5.40}$$

Using the relations determined from section 5.1 this can be further simplified to

$$\bar{f} = (1-\alpha)\,\bar{f}_{thermalized} + \alpha\gamma\bar{f}_{specular} + \alpha\,(1-\gamma)\,\bar{f}_{scatter} \quad . \tag{5.41}$$

5.3 Phonon Energy Flux Through a Boundary

The microscopic model can now be used to make macroscopic boundary conditions for the state variables of the system of moment equations. We first consider energy flux, since it must be conserved across the boundary,

$$q_k^{phonon} = \int \hbar\omega c n_k f \, d\mathbf{k} \quad . \tag{5.42}$$

The energy flux inside the boundary must be continuous with an external flux to prevent the surface from changing properties,

$$q_k^{ext}\nu_k = q_k^{phonon}\nu_k \quad . \tag{5.43}$$

To evaluate the external flux we evaluate the phonon's energy flux at the surface. We do this by breaking up the full integral into two half space integrals. One half space accounts for phonons travelling towards the wall and the other accounts for phonons travelling away from the wall. Incoming phonons have distribution

f and outgoing phonons have distribution $\bar{f}$,

$$\int_{n_k\nu_k<0} \hbar\omega c n_k \nu_k f \, d\mathbf{k} + \int_{n_k\nu_k>0} \hbar\omega c n_k \nu_k \bar{f} \, d\mathbf{k} = q_k^{ext} \nu_k \quad . \tag{5.44}$$

We then multiply equation (5.42) by ν_k, subtract it from equation (5.44) and simplify to obtain

$$\int_{n_k\nu_k>0} \hbar\omega c n_k \nu_k \bar{f} \, d\mathbf{k} = \int_{n_k\nu_k>0} \hbar\omega c n_k \nu_k f \, d\mathbf{k} \quad , \tag{5.45}$$

which is the energy boundary condition for a surface, where the temperature of the surface T_s is controlled.

5.4 General Boundary Conditions for the Moment Equations

General boundary conditions must be formed so that for an arbitrary number of moment equations there are an appropriate number of boundary conditions. The general boundary conditions can be formed by equating the moments of f with the moments of $\bar{f}$. We do this by assuming that once a phonon has just touched the wall it has the distribution $\bar{f}$ but once it moves a distance $\Delta\mathbf{x}$ into the domain its moment's fluxes are equal to the fluxes of f. We then take the limit as Δx goes to zero. This condition assures that the fluxes of f and $\bar{f}$ are the same at the wall but it does not require that the actual distributions must be equal. Essentially there is a microscopic discontinuity but all macroscopic fluxes are continuous. This boundary condition can be written as

$$\int_{n_k\nu_k>0} k n_{\langle i_1 \ldots i_n \rangle} c n_{i_{n+1}} \bar{f} \, d\mathbf{k} = \int_{n_k\nu_k>0} k n_{\langle i_1 \ldots i_n \rangle} c n_{i_{n+1}} f \, d\mathbf{k} \quad , \tag{5.46}$$

where the integrals are computed at the boundary.

5.4.1 Reduction of the General Boundary Conditions

Equation (5.46) makes one boundary condition for each moment equation for each surface in the domain. This overconstrains the system of equations by making about twice as many boundary conditions as necessary. This is because the general moment equations only have first order derivatives in $\mathbf{x}$ which means only one constant of integration is created, however equation (5.46) creates two boundary conditions for each dimension of $\mathbf{x}$.

The problem of too many boundary conditions can be reduced using an argument first put forward by Grad in gas kinetics [10], [23]. Grad first considered a special case where at a surface there was only specular reflection and the distribution in the bulk was in a local equilibrium. In this case it means β and ρ are both zero, α is one and f is a Bose distribution. This reduces the distribution function for phonons that have just interacted with the wall to

$$\bar{f} = f\left(k_i - 2k_k\nu_k\nu_i\right) \quad . \tag{5.47}$$

The boundary condition is therefore

$$\int_{n_k\nu_k>0} u_{\langle i_1\ldots i_n\rangle} c n_k\nu_k f\left(k_i - 2k_k\nu_k\nu_i\right)\, d\mathbf{k} = \int_{n_k\nu_k>0} u_{\langle i_1\ldots i_n\rangle} c n_k\nu_k f\left(k_i\right) d\mathbf{k} \quad . \tag{5.48}$$

By substitution, this simplifies to

$$\begin{aligned} \int_{\infty} u_{\langle i_1\ldots i_n\rangle} c n_k\nu_k f\left(k_i\right) d\mathbf{k} &= 0 \text{ if } u_{\langle i_1\ldots i_n\rangle} c n_k\nu_k \text{ is even in } n_k\nu_k \text{ and} & \text{(5.49a)} \\ \int_{n_k\nu_k>0} u_{\langle i_1\ldots i_n\rangle} c n_k\nu_k \left[f\left(k_i\right) - f\left(k_i - 2k_k\nu_k\nu_i\right)\right] &= 0 \text{ if } u_{\langle i_1\ldots i_n\rangle} c n_k\nu_k \text{ is odd in } n_k\nu_k. \end{aligned}$$

Grad argued that if f was even in the $n_k\nu_k$ direction which implies that $f\left(k_i\right) = f\left(k_i - 2k_k\nu_k\nu_i\right)$, the boundary conditions with even $u_{\langle i_1\ldots i_n\rangle} c n_k\nu_k$ are reduced to an identity and therefore provide no information about f. Grad argued further that if the boundary condition gave no information in the special case, then it could not be used in the general case either, so he rejected all boundary conditions with even $u_{\langle i_1\ldots i_n\rangle} c n_k\nu_k$.

5.4.2 Explicit Breakdown of the General Boundary Conditions

The boundary conditions can be further simplified in order to generate an explicit form without any integrals by using the Grad closure distribution function from equation (4.40). We first simplify equation (5.46) by cancelling out any part of $u_{\langle i_1\ldots i_n\rangle}$ that is independent of $\mathbf{k}$ as well as the constant, c, resulting in

$$\int\limits_{n_k\nu_k>0} k\left(n_{\langle\, i_1\ldots i_m\rangle}\right) n_{i_{m+1}}\nu_{i_{m+1}}\bar{f}\, d\mathbf{k} = \int\limits_{n_k\nu_k>0} k\left(n_{\,\langle i_1\ldots i_m\rangle}\right) n_{i_{m+1}}\nu_{i_{m+1}} f\, d\mathbf{k} \quad , \tag{5.50}$$

where the integral must be odd in $n_k\nu_k$ (which implies even $u_{\langle i_1\ldots i_n\rangle}$). This is more easily seen if the tensor equation is broken into tangential and normal parts using the definition of τ_A and ν from equations (5.18) and (5.19) and bring $n_k\nu_k$ into the brackets

$$\int\limits_{\nu>0} k\left(\tau_{B_1\ldots B_s}\right)\nu^{m-s+1}\bar{f}\, d\mathbf{k} = \int\limits_{\nu>0} k\left(\tau_{B_1\ldots B_s}\right)\nu^{m-s+1} f\, d\mathbf{k} \text{ for odd } m-s+1 \quad . \tag{5.51}$$

Note the use of m instead of n and B instead of A. This is simply because n and A will be used shortly to denote other indices.

The right hand side of the equation is the simpler one, so it will be simplified first. We expand the integral by substituting in the distribution function, f from equation (4.40)

$$\int\limits_{\nu>0} k\left(\tau_{B_1\ldots B_s}\right)\nu^{m-s+1} f\, d\mathbf{k} = \int\limits_{\nu>0} k\left(\tau_{B_1\ldots B_s}\right)\nu^{m-s+1} f_{Bose}\, d\mathbf{k} + \int\limits_{\nu>0} k^2\left(\tau_{B_1\ldots B_s}\right)\nu^{m-s+1}\frac{k_B T}{\hbar c}\frac{\partial f_{Bose}}{\partial k}\left(\sum_{n=1}^{N} HJ_n u_{\langle i_1\ldots i_n\rangle} n_{<i_1}\ldots n_{i_n>}\right) d\mathbf{k} \quad . \tag{5.52}$$

Using a similar argument as outlined in section 5.2 the scalar product $u_{\langle i_1\ldots i_n\rangle} n_{<i_1}\ldots n_{i_n>}$ can be broken down into a sum of tangential and normal parts

$$\int\limits_{\nu>0} k\left(\tau_{B_1\ldots B_s}\right)\nu^{m-s+1} f\, d\mathbf{k} = \int\limits_{\nu>0} k\left(\tau_{B_1\ldots B_s}\right)\nu^{m-s+1} f_{Bose}\, d\mathbf{k} + \int\limits_{\nu>0} k^2\left(\tau_{B_1\ldots B_s}\right)\nu^{m-s+1}\frac{k_B T}{\hbar c}\frac{\partial f_{Bose}}{\partial k}\left(\sum_{n=1}^{N} HJ_n \sum_{r=0}^{n}\chi_r^n u_{\langle A_1\ldots A_r v_1\ldots\nu_{n-r}\rangle}\tau_{A_1}\ldots\tau_{A_r}\nu^{n-r}\right) d\mathbf{k} \quad . \tag{5.53}$$

The integral can be split into parts dependent on k and parts dependent on the solid angle, Ω, where $d\mathbf{k}$ is $k^2 dk d\Omega$

$$\int\limits_{\nu>0} k\left(\tau_{B_1\ldots B_s}\right)\nu^{m-s+1} f\, d\mathbf{k} = \int\limits_{0}^{\infty} k^3 f_{Bose} dk \int\limits_{\nu>0}\left(\tau_{B_1\ldots B_s}\right)\nu^{m-s+1}\, d\Omega + \int\limits_{0}^{\infty} k^4\frac{k_B T}{\hbar c}\frac{\partial f_{Bose}}{\partial k}dk \int\limits_{\nu>0}\left(\tau_{B_1\ldots B_s}\right)\nu^{m-s+1}\left(\sum_{n=1}^{N} HJ_n \sum_{r=0}^{n}\chi_r^n u_{\langle A_1\ldots A_r v_1\ldots\nu_{n-r}\rangle}\tau_{A_1}\ldots\tau_{A_r}\nu^{n-r}\right) d\Omega \quad . \tag{5.54}$$

The integration over k is fairly straightfoward,

$$\int\limits_{\nu>0} k\left(\tau_{B_1\ldots B_s}\right)\nu^{m-s+1} f\, d\mathbf{k} = \frac{\pi^4}{15}\left(\frac{k_B T}{\hbar c}\right)^4 \int\limits_{\nu>0}\left(\tau_{B_1\ldots B_s}\right)\nu^{m-s+1}\, d\Omega + \frac{4\pi^4}{15}\left(\frac{k_B T}{\hbar c}\right)^5 \int\limits_{\nu>0}\left(\tau_{B_1\ldots B_s}\right)\nu^{m-s+1}\left(\sum_{n=1}^{N} HJ_n \sum_{r=0}^{n}\chi_r^n u_{\langle A_1\ldots A_r v_1\ldots\nu_{n-r}\rangle}\tau_{A_1}\ldots\tau_{A_r}\nu^{n-r}\right) d\Omega \quad . \tag{5.55}$$

The first term's integration over Ω is the same as the integration in equation (5.25) with the the boundary $\nu > 0$ rather than $v < 0$. This change in bound gives the same answer except that all terms are positive. We define ξ_r^n as

$$\xi_r^n = |\sigma_r^n| \quad . \tag{5.56}$$

The second term of equation (5.55) also reduces to a similar integral when the τ_A's and τ_B's are combined and the sums and integrals are rearranged

$$\int\limits_{\nu>0} k\left(\tau_{B_1\ldots B_s}\right)\nu^{m-s+1} f\, d\mathbf{k} = \frac{\pi^4}{15}\left(\frac{k_B T}{\hbar c}\right)^4 \xi_s^m \delta_{\{B_1\ldots B_s\}} + \frac{4\pi^4}{15}\left(\frac{k_B T}{\hbar c}\right)^5 \sum_{n=1}^{N}\sum_{r=0}^{n} H J_n \chi_r^n \xi_{r+s}^{n+m} u_{\langle A_1\ldots A_r \nu_1\ldots\nu_{n-r}\rangle}\delta_{\{A_1\ldots A_r B_1\ldots B_s\}} \quad . \tag{5.57}$$

The left hand side of the equation (5.50) can be determined in a similar way. It is first broken down into its individual terms according to Section 5.2.

$$\int\limits_{\nu>0} k\left(\tau_{B_1\ldots B_s}\right)\nu^{m-s+1}\bar{f}\, d\mathbf{k} = (1-\alpha)\int\limits_{\nu>0} k\left(\tau_{B_1\ldots B_s}\right)\nu^{m-s+1}\bar{f}_{\,thermalized} d\mathbf{k} + \gamma\alpha\int\limits_{\nu>0} k\left(\tau_{B_1\ldots B_s}\right)\nu^{m-s+1}\bar{f}_{specular}\, d\mathbf{k} + \alpha(1-\gamma)\int\limits_{\nu>0} k\left(\tau_{B_1\ldots B_s}\right)\nu^{m-s+1}\bar{f}_{scatter}\, d\mathbf{k} \; . \tag{5.58}$$

For simplicity, each term in the above equation will be determined separately, starting with $\bar{f}_{\,thermalized}$,

$$(1-\alpha)\int\limits_{\nu>0} k\left(\tau_{B_1\ldots B_s}\right)\nu^{m-s+1}\bar{f}_{\,thermalized} d\mathbf{k} = (1-\alpha)\int\limits_{\nu>0} k\left(\tau_{B_1\ldots B_s}\right)\nu^{m-s+1}\bar{f}_{\,Bose}\left(T_s,k\right) d\mathbf{k} = (1-\alpha)\frac{\pi^4}{15}\left(\frac{k_B T_s}{\hbar c}\right)^4 \xi_s^m \delta_{\{B_1\ldots B_s\}} \quad . \tag{5.59}$$

The specular reflection term can be solved by using a substitution $x_i = \{k_\tau, -k_\nu\}$,

$$\gamma\alpha\int\limits_{\nu>0} k\left(\tau_{B_1\ldots B_s}\right)\nu^{m-s+1}\bar{f}_{specular}\, d\mathbf{k} = \gamma\alpha\int\limits_{\nu>0} k\left(\tau_{B_1\ldots B_s}\right)\nu^{m-s+1} f\left(k_i - 2k_k\nu_k\nu_i\right) d\mathbf{k} = -\gamma\alpha\int\limits_{\nu<0} x\left(\tau_{B_1\ldots B_s}\right)\nu^{m-s+1} f\left(x_i\right) d\mathbf{x} \quad . \tag{5.60}$$

The negative sign is a result of the fact that $m-s+1$ is always odd. The result is an integration just like the right hand side of equation (5.50) except over $\nu < 0$,

$$\gamma\alpha\int\limits_{\nu>0} k\left(\tau_{B_1\ldots B_s}\right)\nu^{m-s+1}\bar{f}_{specular}\, d\mathbf{k} = \gamma\alpha\frac{\pi^4}{15}\left(\frac{k_B T}{\hbar c}\right)^4 \sigma_s^m \delta_{\{B_1\ldots B_s\}} + \gamma\alpha\frac{4\pi^4}{15}\left(\frac{k_B T}{\hbar c}\right)^5 \sum_{n=1}^{N}\sum_{r=0}^{n} H J_n \chi_r^n \sigma_{r+s}^{n+m} u_{\langle A_1\ldots A_r \nu_1\ldots\nu_{n-r}\rangle}\delta_{\{A_1\ldots A_r B_1\ldots B_s\}} \quad . \tag{5.61}$$

Since $m-s$ is always even, σ_s^m will always be equal to ξ_s^m, which is important for simplification later on

$$\gamma\alpha \int\limits_{\nu>0} k\left(\tau_{B_1\ldots B_s}\right)\nu^{m-s+1}\bar{f}_{specular}\,d\mathbf{k} = \gamma\alpha\frac{\pi^4}{15}\left(\frac{k_BT}{\hbar c}\right)^4\xi_s^m\delta_{\{B_1\ldots B_s\}} + \gamma\alpha\frac{4\pi^4}{15}\left(\frac{k_BT}{\hbar c}\right)^5\sum_{n=1}^{N}\sum_{r=0}^{n}HJ_n\chi_r^n\sigma_{r+s}^{n+m}u_{\langle A_1\ldots A_rv_1\ldots\nu_{n-r}\rangle}\delta_{\{A_1\ldots A_rB_1\ldots B_s\}} \quad . \quad (5.62)$$

Although $f_{scatter}$ is a complicated term, it is simple to integrate because it is independent of Ω,

$$\alpha\left(1-\gamma\right)\int\limits_{\nu>0} k\left(\tau_{B_1\ldots B_s}\right)\nu^{m-s+1}\bar{f}_{scatter}\,d\mathbf{k} = \alpha\left(1-\gamma\right)\frac{\pi^4}{15}\left(\frac{k_BT}{\hbar c}\right)^4\xi_s^m\delta_{\{B_1\ldots B_s\}} + \alpha\left(1-\gamma\right)\frac{4\pi^4}{15}\left(\frac{k_BT}{\hbar c}\right)^5\left(\sum_{n=1}^{N}\sum_{r=0}^{n}HJ_n\left(-1\right)^{\frac{r}{2}}\chi_r^n\sigma_r^nZ_ru_{\langle\nu_1\ldots\nu_n\rangle}\right)\xi_s^m\delta_{\{B_1\ldots B_s\}} \quad . \quad (5.63)$$

Combining all terms results in the generalized boundary condition

$$\begin{aligned}&\left(1-\alpha\right)\frac{\pi^4}{15}\left(\frac{k_BT_s}{\hbar c}\right)^4\xi_s^m\delta_{\{B_1\ldots B_s\}} + \gamma\alpha\frac{\pi^4}{15}\left(\frac{k_BT}{\hbar c}\right)^4\xi_s^m\delta_{\{B_1\ldots B_s\}} + \alpha\left(1-\gamma\right)\frac{\pi^4}{15}\left(\frac{k_BT}{\hbar c}\right)^4\xi_s^m\delta_{\{B_1\ldots B_s\}}\\ &\quad+\gamma\alpha\frac{4\pi^4}{15}\left(\frac{k_BT}{\hbar c}\right)^5\sum_{n=1}^{N}\sum_{r=0}^{n}HJ_n\chi_r^n\sigma_{r+s}^{n+m}u_{\langle A_1\ldots A_rv_1\ldots\nu_{n-r}\rangle}\delta_{\{A_1\ldots A_rB_1\ldots B_s\}}\\ &\quad+\alpha\left(1-\gamma\right)\frac{4\pi^4}{15}\left(\frac{k_BT}{\hbar c}\right)^5\left(\sum_{n=1}^{N}\sum_{r=0}^{n}HJ_n\left(-1\right)^{\frac{r}{2}}\chi_r^n\sigma_r^nZ_ru_{\langle\nu_1\ldots\nu_n\rangle}\right)\xi_s^m\delta_{\{B_1\ldots B_s\}}\\ &=\frac{\pi^4}{15}\left(\frac{k_BT}{\hbar c}\right)^4\xi_s^m\delta_{\{B_1\ldots B_s\}}+\frac{4\pi^4}{15}\left(\frac{k_BT}{\hbar c}\right)^5\sum_{n=1}^{N}\sum_{r=0}^{n}HJ_n\chi_r^n\xi_{r+s}^{n+m}u_{\langle A_1\ldots A_rv_1\ldots\nu_{n-r}\rangle}\delta_{\{A_1\ldots A_rB_1\ldots B_s\}} \quad . \quad (5.64)\end{aligned}$$

Finally, this equation can be simplified by collecting like terms and cancelling common multiples

$$\begin{aligned}&\left[\left(1-\alpha\right)\left(T_s^4-T^4\right)+\alpha\left(1-\gamma\right)\frac{c^4\hbar^3}{4\pi yk_B^4}\sum_{n=1}^{N}\sum_{r=0}^{n}\left(J_n\left(-1\right)^{\frac{r}{2}}\chi_r^n\sigma_r^nZ_ru_{\langle\nu_1\ldots\nu_n\rangle}\right)\right]\xi_s^m\delta_{\{B_1\ldots B_s\}}\\ &\quad+\frac{c^4\hbar^3}{4\pi yk_B^4}\sum_{n=1}^{N}\sum_{r=0}^{n}J_n\chi_r^n\left(\gamma\alpha\sigma_{r+s}^{n+m}-\xi_{r+s}^{n+m}\right)u_{\langle A_1\ldots A_rv_1\ldots\nu_{n-r}\rangle}\delta_{\{A_1\ldots A_rB_1\ldots B_s\}}=0 \quad . \quad (5.65)\end{aligned}$$

Although the general boundary condition seems quite cumbersome, in its current presentation it is an explicit equation without any integration that provides sufficient boundary conditions for an arbitrary number of moments in three dimensions.

6 Summary of Equations Used For Further Analysis

6.1 Summary of Assumptions

For the most part, the theory presented previously has been fairly general in nature. However, a number of assumptions were necessary to arrive to the general equations that have been presented, and it is important that those assumptions are clear before interpreting results.

The first assumption is that phonons have a linear dispersion (i.e. $\omega = ck$) and an infinite Brillioun zone. This is assumption is used to linearize the left hand side of the phonon Boltzmann equation and was shown to have little relative error if the temperature of the material in question was less than or equal to approximately 0.6 of the material's Debye temperature.

The next assumption was the gray matter Callaway model. This assumption is necessary for linearizing the right hand side of the phonon Boltzmann equation and assumes that phonons have the same collision frequency regardless of wavenumber. Since this research is a first step, the gray matter assumption was used because of its simplicity, however it is recommended that wavenumber dependent collisions be examined in the future.

Finally, the microscopic boundary conditions were developed simply by thinking about what a phonon could possibly do when it interacted with a boundary and how that could be modeled in both a general and mathematically simple way, with the end goal of providing fitting coefficients that could be used to match experimental results and hopefully become predictive.

The bulk equations used in this report are derived from Grad's closure method, using the Callaway model for the collision term. We start with equation (4.36), the general balance equation. The first two moments (energy and momentum) have already been derived in Section 4.4:

$$\begin{aligned} \frac{\partial e}{\partial t} + c^2 \frac{\partial p_i}{\partial x_i} &= 0 \\ \frac{\partial p_j}{\partial t} + \frac{1}{3}\frac{\partial e}{\partial x_j} + c\frac{\partial N_{\langle ij \rangle}}{\partial x_i} &= -\frac{1}{\tau_R} p_j \end{aligned}$$

With the general equation for all higher order moments

$$\frac{\partial u_{\langle i_1 \ldots i_n \rangle}}{\partial t} + c\frac{n}{2n+1}\frac{\partial u_{<<i_1 \ldots i_{n-1}>}}{\partial x_{i_n>}} + c\frac{\partial u_{\langle i_1 \ldots i_n k \rangle}}{\partial x_k} = \frac{1}{\tau} u_{\langle i_1 \ldots i_n \rangle};\ n = 1, \ldots, N \quad , \tag{6.1}$$

where $u_{\langle i_1 \ldots i_N k \rangle} = 0$.

6.2 Dimensionless Form

6.2.1 Bulk Equations

A dimensionless form of the equations requires few steps because the moments, $u_{\langle i_1 \ldots i_n \rangle}$ all have the same dimension as p_i. The only variable with a different dimension is the energy e. For ease of notation, we define E as

$$E \equiv \frac{e}{c} \quad . \tag{6.2}$$

While τ has already been defined as the average time between two phonon collisions, we define the mean free path λ as the average distance a particle travels between collisions. λ is related to τ by the Debye velocity, c

$$\lambda = c\tau \quad . \tag{6.3}$$

Dimensionless length is defined using a characteristic length scale L,

$$\hat{x} \equiv \frac{x}{L} \quad . \tag{6.4}$$

Dimensionless time is also defined using L and the speed of sound,

$$\hat{t} \equiv \frac{tc}{L} \quad . \tag{6.5}$$

All of the moments have the same unit and every term in the moment equations have one moment in them, so the equations could be made dimensionless using any constant without having any ramifications, however it is useful to relate the moments to temperauture, especially since temperature is in the boundary conditions. Therefore using the T^4 relation to e from equation (3.28) and remembering that $u_{\langle i_1 \ldots i_n \rangle}$ has the dimensions of $\frac{e}{c}$ results in a useful dimensionless form

$$\hat{u}_{\langle i_1 \ldots i_n \rangle} = u_{\langle i_1 \ldots i_n \rangle} \left(\frac{4\pi y k_B^4}{\hbar^3} \frac{T_o^4}{c^4} \right)^{-1} \quad , \tag{6.6}$$

where T_o is a relevant temperature in the model, such as a surface temperature or possibly the Debye temperature. This equation applies for p_i and E as well.

Finally, we define the Knudsen number, Kn

$$Kn \equiv \frac{L}{\lambda} = \frac{L}{c\tau} \quad . \tag{6.7}$$

Equation 4.46 is made non-dimensional by dividing by c, multiplying by L and by non-dimensionalizing the moments using equation 6.6. Using the above definition results in the following system of equations

$$\begin{aligned}
\frac{\partial \hat{E}}{\partial \hat{t}} + \frac{\partial \hat{p}_i}{\partial \hat{x}_i} &= 0 \\
\frac{\partial \hat{p}_j}{\partial \hat{t}} + \frac{1}{3}\frac{\partial \hat{E}}{\partial \hat{x}_j} + \frac{\partial \hat{N}_{\langle ij \rangle}}{\partial \hat{x}_i} &= -\frac{1}{Kn_R}\hat{p}_j \\
\frac{\partial \hat{u}_{\langle i_1 \ldots i_n \rangle}}{\partial \hat{t}} + \frac{n}{2n+1}\frac{\partial \hat{u}_{<<i_1 \ldots i_{n-1}>}}{\partial \hat{x}_{i_n>}} + \frac{\partial \hat{u}_{\langle i_1 \ldots i_n k \rangle}}{\partial \hat{x}_k} &= -\frac{1}{Kn}\hat{u}_{\langle i_1 \ldots i_n \rangle}; \quad n = 1, ..., N \quad ,
\end{aligned} \tag{6.8}$$

where $Kn_R = \frac{L}{c\tau_R}$ and $\hat{u}_{\langle i_1 \ldots i_N k \rangle} = 0$. Finally, it is useful to present the equations in a general 3-D matrix form where the vector[5] $\hat{\mathbf{u}}_\alpha$ represents all of the moments such that

$$\hat{\mathbf{u}}_\alpha = \left\{ \hat{E}, \hat{p}_i, \hat{u}_{\langle ij \rangle}, ..., \hat{u}_{\langle i_1 \ldots i_n \rangle} \right\}_\alpha \quad . \tag{6.9}$$

The entire system of moment equations can thus be represented in the matrix form

$$\frac{\partial \hat{\mathbf{u}}_\alpha}{\partial \hat{t}} + \mathbf{A}_{\alpha\beta}\frac{\partial \hat{\mathbf{u}}_\beta}{\partial \hat{x}} + \mathbf{B}_{\alpha\beta}\frac{\partial \hat{\mathbf{u}}_\beta}{\partial \hat{y}} + \mathbf{C}_{\alpha\beta}\frac{\partial \hat{\mathbf{u}}_\beta}{\partial \hat{z}} = -\mathbf{P}_{\alpha\beta}\hat{\mathbf{u}}_\beta \quad . \tag{6.10}$$

The expanded equations in three dimensions up to $\hat{u}_{\langle ijkl \rangle}$ (i.e. 25 independent moments in 3-D) are presented in Appendix B.

6.2.2 Boundary Conditions

The general boundary condition shown in equation (5.65) can also be simplified using the same process. We start by dividing equation (5.65) by T_0^4,

$$\begin{aligned}
&\left[(1-\alpha)\left(\frac{T_s^4}{T_0^4} - \frac{T^4}{T_0^4} \right) + \alpha(1-\gamma)\frac{c^4\hbar^3}{4\pi y k_B^4 T_0^4} \sum_{n=1}^{N}\sum_{r=0}^{n} \left(J_n (-1)^{\frac{r}{2}} \chi_r^n \sigma_r^n Z_r u_{\langle \nu_1 \ldots \nu_n \rangle} \right) \right] \xi_s^m \delta_{\{B_1 \ldots B_s\}} \\
&\qquad + \frac{c^4\hbar^3}{4\pi y k_B^4 T_0^4} \sum_{n=1}^{N}\sum_{r=0}^{n} J_n \chi_r^n \left(\gamma\alpha\sigma_{r+s}^{n+m} - \xi_{r+s}^{n+m} \right) u_{\langle A_1 \ldots A_r \nu_1 \ldots \nu_{n-r} \rangle} \delta_{\{A_1 \ldots A_r B_1 \ldots B_s\}} = 0 \quad .
\end{aligned} \tag{6.11}$$

[5] Since latin letters have been typically used as indices for spatial vectors and tensors, we use greek indices to represent vectors representing the combined moments.

The equation is now dimensionless and is simplified by replacing $\frac{c^4\hbar^3}{4\pi y k_B^4 T_0^4} u_{\langle A_1 \ldots A_r v_1 \ldots \nu_{n-r}\rangle}$ with $\hat{u}_{\langle A_1 \ldots A_r v_1 \ldots \nu_{n-r}\rangle}$ according to equation (6.6) and $\frac{T^4}{T_0^4}$ with $\hat{T}^4$,

$$\left[(1-\alpha)\left(\hat{T}_s^4 - \hat{T}^4\right) + \alpha(1-\gamma)\sum_{n=1}^{N}\sum_{r=0}^{n}\left(J_n(-1)^{\frac{r}{2}}\chi_r^n\sigma_r^n Z_r \hat{u}_{\langle\nu_1\ldots\nu_n\rangle}\right)\right]\xi_s^m\delta_{\{B_1\ldots B_s\}} + \sum_{n=1}^{N}\sum_{r=0}^{n} J_n\chi_r^n\left(\gamma\alpha\sigma_{r+s}^{n+m} - \xi_{r+s}^{n+m}\right)\hat{u}_{\langle A_1\ldots A_r v_1\ldots\nu_{n-r}\rangle}\delta_{\{A_1\ldots A_r B_1\ldots B_s\}} = 0 \quad . \tag{6.12}$$

Although equation (6.12) is a valid dimensionless form of the boundary condition, T is not a moment variable. To simplify the equation, it is convenient to replace $\hat{T}^4$ with $\hat{E}$. Using equation (6.6) as a guide,

$$T^4 = \frac{\hbar^3c^4}{4\pi k_B^4 y}E = \frac{\hbar^3c^4}{4\pi k_B^4 y}\left(\frac{\hbar^3c^4}{4\pi k_B^4 y}\right)^{-1} T_0^4\hat{E} \quad . \tag{6.13}$$

Rearanging and cancelling terms yeilds

$$\frac{T^4}{T_0^4} = \hat{T}^4 = \hat{E} \quad . \tag{6.14}$$

Substituting into equation (6.12) results in the final dimensionless form

$$\left[(1-\alpha)\left(\hat{E}_s - \hat{E}\right) + \alpha(1-\gamma)\sum_{n=1}^{N}\sum_{r=0}^{n}\left(J_n(-1)^{\frac{r}{2}}\chi_r^n\sigma_r^n Z_r \hat{u}_{\langle\nu_1\ldots\nu_n\rangle}\right)\right]\xi_s^m\delta_{\{B_1\ldots B_s\}} + \sum_{n=1}^{N}\sum_{r=0}^{n} J_n\chi_r^n\left(\gamma\alpha\sigma_{r+s}^{n+m} - \xi_{r+s}^{n+m}\right)\hat{u}_{\langle A_1\ldots A_r v_1\ldots\nu_{n-r}\rangle}\delta_{\{A_1\ldots A_r B_1\ldots B_s\}} = 0 \quad , \tag{6.15}$$

where $\hat{E}_s$ is the dimensionless surface energy.

The expanded form of the general boundary condition is quite complex. The boundary conditions for a two dimensional system of equations up to $u_{\langle ijkl\rangle}$ in Cartesian coordinates are presented in Appendix C.

7 Discussion and Results

7.1 1-D Heat Conduction Between Parallel Plates

For a few specific geometries, analytic results can be obtained for a closed (i.e. finite) set of moment equations. A simple 1 dimensional problem that can be solved analytically is heat conduction between parallel surfaces, illustrated in Figure 7.1. A flux is introduced to a solid by establishing differing temperatures (or energies) at the two surfaces. The problem is steady state and only dependent on one direction (x in this case) because the solid is semi-infinite in the y and z directions. The problem is solved below for the 9, 16 and 25 moment cases and compared to Fourier's law in dimensionless form using the process described in Section 6.2.

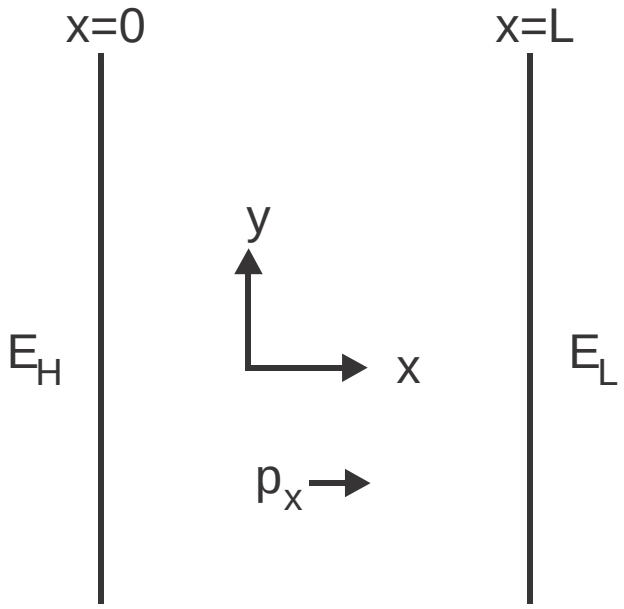

Figure 7.1: Heat conduction between parallel plates.

7.1.1 The 9 Moment Solution

Despite the large number of equations in the moment method, the properties of this problem allow for many of them to be ignored or greatly simplified. In order to compare the moment method to Fourier's law only two properties are needed, $\hat{E}$ (which is proportional to internal energy), and $\hat{p}_x$ (which is proportional to heat flux). The simplified set of equations (derived from Appendix B) with all y, z, t, and higher moment terms removed are

$$\begin{aligned} \frac{\partial \hat{p}_x}{\partial \hat{x}} &= 0 \\ \frac{1}{3}\frac{\partial \hat{E}}{\partial \hat{x}} + \frac{\partial \hat{N}_{\langle xx \rangle}}{\partial \hat{x}} &= -\frac{1}{Kn_R}\hat{p}_x \qquad (7.1a) \\ \frac{4}{15}\frac{\partial \hat{p}_x}{\partial \hat{x}} &= -\frac{1}{Kn}\hat{N}_{\langle xx \rangle} \quad . \qquad (7.1b) \end{aligned}$$

Solving for $\hat{p}_x$ yields

$$\hat{p}_x = C_1 \quad , \qquad (7.2a)$$

where C_1 is a constant of integration. This can be substituted into equation (7.1a)

$$\frac{1}{3}\frac{\partial \hat{E}}{\partial x} + \frac{\partial \hat{N}_{\langle xx \rangle}}{\partial x} = -\frac{1}{Kn_R}\hat{p}_x = -\frac{1}{Kn_R}C_1 \quad . \qquad (7.3)$$

Equation (7.1b) is used to solve for $\frac{\partial \hat{N}_{\langle xx \rangle}}{\partial x}$,

$$-\frac{1}{Kn}\hat{N}_{\langle xx \rangle} = \frac{4}{15}\frac{\partial \hat{p}_x}{\partial \hat{x}} = 0 \tag{7.4a}$$

$$\frac{\partial \hat{N}_{\langle xx \rangle}}{\partial x} = 0 \ . \tag{7.4b}$$

Substituting into equation (7.3) and solving for $\hat{E}$ yields

$$\hat{E} = -\frac{3}{Kn_R}C_1 x + C_2 \tag{7.5}$$

where C_2 is another constant of integration.

At this point, the solution is exactly the same as Fourier's law, however the boundary conditions are different. Equation C.1 is used to determine both constants of integration by applying it at either wall. For this geometry in the 9 moment case it reads

$$\hat{E} = -2\nu_x \hat{p}_x \frac{(1+\alpha)}{(1-\alpha)} + \hat{E}_s \tag{7.6}$$

where $\hat{E}_s$ is the boundary energy and ν_x is the wall normal, which in this case is 1 at $x = 0$ and -1 at $x = L$. Equation (7.6) is known as a jump condition because $\hat{E}$ is equal to $\hat{E}_s$ plus an extra term (the typical boundary condition for Fourier's law is the no slip condition, $\hat{E} = \hat{E}_s$).

Applying this boundary condition to equation (7.5) gives the full solution to the problem

$$\hat{E} = -\frac{3\left(\hat{E}_H - \hat{E}_L\right)(1-\alpha)}{3 - 3\alpha + 4Kn_R(1+\alpha)}x + \frac{2\hat{E}_H Kn_R}{3 - 3\alpha + 4Kn_R(1+\alpha)} \ . \tag{7.7}$$

Figure 7.2 shows a plot of $\hat{E}$ as a function of $\hat{x}$ for several different Knudsen numbers with $\hat{E}_H = 1.1$ at $\hat{x} = 0$ and $\hat{E}_L = 1$ at $\hat{x} = 1$. The results show a linear profile, like Fourier's law, except for jumps at the boundaries, which increase as Knudsen number increases.

The temperature jump can also be affected by changing the proportion of phonons that simply bounce off the surface (α) and the number of phonons that thermalize at the surface ($1 - \alpha$). Figure 7.3 shows the same plot except the Knudsen number remains at 0.1 and α is varied from 0 to 1. As α increases, the temperature jump also increases. Note that for $\alpha = 1$, all phonons are reflected at the surface. Therefore no energy exchange occurs and the surface is adiabatic. Accordingly, there is no temperature profile in the crystal and no heat transfer through it.

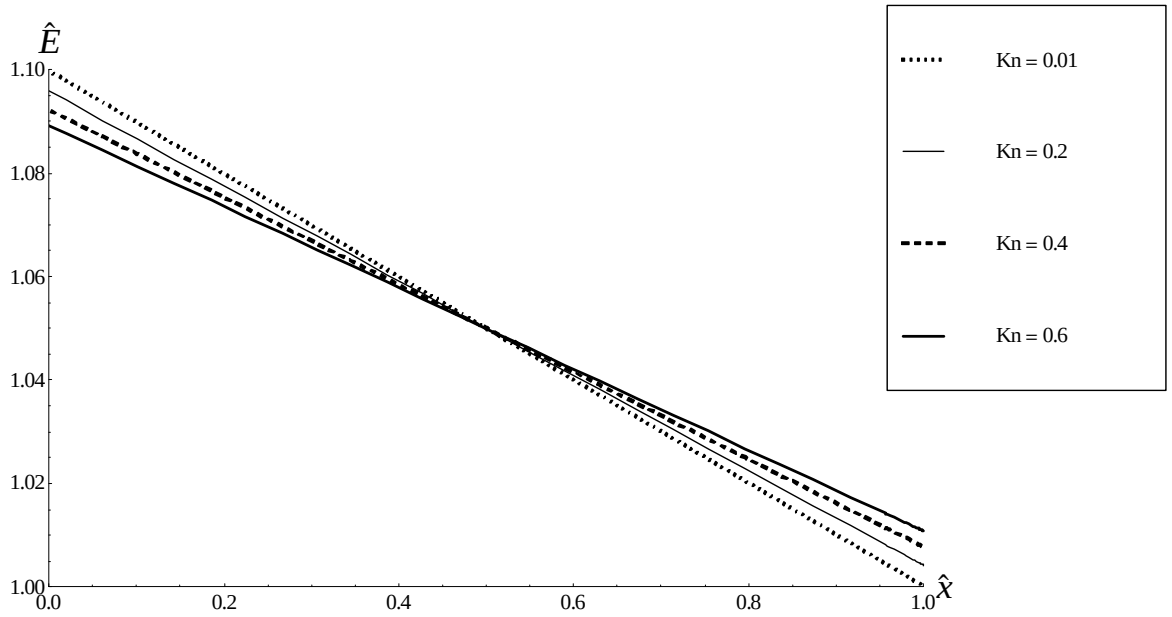

Figure 7.2: Heat conduction between two parallel surfaces for varying Knudsen number using the 9 moment equations.

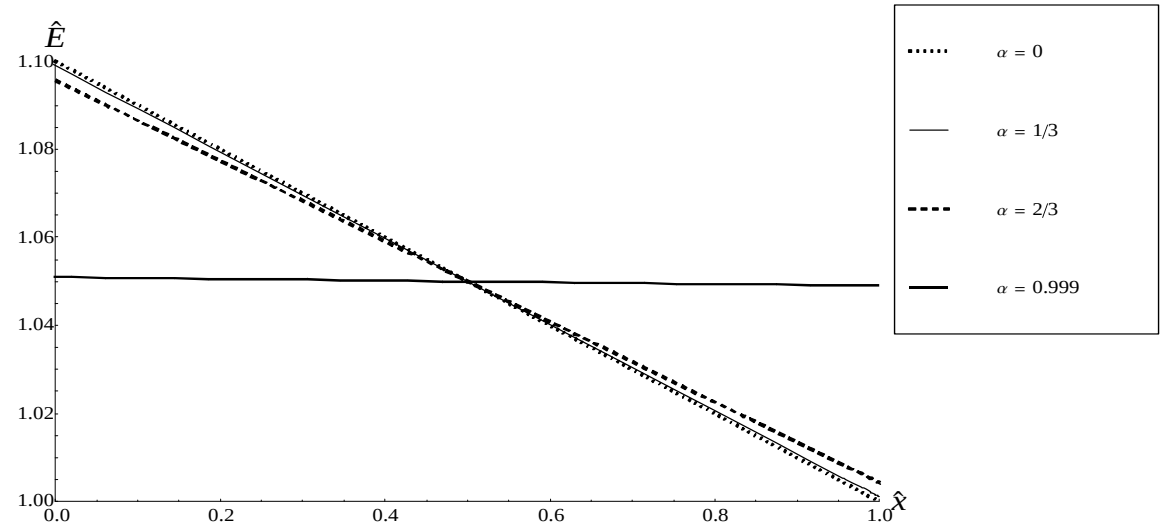

Figure 7.3: Heat conduction between parallel surfaces for varying values of α using the 9 moment equations with $Kn = 0.1$.

7.1.2 The 16 and 25 Moment Solution

The problem can be solved with more moment equations by using the same process as the 9 moment solution except more equations are needed. For the 16 moment case, in this geometry, the equations are

$$\frac{\partial \hat{p}_x}{\partial \hat{x}} = 0 \tag{7.8a}$$

$$\frac{1}{3}\frac{\partial \hat{E}}{\partial \hat{x}} + \frac{\partial \hat{N}_{\langle xx\rangle}}{\partial \hat{x}} = -\frac{1}{Kn_R}\hat{p}_x \tag{7.8b}$$

$$\frac{4}{15}\frac{\partial \hat{p}_x}{\partial \hat{x}} + \frac{\partial \hat{M}_{\langle xxx\rangle}}{\partial \hat{x}} = -\frac{1}{Kn}\hat{N}_{\langle xx\rangle} \tag{7.8c}$$

$$\frac{9}{35}\frac{\partial \hat{N}_{\langle xx\rangle}}{\partial \hat{x}} = -\frac{1}{Kn}\hat{M}_{\langle xxx\rangle} \quad . \tag{7.8d}$$

The first two equations are the same as the 9 moment case but higher moment equations need to be solved. For instance, in the 16 moment case, $\hat{M}_{\langle xxx\rangle}$ is non-zero, so now equation (7.8c) simplifies to

$$\frac{\partial \hat{M}_{\langle xxx\rangle}}{\partial x} = -\frac{1}{Kn}\hat{N}_{\langle xx\rangle} \quad . \tag{7.9}$$

The $\hat{M}_{\langle xxx\rangle}$ term requires equation (7.8d), which is simplified to

$$\frac{9}{35}\frac{\partial \hat{N}_{\langle xx\rangle}}{\partial x} = -\frac{1}{Kn}\hat{M}_{\langle xxx\rangle} \tag{7.10a}$$

$$\frac{\partial \hat{M}_{\langle xxx\rangle}}{\partial x} = -\frac{9Kn}{35}\frac{\partial^2 \hat{N}_{\langle xx\rangle}}{\partial x^2} \quad . \tag{7.10b}$$

With further back substitution, a general solution for $\hat{E}$ can be found

$$\hat{E} = -\frac{3}{Kn_R}C_1 x + C_2 + C_3 \cosh\left(\frac{1}{Kn}\frac{3}{\sqrt{35}}x\right) + C_4 \sinh\left(\frac{1}{Kn}\frac{3}{\sqrt{35}}x\right) \quad . \tag{7.11}$$

where C_1, C_2, C_3, C_4 are constants of integration which are determined using equations (C.1) and (C.3). The linear system for the constants was solved using Mathematica; the resulting lengthy expressions will not be shown. Curves were produced directly in Mathematica.

The 25 moment system can be solved in a similar fashion. The simplified equations for this geometry are

$$\frac{\partial \hat{p}_x}{\partial \hat{x}} = 0 \tag{7.12a}$$

$$\frac{1}{3}\frac{\partial \hat{E}}{\partial \hat{x}} + \frac{\partial \hat{N}_{\langle xx\rangle}}{\partial \hat{x}} = -\frac{1}{Kn_R}\hat{p}_x \tag{7.12b}$$

$$\frac{4}{15}\frac{\partial \hat{p}_x}{\partial \hat{x}} + \frac{\partial \hat{M}_{\langle xxx\rangle}}{\partial \hat{x}} = -\frac{1}{Kn}\hat{N}_{\langle xx\rangle} \tag{7.12c}$$

$$\frac{\partial \hat{M}_{\langle xxx\rangle}}{\partial \hat{t}} + \frac{9}{35}\frac{\partial \hat{N}_{\langle xx\rangle}}{\partial \hat{x}} + \frac{\partial \hat{R}_{\langle xxxx\rangle}}{\partial \hat{x}} = -\frac{1}{Kn}\hat{M}_{\langle xxx\rangle} \tag{7.12d}$$

$$\frac{16}{63}\frac{\partial \hat{M}_{\langle xxx\rangle}}{\partial \hat{x}} = -\frac{1}{Kn}\hat{R}_{\langle xxxx\rangle} \quad . \tag{7.12e}$$

Using the same process of substitution as the 9 and 16 moment equations results in

$$\hat{E} = -\frac{3}{Kn_R}C_1 x + C_2 + C_3 \cosh\left(\frac{1}{Kn}\sqrt{\frac{23}{45}}x\right) + C_4 \sinh\left(\frac{1}{Kn}\sqrt{\frac{23}{45}}x\right) \quad , \tag{7.13}$$

where the constants of integration are solved once again using equations (C.1) and (C.3).

To compare the results of the 9, 16 and 25 moment equations, Figure 7.4 shows a plot of $\hat{E}$ as a function of distance $\hat{x}$ for each moment equation with $\hat{E}_H = 1.1$ at $\hat{x} = 0$ and $\hat{E}_L = 1$ at $\hat{x} = 1$. In all cases, the results show a profile that looks quite linear. There is some curvature in the 16 and 25 moment solutions because of the hyperbolic sine functions, however their effect is negligible.

7.1.3 Discussion

The geometry of heat conductivity between parallel surfaces allows for a simple problem that can be solved and analyzed by the moment method and compared to Fourier's law. This can be used to get a basic understanding of what effects can occur when phonon rarefaction causes the continuum assumption to break down. Clearly, the dominant effect in this case is the temperature jump (although the equations solve for $\hat{E}$, this is proportional to temperature). Another interesting result is that the 9 moment solution is almost exactly the same as the 25 moment solution for Knudsen numbers in the range that these equations could work for (since the equations are linearized by a small Knudsen number approximation, it does not make sense to extend the solutions to cases where Knudsen number is greater than 1).

The property that could be particularly useful in design work would be an equivalent heat conductivity for a material dependent on the Knudsen number of the system. Since heat flux (which is proportional to

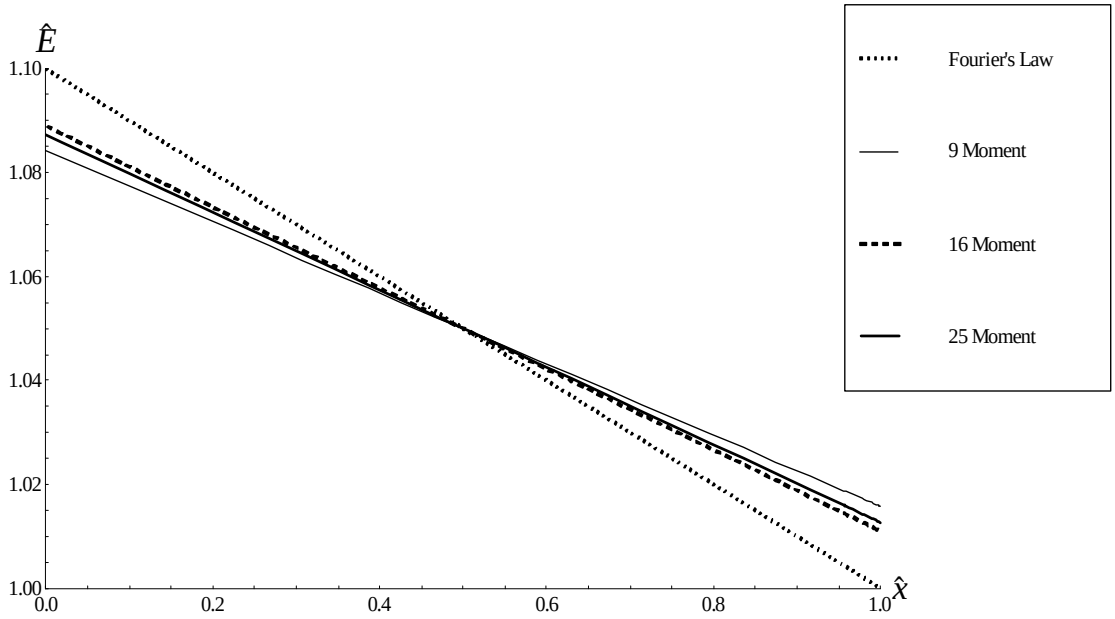

Figure 7.4: Heat conduction between parallel surfaces for various systems of equations. In all cases $Kn = 0.2$, $Kn_R = 0.4$, $\alpha = 0.5$.

p) is not necessarily proportional to the local temperature gradient in the moment method, we define heat conductivity over a finite distance

$$q_i = \kappa \frac{\Delta T}{\Delta x} \quad . \tag{7.14}$$

Since p_i is proportional to q_i an equivalent heat conductivity can be measured

$$\frac{\kappa}{\kappa_{Fourier}} = \frac{p}{p_{Fourier}} \quad . \tag{7.15}$$

Figure 7.5 shows that the equivalent heat conductivity for the moment method drops as Knudsen number gets larger. This means that for a nano-device, with similar geometry to the parallel surface problem would transfer less heat than expected by Fourier's law for a given temperature or be hotter than expected for a given heat flux. It should be noted that Figure 7.5 assumes the same proportion of resistive and normal phonon process (i.e. the ratio of Kn to Kn_R remains constant) as Kn increases (which essentially signifies a decreasing length scale). This may not be the case in typical experiment because resistive process include phonon interaction with grain boundaries, which could become less significant at smaller length scales.

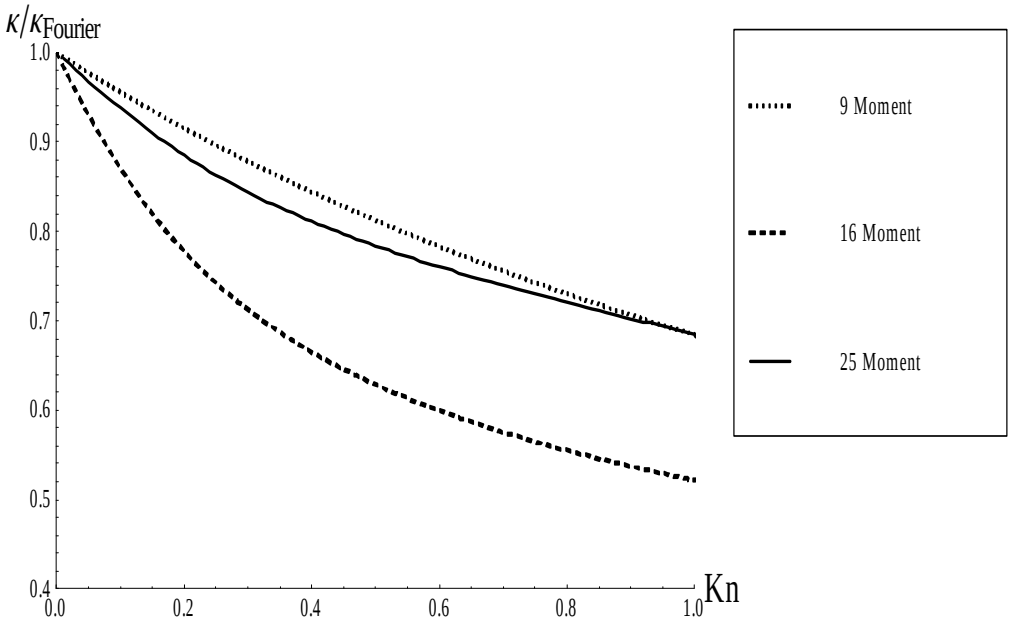

Figure 7.5: Equivalent heat conductivity compared to Fourier's law as a function of Knudsen number for the 9, 16 and 25 moment equations. In this case $Kn_R = 2Kn$, $\alpha = 0.5$ and $\gamma = 0.5$.

7.2 1-D Poiseuille Flow

Another geometric configuration with an analytic solution is a constant energy gradient in one direction in a semi-infinite solid. This is roughly analagous to Poiseuille flow in fluid mechanics. In Figure 7.6 the direction of the gradient is in the x direction and the y direction has a thickness of $2L$. We assume that the only x dependent property is the gradient of temperature such that $\frac{d\hat{E}}{d\hat{x}}$ is a constant. Since the z dimension is infinite, no properties are dependent on it. Furthermore, the process is steady state.

7.2.1 General Solution

We begin with a reduced form of equation (6.10), where t and z derivatives are elimanted,

$$A_{\alpha\beta}\frac{\partial \hat{u}_\beta}{\partial \hat{x}} + B_{\alpha\beta}\frac{\partial \hat{u}_\beta}{\partial \hat{y}} = -P_{\alpha\beta}\hat{u}_\beta \quad . \tag{7.16}$$

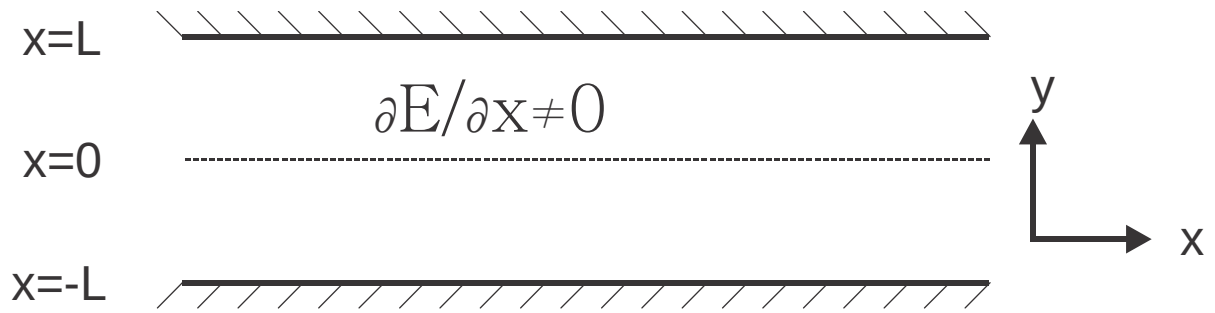

Figure 7.6: Poiseuille Flow

The only equation with an x dependent term is the moment p_x. Using the expanded moment equations in Appendix B as a starting reference and removing all terms without y dependency except for $\frac{d\hat{E}}{d\hat{x}}$ gives

$$\frac{1}{3}\frac{d\hat{E}}{d\hat{x}} + \frac{d\hat{N}_{\langle xy\rangle}}{d\hat{y}} = -\frac{1}{Kn_R}\hat{p}_x \quad . \tag{7.17}$$

We define $\tilde{p}_x$ as

$$\tilde{p}_x = \hat{p}_x + Kn_R\frac{d\hat{E}}{d\hat{x}} \quad . \tag{7.18}$$

Since $\frac{d\hat{E}}{d\hat{x}}$ is constant

$$\frac{\partial\tilde{p}_x}{\partial\hat{x}} = \frac{\partial\hat{p}_x}{\partial\hat{x}} = 0 \quad .$$

Furthermore, inspection of equation (B.1) with all non y dependencies removed leads to a trivial equation

$$\frac{\partial\hat{p}_y}{\partial\hat{y}} = 0 \quad . \tag{7.19}$$

To simplify our equations we redefine our variables such that

$$\tilde{u}_\alpha = \left\{\tilde{p}_x, \hat{u}_{\langle ij\rangle}, ..., \hat{u}_{\langle i_1...i_n\rangle}\right\} \quad . \tag{7.20}$$

Equation (7.16) can be simplified to

$$\tilde{B}_{\alpha\beta}\frac{\partial\tilde{u}_\beta}{\partial\hat{y}} = -\tilde{P}_{\alpha\beta}\tilde{u}_\beta \quad . \tag{7.21}$$

Redefining $\hat{p}_x$ to $\tilde{p}_x$ made the system of equations only dependent on y. $\tilde{P}_{\alpha\beta}$ is now an invertible matrix

because energy balance was removed from the system of equations

$$\tilde{P}_{\alpha\beta} = \begin{bmatrix} \frac{1}{Kn_R} & 0 & \cdots & 0 \\ 0 & \frac{1}{Kn} & & \vdots \\ \vdots & & \ddots & 0 \\ 0 & \cdots & 0 & \frac{1}{Kn} \end{bmatrix} \quad . \tag{7.22}$$

Therefore $\tilde{\mathbf{u}}_\alpha$ can be isolated

$$\tilde{u}_\alpha = -\tilde{P}^{-1}_{\alpha\gamma}\tilde{B}_{\gamma\beta}\frac{\partial \tilde{u}_\beta}{\partial \hat{y}} \quad . \tag{7.23}$$

This system of differential equations can be solved by diagonalizing the $P^{-1}_{ik}B_{kj}$ matrix using its eigenvectors, Q_{ij} and corresponding eigenvalues in the diagonal matrix Λ_{ij}. We define Λ_{ij} as

$$\Lambda_{\alpha\beta} \equiv \begin{bmatrix} \lambda_1 & 0 & \cdots & 0 \\ 0 & \lambda_2 & & \vdots \\ \vdots & & \ddots & 0 \\ 0 & \cdots & 0 & \lambda_n \end{bmatrix}$$

Using the substitution

$$\tilde{u}_\alpha = Q_{\alpha\beta}w_\beta \tag{7.24}$$

leads to the equation

$$w_\alpha = -Q^{-1}_{\alpha\varepsilon}\tilde{P}^{-1}_{\varepsilon\gamma}B_{\gamma\kappa}Q_{\kappa\beta}\frac{\partial w_\beta}{\partial \hat{y}} = -\Lambda_{\alpha\beta}\frac{\partial w_\beta}{\partial \hat{y}} \quad . \tag{7.25}$$

This equation is solved using the hyperbolic sine functions

$$w_\alpha = C^1_\alpha \cosh\left(-\frac{1}{\lambda_a}y\right) + C^2_\alpha \sinh\left(-\frac{1}{\lambda_a}y\right) \quad , \tag{7.26}$$

where $C^{1,2}_a$ are constants of integration. $\tilde{u}_\alpha$ can now be determined by inverting equation (7.24).

7.2.2 The 9 Moment Solution

The boundary conditions can be applied to both walls to determine the constants of integration. The process can be simplified by only solving for the variables that are useful for discussion[6]. In this case, the

[6] In general, all moments need to be solved simultaneously, however for the geometry of this problem, some of the equations decouple themselves, so they can be ignored.

most interesting variable is the momentum, because it is proportional to the heat flux. It is essential that the right number of boundary conditions are used, or the system will become overdefined. For the nine moment case, we use equation (C.2). Since $M_{\langle ijk \rangle} = 0$ in the nine moment case, this equation is simplified to

$$\hat{p}_x = -n_y \frac{8\hat{N}_{\langle xy \rangle}(1+\alpha\gamma)}{3(1-\alpha\gamma)} \quad , \tag{7.27}$$

where n_y is the wall normal direction. This boundary condition is then applied at both walls. Assuming an origin in the middle of the flow, this could be applied at $\hat{p}_x(1)$ where $n_y = -1$ and at $\hat{p}_x(-1)$ where $n_y = 1$. For the 9 moment case, the solution for $\hat{p}_x$ is

$$\hat{p}_x = -\frac{Kn_R}{3}\frac{\partial \hat{E}}{\partial x} + K_1 \cosh\left(\sqrt{\frac{5}{KnKn_R}}y\right) \quad , \tag{7.28}$$

where

$$K_1 = \frac{\frac{\partial \hat{E}}{\partial x} Kn_R}{3\cosh\left(\sqrt{\frac{5}{KnKn_R}}\right) + \sqrt{\frac{Kn}{Kn_R}}\frac{8(1+\alpha\gamma)}{3\sqrt{5}(1-\alpha\gamma)}\sinh\left(\sqrt{\frac{5}{KnKn_R}}\right)} \quad . \tag{7.29}$$

The solution for $\hat{p}_x$ is composed of two terms. The first term is what is predicted by Fourier's law. The second term is a hyperbolic cosine function that creates what is known as a Knudsen layer. The Knudsen layer is essentially a form of boundary layer caused by phonon "drag" on a boundary. This drag is caused by the scattering of phonons when they interact with the surface.

Figure 7.7 shows the profile for $\hat{p}_x$ for various Knudsen numbers. As the Knudsen number approaches zero, $\hat{p}_x$ approches plug flow at 1, which is what is predicted by Fourier's law. As Knudsen number increases, phonon scattering at the boundary becomes significant, increasing the Knudsen layer and therefore reducing $\hat{p}_x$. Knudsen layers exist in all heat flow systems, however they only become significant as the Knudsen number increases.

The boundary conditions used in this solution can be tuned depending on the proportion of phonons that specularly reflect, γ, and isotropically scatter, $1-\gamma$. Figure 7.8 shows $\hat{p}_x$ profiles for $Kn = 0.2$ with varying γ. The figure shows the reduced drag from the boundary as specular reflection increases. In fact, with pure specular reflection ($\gamma = 1$), the Knudsen layer disappears and plug flow is achieved. It is important to realize that this is not the mechanism that predicts Fourier heat transfer on the macro scale. Plug flow can be achieved with γ less than one as long as the Knudsen number is very small, as is shown in Figure 7.7.

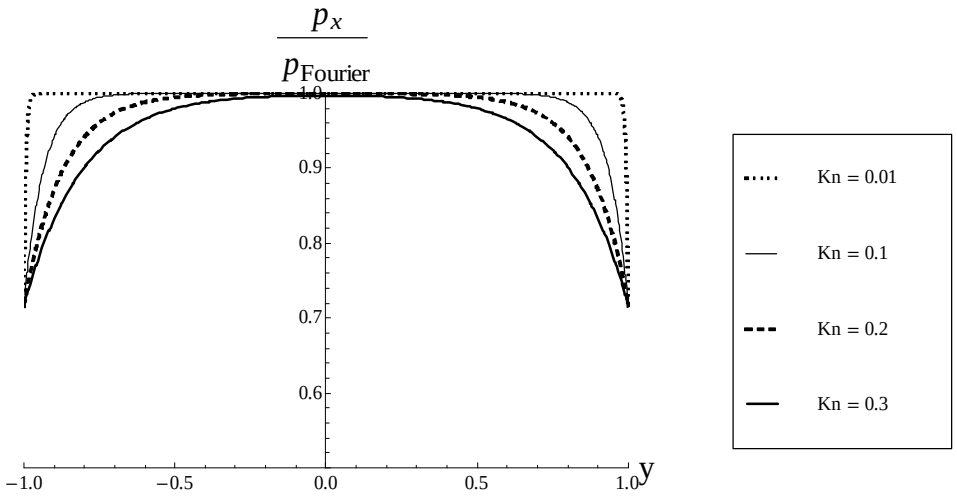

Figure 7.7: Poiseuille flow profile of $\hat{p}_x$ for the 9 moment case with varying Kn where $Kn_R = Kn$, $\alpha = 1$, $\gamma = 0.5$. As Kn approaches zero, the 9 moment case approaches the same profile predicted by Fourier's law. At higher Kn, boundary effects reduce $\hat{p}_x$.

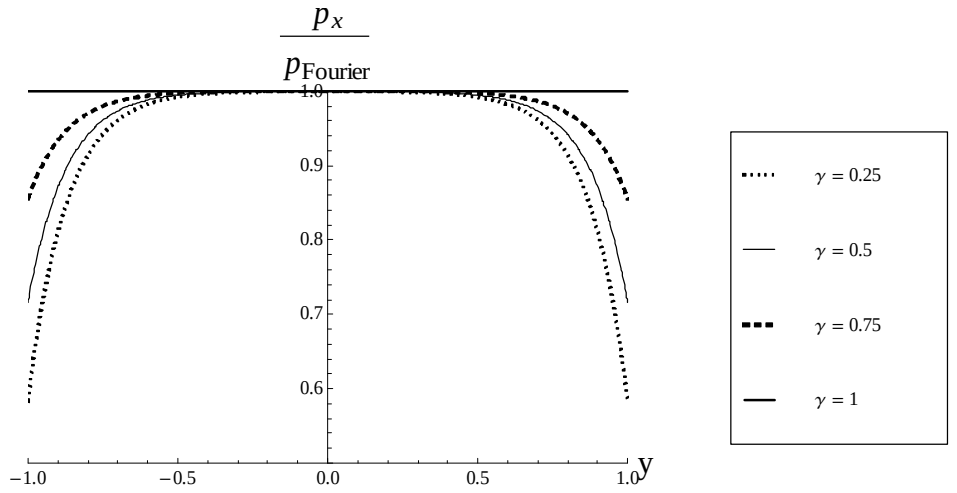

Figure 7.8: Poiseuille flow for the 9 moment equations with $Kn = 0.2$, $Kn_R = 0.4$ and varying γ. Note that as γ increases, the boundary effect diminishes until plug flow is achieved, due to the boundary not inhibiting momentum when there is pure specular reflection.

7.2.3 The 16 and 25 Moment Solutions

For the 16 moment case, the solution for $\hat{p}_x$ is

$$\hat{p}_x = -\frac{Kn_R}{3}\frac{\partial \hat{E}}{\partial x} + K_1 \cosh\left(\sqrt{\frac{35}{8Kn^2 + 7KnKn_R}}y\right) \quad , \tag{7.30}$$

where

$$K_1 = \frac{\frac{\partial \hat{E}}{\partial x} Kn_R}{3\sqrt{8Kn^2 + 7KnKn_R}\left[\sqrt{\frac{35}{8Kn^2+7KnKn_R}}\cosh\left(\sqrt{\frac{35}{8Kn^2+7KnKn_R}}\right) + \frac{75(1+\alpha\gamma)\sinh\left(\sqrt{\frac{35}{8Kn^2+7KnKn_R}}\right)}{35(1-\alpha\gamma)}\right]} \quad . \tag{7.31}$$

The solution for the 16 moment case makes an adjustment to the Knudsen layer when compared with the 9 moment solution.

The 25 moment solution adds a second Knudsen layer

$$\begin{aligned}\hat{p}_x = -\frac{Kn_R}{3}\frac{\partial \hat{E}}{\partial x} &+ K_1 \cosh\left(\sqrt{\frac{210}{49Kn^2 + 21KnKn_R - \sqrt{7Kn^2\left(343Kn^2 - 6KnKn_R + 63Kn_R^2\right)}}}y\right) \\ &+ K_2 \cosh\left(\sqrt{\frac{210}{49Kn^2 + 21KnKn_R + \sqrt{7Kn^2\left(343Kn^2 - 6KnKn_R + 63Kn_R^2\right)}}}y\right) \quad ,\end{aligned} \tag{7.32}$$

where the constants of integration, K_1 and K_2 are too lengthy to present; however, they have a similar form to the constant in the 9 and 16 moment cases. Although higher moment equations have not been solved explicitly, it is clear from the general solution to equation (7.16) that more moments lead to more Knudsen layers.

Figure 7.9 compares the 9, 16, and 25 moment equations for $Kn = 0.3$, $Kn_R = 0.6$, $\alpha = 1$ and $\gamma = 0.5$. With these parameters it is clear that the 25 moment equation has significantly more drag than the 16 and 9 moment equations. However, at lower Knudsen numbers, there is not as much difference between 9, 16 and 25 moments (see Figure 7.10). Comparing solutions from the different moment equations is a way of determining convergence. Solutions from higher and higher moment equations can be compared until the difference between two sets is within and acceptable error. It would then be unnecessary to solve larger moment systems for that particular Knudsen number in that particular system.

Phonon momentum is not a typical quantity desired by design engineers, however heat conductivity is. Since p_i is proportional to q_i and equivalent heat conductivity can be determined by integrating p_i over

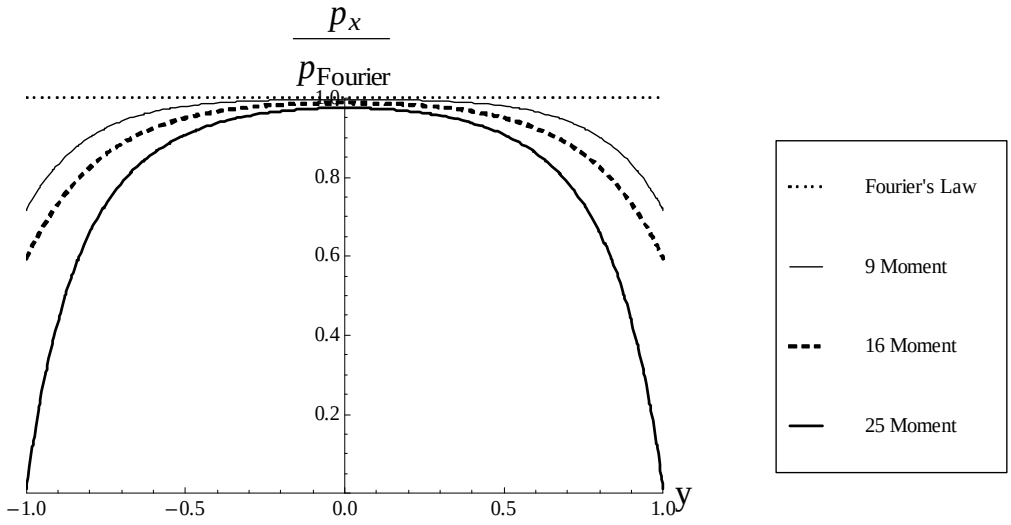

Figure 7.9: Phonon momentum p_x as a function of y in a Poiseuille flow situation where $Kn = 0.3$, $Kn_R = 0.6$, $\alpha = 1$, $\gamma = 0.5$. Fourier's law would give a flat "plug" flow. Boundary drag which reduces total heat flux occurs in the moment equations. Higher moment equations display greater dependency on boundary effects.

an area and comparing it to the heat flux that would be predicted by Fourier's law. This comparison can be used to create a bulk heat conductivity for the entire system that could be compared to the material's heat conductivity in the macro-scale. Figure 7.10 compares the equivalent heat conductivity as a function of Knudsen number for the 9, 16 and 25 moment equations.

7.3 1-D Heat Conduction with Periodic Initial Conditions

Another simple geometric configuration that can be solved analytically is a one dimensional body with periodic initial conditions such as in Figure 7.11. This was conducted experimentally by Johnson et al [24] by interfering two lasers and exposing a wafer to the diffraction pattern specifically because it is a configuration that is possible to analyze both theoretically and experimentally. In the experiment, a sinusoidal energy pattern was initialized in a thin silicon wafer at room temperature and the thermal decay was measured to determine a wave-length dependent damping coefficient. The damping behaviour as a function of the laser diffraction grating's wavelength can be determined from the moment equations, and then be compared to Fourier's law and the experimental results. The periodic nature of the problem eliminates the boundary

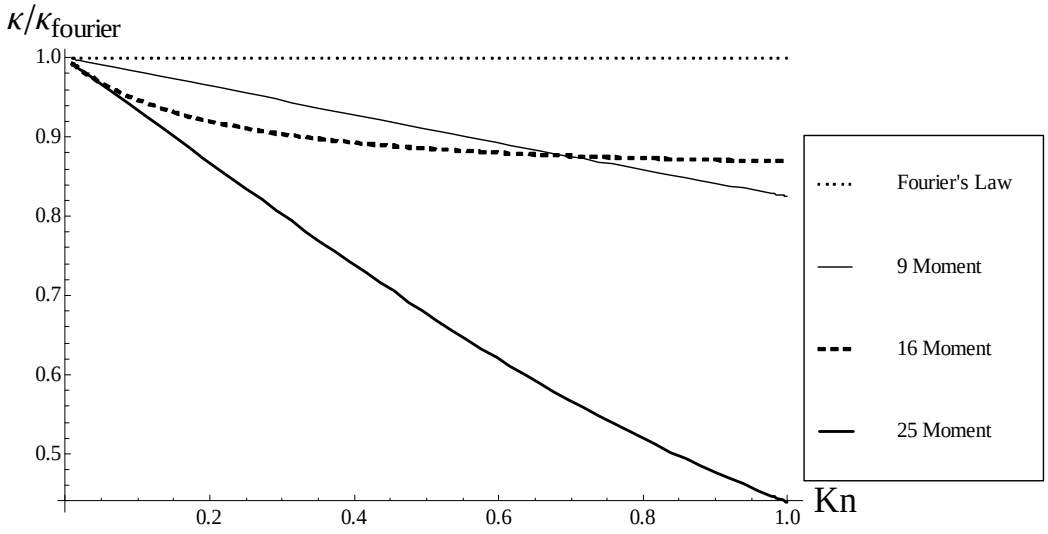

Figure 7.10: Equivalent thermal conductivity for the 9, 16 and 25 moment equations compared to Fourier's law as a function of Knudsen number.

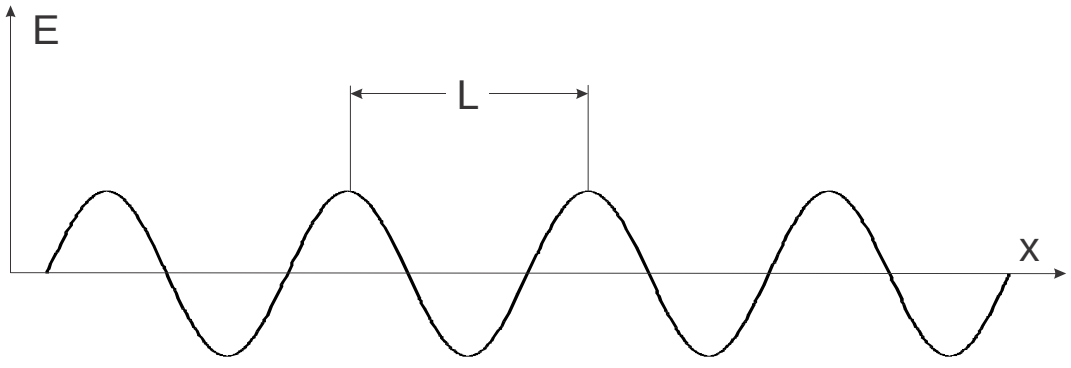

Figure 7.11:

conditions, allowing study of bulk behaviour.

The thin wafer was required by the experiment so that the sinusoidal pattern would be homogenous throughout the entire specimen. Results from Section 7.2 indicate this causes a reduction in heat flow. Incorporating this effect into this model would require a two dimensional solution, which is ignored for this simple analysis.

7.3.1 Fourier's Law Solution

The dispersion relation for Fourier's law can be determined starting with the heat equation in one dimension

$$\frac{\partial e}{\partial t} - \frac{\kappa}{\tilde{c}_v}\frac{\partial^2 e}{\partial x^2} = 0 \quad . \tag{7.33}$$

Since the problem is periodic, the wave ansatz is used

$$e = e_0 \exp\left[-i\left(\bar{K}x - \omega t\right)\right] \quad , \tag{7.34}$$

where $\bar{K} = \frac{2\pi}{L}$ is the wave vector of the diffraction pattern and ω is the frequency. The frequency response is split into two parts. The real part of ω is the phase velocity of the wave and the imaginary part is the wave damping. By substituting the ansatz into the differential equation, the dispersion relation is determined to be quadratic in $\bar{K}$

$$i\omega = \frac{\kappa}{\tilde{c}_v}\bar{K}^2 \quad . \tag{7.35}$$

7.3.2 The 9 Moment Solution

The experimental results were compared to the analytical solution for the 9 moment method using x as the relevant direction. In order to compare it to the experiment, the dimensional form of the equations are used. The necessary equations are

$$\frac{\partial e}{\partial t} + c^2\frac{\partial p_x}{\partial x} = 0 \tag{7.36a}$$

$$\frac{\partial p_x}{\partial t} + \frac{1}{3}\frac{\partial e}{\partial x} + c\frac{\partial N_{\langle xx\rangle}}{\partial x} = -\frac{1}{\tau_R}p_x \tag{7.36b}$$

$$\frac{\partial N_{\langle xx\rangle}}{\partial t} + \frac{4}{15}c\frac{\partial p_x}{\partial x} = -\frac{1}{\tau}N_{\langle xx\rangle} \quad . \tag{7.36c}$$

We define the vector u_α as

$$u_\alpha(x,t) = \begin{bmatrix} e \\ p_x \\ N_{\langle xx \rangle} \end{bmatrix} , \tag{7.37}$$

the matrix $A_{\alpha\beta}$ as

$$A_{\alpha\beta} = \begin{bmatrix} 0 & c^2 & 0 \\ \frac{1}{3} & 0 & c \\ 0 & \frac{4}{15}c & 0 \end{bmatrix} , \tag{7.38}$$

and the matrix $P_{\alpha\beta}$ as

$$P_{\alpha\beta} = \begin{bmatrix} 0 & 0 & 0 \\ 0 & \frac{1}{\tau_R} & 0 \\ 0 & 0 & \frac{1}{\tau} \end{bmatrix} . \tag{7.39}$$

which simplifies equation 7.36 to

$$\frac{\partial u_a}{\partial t} + A_{\alpha\beta}\frac{\partial u_\beta}{\partial x} = -P_{\alpha\beta}u_\beta , \tag{7.40}$$

with initial condition

$$u_a(x,0) = \begin{bmatrix} e_0 \cos\left(\bar{K}x\right) \\ 0 \\ 0 \end{bmatrix} , \tag{7.41}$$

Since the problem is periodic, we use the wave ansatz for the solution

$$u_a = u_a^0 e^{i\left(\bar{K}_n x - \omega_n t\right)} . \tag{7.42}$$

Substituting into equation (7.40) and rearranging yields the equation

$$i\omega u_a - i\bar{K}A_{\alpha\beta}u_\beta + P_{\alpha\beta}u_\beta = 0 . \tag{7.43}$$

For non trivial solutions of u_a, the characteristic equation must hold

$$\left(i\omega\delta_{\alpha\beta} - i\bar{K}A_{\alpha\beta} + P_{\alpha\beta}\right)u_\beta = 0 . \tag{7.44}$$

Equation (7.44) is an eigenvalue equation for the matrix $-i\bar{K}A_{\alpha\beta}+P_{\alpha\beta}$. For each eignevalue, $i\omega$, there is a specific solution to the wave ansatz. Since the problem is linear, they can be added together to form the

general solution

$$u_\alpha(x,t) = \sum_\beta a_\beta Q_{\alpha\beta} e^{i(\bar{K}x - \omega_\beta t)} \quad , \tag{7.45}$$

where $Q_{\alpha\beta}$ is the matrix of eigenvectors corresponding to the eigenvalues $i\omega_\beta$. The amplitude a_β must be determined from the initial condition shown in equation (7.41). Substituting the initial condition into the general boundary solution yields,

$$u_\alpha(x,0) = \sum_\beta a_\beta Q_{\alpha\beta} e^{i\bar{K}x} \quad . \tag{7.46}$$

This can be simplified such that

$$a_\alpha = e_0 Q^{-1}_{\alpha 1} \quad . \tag{7.47}$$

Note that e_0 was previously defined as the energy amplitude for the initial condition in equation (7.41). The final solution is

$$u_\alpha(x,t) = e_0 \sum_\beta Q_{\alpha\beta} Q^{-1}_{\beta 1} e^{i(\bar{K}x - \omega_\beta t)} \quad . \tag{7.48}$$

This solution can be generated for an arbitrary number of moments by simply expanding the dimensions of u_α, $A_{\alpha\beta}$, and $P_{\alpha\beta}$ and determining their coefficients from the moment equations. For simplicity, only results from the 9 moment equations are presented.

7.3.3 Mathematical Method to Compare Results

The experimental results (see Figure 7.12) were determined by fitting an exponential function to the wave decay. Since the moment model's solution is a specific solution, it was approximated by finding an aggregate frequency, $\bar{\omega}$, such that

$$\sum_\beta Q_{\alpha\beta} Q^{-1}_{\beta 1} e^{i(\bar{K}x - \omega_\beta t)} = e^{i(\bar{K}x - \bar{\omega}t)} \quad . \tag{7.49}$$

$\bar{\omega}$ can be determined by taking the natural logarithm of equation (7.49) and simplifying for a constant value of x (in this case $x = 0$ is used for simplicity but any value will work)

$$-i\bar{\omega}t = \ln\left[\sum_\beta Q_{\alpha\beta} Q^{-1}_{\beta 1} e^{-i\omega_\beta t)}\right] \quad . \tag{7.50}$$

The resultant equation is linear with respect to t. Essentially $\bar{\omega}$ determined by taking the slope of least squares fit to the right hand side of equation (7.50). The least squares fit was computed between $t = 0$ and a time that was sufficiently large enough for most of the decay to occur, which was consistent with the experiment [24].

7.3.4 Results and Discussion

The results from the one dimensional 9 moment model are qualitatively similar to the experimental results. There was difficulty matching the data quantitatively for a variety of reasons. The dispersion relation of Fourier's law (as measured in [24]), the 9 moment method and the data from [24] are shown in Figure 7.12.

In the experiment, Johnson used silicon wafers, which have a tabulated mean free path, $\lambda = 43$ nm [25]. Using a specific heat of 700 J/kgK, a conductivity of 130 W/mK, a density of 2329 kg/m^3, and a speed of sound of 8430 m/s [26] equation 4.31 gives a resistive mean free path, λ_R, of 28 nm. However, since the Johnson experiment used a thin wafer which reduces heat conductivity because of phonon boundary scattering, essentially experiencing the result predicted in Section 7.2. As a result, inspection of the slope of the line for Fourier's law in Figure 7.12 actually predicts a bulk conductivity of 89 W/mK.

This effect is not a part of the 1-D, 9 moment solution because it is essentially a two dimensional side effect. The only two parameters in the 9 moment solution are the resistive mean free path and the total mean free path. In order to fit the data from the Johnson experiment, the resistive mean free path was adjusted to fit the slope of Fourier's law as measured in the experiment, and then the total mean free path was adjusted to fit the experiment's dispersion relation. The results require a resitive mean free path of 19 nm and a total mean free path of 9300 nm.

The results of the 9 moment theory are not entirely accurate, but they do predict the general characteristics of the equation. Furthermore, the frequency dependence of phonon mean free path has an important effect on the results. In fact, in thin films, there has been research suggesting that the importance of low frequency phonons (and their longer mean free paths) should be taken into consideration to make the "effective" mean free path on the order of 300 nm [27].

Ultimately the solution should be tested using a two dimensional solution to the moment equations.

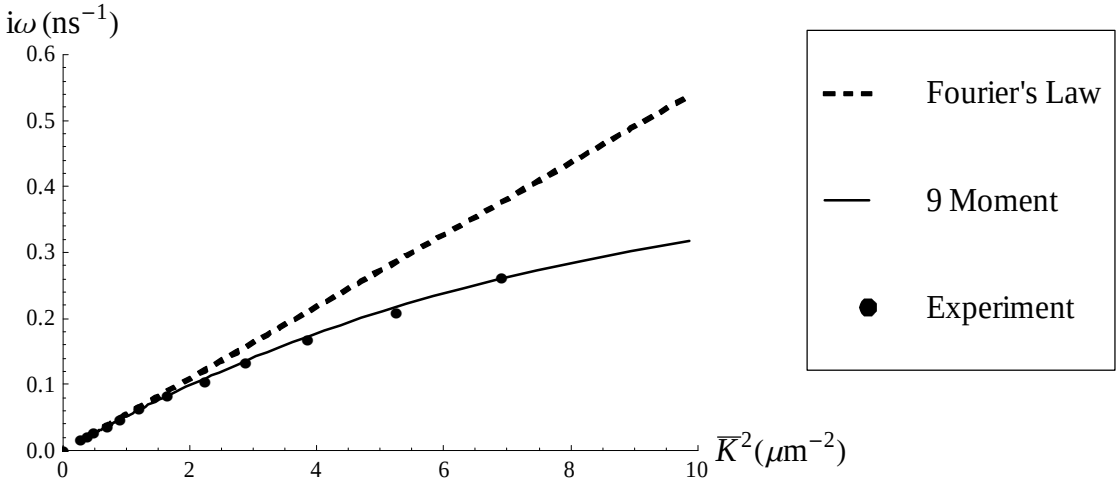

Figure 7.12: Dispersion relation of the wavevector ($\bar{K}$) of a sinusoidal initial condition and the temperature relaxation frequency (ω). The Fourier's Law slope and the experimental data plots are from [24]. Fitting the 9 moment theory to the experimental data required a resistive mean free path of 19 nm and a total mean free path of 9300 nm.

This would create a model that could capture the effects of the thin film boundary scattering as well as the periodic initial conditions. The boundary scattering parameters α and γ could be used to reduce the effective thermal conductivity which would hopefully result in more accurate values for the phonon mean free path. A time dependent finite volume method using the Roe (i.e. upwind) scheme was in development but was not completed at the time of writing.

7.4 2-D Heat Conduction

7.4.1 Numerical Method

Numerical models are an essential tool for solving problems with anything but the simplest of geometries. A simple 2-D steady state numerical model for a square domain was adapted from a gas kinetic moment model [32], [31]. There is no fundamental reason preventing extension of this scheme to arbitrary geometries.

The system of steady state, 2-D moment equations are[7]

[7]For the numerical section, index notation will not be used to avoid any confusion with discretized equations. For example

$$\mathcal{A}\frac{\partial \mathcal{U}}{\partial x} + \mathcal{B}\frac{\partial \mathcal{U}}{\partial y} + \mathcal{P}\mathcal{U} = 0 \quad , \tag{7.51}$$

where

$$\mathcal{U} = \begin{bmatrix} \hat{E} & \hat{p}_x & \hat{p}_y & \hat{N}_{\langle xx \rangle} & \hat{N}_{\langle xy \rangle} & \hat{N}_{\langle yy \rangle} \end{bmatrix} \quad .$$

$\mathcal{A}$, $\mathcal{B}$, and $\mathcal{P}$ are coefficient matrices that are presented for the 9 moment equations in Appendix D.

7.4.2 Finite difference approximation

The equation can be discretized over an $N \times M$ grid for such that $x_i = i\Delta x$ and $y_j = j\Delta y$ results in

$$\mathcal{A}\frac{\partial \mathcal{U}_{i,j}}{\partial x} + \mathcal{B}\frac{\partial \mathcal{U}_{i,j}}{\partial y} + \mathcal{P}\mathcal{U}_{i,j} = 0 \ \ \forall\ (i,j) \in [1,N] \times [1,M]\,, \text{ where } \mathcal{U}_{i,j} = \mathcal{U}(x_i, y_j)\ . \tag{7.52}$$

The boundary conditions are applied at all nodes where $i = 0$, $i = N$, $j = 0$, and $j = M$. The boundary conditions in Appendix C are used to determine the boundary nodes (for the 9 moment case, only equations (C.1) and (C.2) are needed, while the 25 moment equations require all six). The boundary conditions are applied using linear extrapolation to determine the boundary nodes. For x-walls (i.e. walls with a normal vector in the x direction) the boundary condition is

$$\mathcal{U}_{0,j} = \mathcal{X}^{+}\ (2\mathcal{U}_{1,j} - \mathcal{U}_{2,j}) + \mathcal{X}^{d+}\,, \tag{7.53a}$$

$$\mathcal{U}_{N+1,j} = \mathcal{X}^{-}\ (2\mathcal{U}_{N,j} - \mathcal{U}_{N-1,j}) + \mathcal{X}^{d-} \quad \forall\ j \in [1,M]\,, \tag{7.53b}$$

Where $\mathcal{X}$ is a coefficient matrix multiplied by the variables $\mathcal{U}$ for an x-wall and $\mathcal{X}^d$ is an inhomogenous component representing the surface energy, $\hat{E}_s$. The $+$ or $-$ sign represents the sign of the wall normal vector. $\mathcal{X}$, and $\mathcal{X}^d$ for an adiabatic wall are shown in Appendix D for the 9 moment case. The matrix $\mathcal{X}$ only gives boundary conditions for the moments $\hat{p}_x$ and $\hat{N}_{\langle xy \rangle}$ because these are the only moments that are odd in x for the 9 moment case. For more information refer to boundary condition reduction in Section 5.4.1. For all of the other moments $\mathcal{X}$ is an identity.

in this section, $\mathcal{A}_{i,j}U_{i,j}$ denotes the i-th and j-th component of $\mathcal{A}$ multiplied by the i-th and j-th component of U, instead of summation over all components of $\mathcal{A}$ and U.

The same scheme is used for the y-walls

$$\mathcal{U}_{i,0} = \mathcal{Y}^{+}\ (2\mathcal{U}_{i,1} - \mathcal{U}_{i,2}) + \mathcal{Y}^{d+}\,, \tag{7.54a}$$

$$\mathcal{U}_{i,M+1} = \mathcal{Y}^{-}\ (2\mathcal{U}_{i,M} - \mathcal{U}_{i,M-1}) + \mathcal{Y}^{d-}\ \ \forall\ i \in [1,N]\quad . \tag{7.54b}$$

$\mathcal{Y}$ and $\mathcal{Y}^d$ are presented in Appendix D as a boundary with controlled surface energy $\hat{E}_s$.

The matrix $\mathcal{U}_{i,j}$ can be solved using the central difference method to replace the derivatives in equation (7.52)

$$\mathcal{A}\frac{\mathcal{U}_{i+1,j}}{2\Delta x} - \mathcal{A}\frac{\mathcal{U}_{i-1,,j}}{2\Delta x} + \mathcal{B}\frac{\mathcal{U}_{i,,j+1}}{2\Delta y} - \mathcal{B}\frac{\mathcal{U}_{i,j-1}}{2\Delta y} + \mathcal{P}\mathcal{U}_{i,j} = 0\ \forall\ (i,j) \in [2,N-1]\times[2,M-1]\,. \tag{7.55}$$

The boundary nodes are determined by substituting the required boundary condition into equation (7.52). For the left wall (i.e. $i = 1$ wall) equation (7.53a) is used,

$$\left(\mathcal{P} - \frac{1}{\Delta x}\mathcal{A}\mathcal{X}^{+}\right)\mathcal{U}_{1,j} + \frac{1}{2\Delta x}\mathcal{A}\left(I + \mathcal{X}^{+}\right)\mathcal{U}_{2,j} + \mathcal{B}\frac{\mathcal{U}_{1,j+1}}{2\Delta y} - \mathcal{B}\frac{\mathcal{U}_{1,j-1}}{2\Delta y}$$
$$= \frac{1}{2\Delta x}\mathcal{A}\mathcal{X}^{+d} \quad \forall\ j \in [2,M-1]\ . \tag{7.56}$$

For the right wall (i.e. $i = N$ wall) equation (7.53b) is used,

$$\left(\mathcal{P} + \frac{1}{\Delta x}\mathcal{A}\mathcal{X}^{-}\right)\mathcal{U}_{N,j} - \frac{1}{2\Delta x}\mathcal{A}\left(I + \mathcal{X}^{-}\right)\mathcal{U}_{N-1,j} +$$
$$+ \mathcal{B}\frac{\mathcal{U}_{N,j+1}}{2\Delta y} - \mathcal{B}\frac{\mathcal{U}_{N,j-1}}{2\Delta y} = -\frac{1}{2\Delta x}\mathcal{A}\mathcal{X}^{-d} \quad \forall\ j \in [2,M-1]\quad . \tag{7.57}$$

The same method is used for the lower ($j = 1$) and upper ($j = M$) walls.

The corners require combining the x and y boundary condition equations with equation (7.52). For example, the lower left ($i = 1$, $j = 1$) wall has the equation

$$\left(\mathcal{P} - \frac{1}{\Delta x}\mathcal{A}\mathcal{X}^{+} - \frac{1}{\Delta y}\mathcal{B}\mathcal{Y}^{+}\right)\mathcal{U}_{1,1} + \frac{1}{2\Delta x}\mathcal{A}\left(I + \mathcal{X}^{+}\right)\mathcal{U}_{2,1} +$$
$$+ \frac{1}{2\Delta y}\mathcal{B}\left(I + \mathcal{Y}^{+}\right)\mathcal{U}_{1,2} = \frac{1}{2\Delta x}\mathcal{A}\ \mathcal{X}^{+d} + \frac{1}{2\Delta y}\mathcal{B}\ \mathcal{Y}^{+d}. \tag{7.58}$$

All values of $\mathcal{U}_{i,j}$ can be combined into a single vector $X = \{\mathcal{U}_{i,j}\}_{(i,j)\in[1,N]\times[1,M]}$ which allows the above equations to be written in the form,

$$\mathcal{M}X = \mathfrak{b}\,. \tag{7.59}$$

X can be solved by inverting this equation which is can be achieved using the QMR iterative method [30]. The method is second order convergent [32].

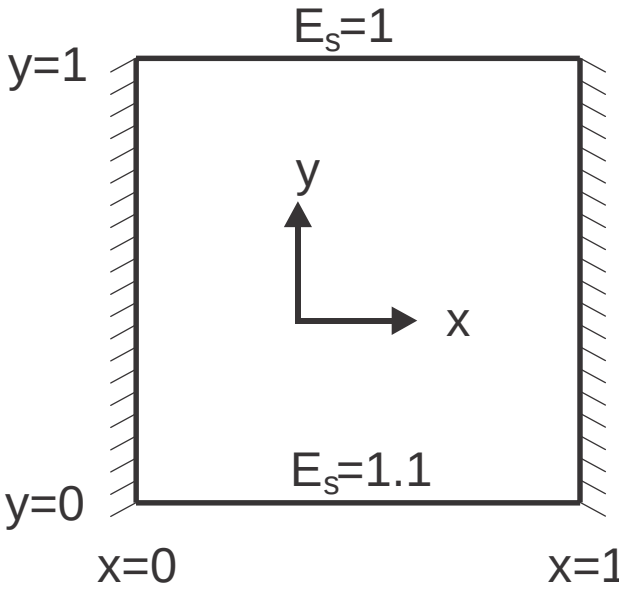

Figure 7.13: The domain of the 2-D steady state numerical model

7.4.3 Numerical Results and Discussion

A numerical model for a steady state square geometry shown in Figure 7.13 was solved for the 9 moment equations. In the problem, the walls at $\hat{x} = 0$ and $\hat{x} = 1$ were adiabatic, the surface at $\hat{y} = 0$ had a surface energy of $\hat{E}_s = 1.1$ and the surface at $\hat{y} = 1$ had a surface energy of $\hat{E}_s = 1$. The problem geometry is similar to a combination of Poiseuille flow and heat flow between parallel plates. All of the coefficient matrices in Appendix D were the specific ones used to solve this problem.

The solution of the 2-D simulation was used to determine the total heat flux in the y direction by integrating $\hat{p}_y$ over $\hat{x}$. Figure 7.14 shows a plot of $\hat{p}_y$ over the entire numerical domain. The plot is similar in shape to 1-D Poiseuille flow except for some effects at the corners. The plot was scaled by the expected value of $\hat{p}_y$ if Fourier's law was used.The total heat flux in the y direction (the adiabatic walls prevent net heat flux in the x direction) can be compared to Fourier's law to determine an effective heat conductivity, as previously described in Sections 7.1 and 7.2. Figure 7.15 shows heat conductivities for all three cases scaled by the expected heat conductivity given by Fourier's law. The 2-D model has a significantly lower conductivity than the 1-D models because it essentially is a combination of both effects. Heat flow is restricted by the temperature jump as well as drag due to phonon scattering on the adiabatic walls.

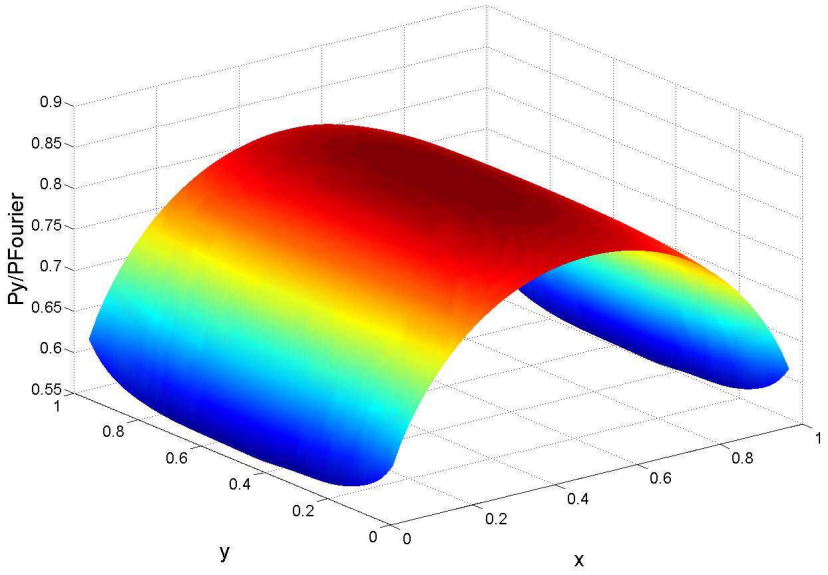

Figure 7.14: A 2-D numerical plot of $\hat{p}_y$ for $Kn = 0.3$, $Kn_R = 0.6$, $\alpha = 0.5$, and $\gamma = 0.5$.

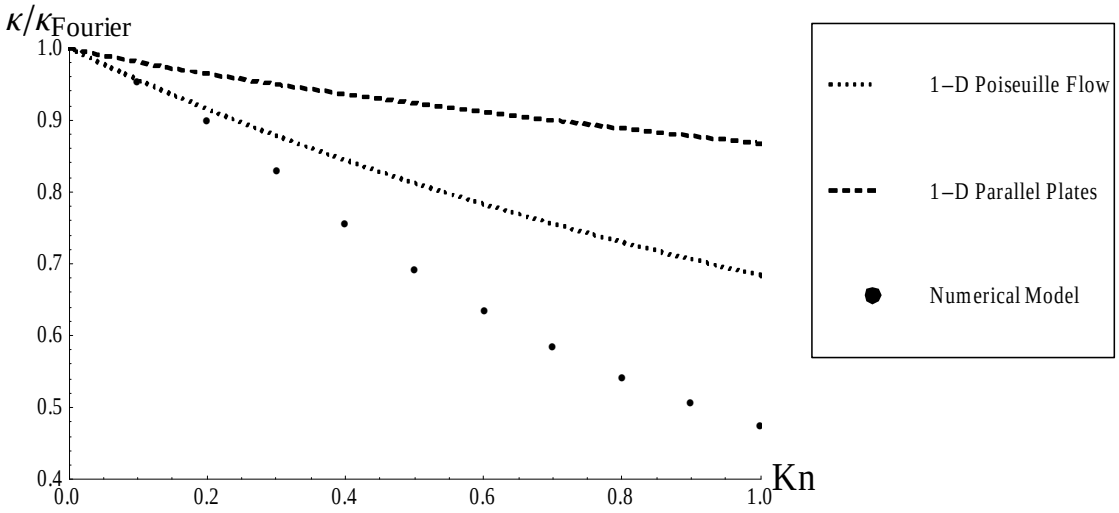

Figure 7.15: Effective heat conductivity for 1-D Poiseuille flow, 1-D heated parallel plates and the 2-D numerical method.

8 Conclusion

8.1 Summary

At macroscopic length scales, heat transfer is governed by Fourier's law. As length scale decreases, surface effects and non-locality begin to dominate heat transfer, making Fourier's law increasingly inaccurate. The Knudsen number, which is the ratio of phonon mean free path to the length scale of the relevant system is a parameter that shows the degree of rarefaction in a given problem. Fourier's law is only accurate when the Knudsen number is very small. In order to develop relevant and accurate constitutive equations for systems with large Knudsen numbers, a microscopic analysis of phonons is necessary.

Phonons are particle representations of crystal lattice vibrations and were derived from quantum mechanics. Phonons conserve energy, but they do not always conserve momentum or number when they collide. Phonon processes can be put into two different categories: normal processes, where phonons conserve momentum; and resistive processes, where they do not. Each type of process has its own mean free path, and hence its own Knudsen number, but it is more useful to use a Knudsen number for resistive processes only, and another Knudsen number for all processes.

The phonon Boltzmann equation governs phonon mechanics, but is time consuming to solve in its full form. The moment method is derived by integrating over the phonon distribution function to develop an infinte set of macroscopic transport equations. This set of equations can be truncated at an arbitrary moment order and is closed using Grad's closure method. The closure method is a linearization of the phonon distribution function which effectively forces any higher order moments to be zero. One prerequisite of this closure is that the Knudsen number is assumed to be less than one. A simple approximation to the phonon collision term is the Callaway model, which replaces the collision term with a relaxation term that is dependent on collision frequency. The Callaway model is based on the assumption that collisions increase entropy and therefore bring the particle distribution function towards an equilibrium distribution. A further simplification is to use the gray matter assumption, which assumes a constant collision frequency regardless of phonon wavevector.

The boundary conditions for the moment method were derived by creating a microscopic model of phonon-

interface interactions that could be both an approximation to what actually occurs and also simple enough so that macroscopic moment boundary conditions could be made. The boundary conditions considered phonon diffuse scattering, specular reflection and interface thermalization. The boundary conditions were derived for the moment equations in an explicit form in three dimensions for an arbitrary number of moment equations. They were also reduced using Grad's argument so that the moment equations would not be overdefined. The resulting macroscopic boundary conditions can be adjusted by changing the scattering, reflection, and thermalization parameters in order to compare and analyze experimental results and other models.

Basic analytic problems were solved for the 9, 16 and 25 moment systems of equations. Heat flow between parallel plates of differing energy was solved. The solution showed a similar solution to Fourier's law except for a temperature jump at the boundaries, which increased with Knudsen number and by decreasing the proportion of phonons that thermalized at the surface. Heat transfer (and consequently the effective heat conductivity) was reduced compared to what Fourier's law would predict.

Another simple analytic problem is one dimensional Poiseuille flow. The solution to the problem showed phonon "drag" at the walls which reduced heat transfer with increasing Knudsen number. Drag could also be affected by changing the proportion of phonons that are scattered or reflected. Once again, an effective heat conductivity was calculated and shown to be lower than what Fourier's law would predict. This reduction in heat conductivity was observed as a side effect in an experiment [24].

The moment model was compared to an experiment where a laser diffraction pattern was used to heat a silicon wafer in a periodic pattern. The periodicity of the system allowed it to be solved analytically in one dimension. The moment method qualitatively matched the measured dispersion relation of the energy relaxation frequency versus the diffraction pattern's wavevector. The moment method could be "fit" to the experimental data, but only by using mean free path lengths that are not accepted for silicon. The moment method could be compared more completely by developing a time dependent, 2 dimensional numerical model.

A steady state 2 dimensional numerical model was created by adapting code used for rarefied gas transport equations [31], [32]. The method was used to develop code for a 2-D square domain analysis. A problem with two parallel adiabatic walls combined with two parallel heated surfaces was solved numerically. The resultant effective heat conductivity was lower than Fourier's law as expected. It was also lower than the

effective heat conductivities calculated for 1-D Poiseuille flow and 1-D heat conduction between parallel plates because it combined both effects.

8.2 Recommendations

The moment method provides a macroscopic model that approximates microscopic phonon interactions with several attractive properties. It is computationally efficient, it can be easily adapted to varying surface and interface conditions by changing its boundary parameters, and it can be extended to arbitrary precision by increasing the number of moments. Finally, it provides solutions in the form of equations, such as equation 7.7, that provide insight into nanoscale heat transfer as opposed to only numerical results. These properties make the moment method a useful modeling tool for engineers. Its efficiency lends itself well to engineering design optimization. In order for it to gain widespread adoption, there are several major steps that need to be taken, both in verification and model improvement.

8.2.1 Verification

The moment method for phonons needs more verification. At the current stage, this can be attained by comparing the moment method with other models, such as direct simulation monte carlo or with experimental results. This is an obvious "next step" for this method. In order to verify the model, a widespread literature review of current experiments and models should be combined with making a versatile numerical model. Simple problems can already be solved using the current numerical model, but extension to more arbitrary geometries would be a significant improvement. A time dependent model would also be useful to solve unsteady problems. A time dependent two dimensional model was under development but was not finished by the time of writing.

8.2.2 Theoretical Model Improvement

There are several ways that could improve the accuracy and the versatility of the moment method. One of the severe limitations of the model is the assumption that the mean free path is not a function of phonon frequency (the gray matter assumption). Frequency dependent mean free path has a significant effect at the

nanoscale [27]. Removing the gray matter assumption significantly increases the complexity of the Callaway model because the collision frequency can no longer be removed from the integral in equation 4.20.

In general, the model could be improved simply by removing as many assumptions as possible. This obviously sacrifices the simplicity and linearity of the equations, but could improve its accuracy. One useful improvement would be to integrate the moments over a finite Brillouin zone instead of an infinite one. This could help the model be more accurate at higher temperatures and would be especially useful for modeling materials with a low Debye temperature. Finally, non-linear phonon dispersion could improve the model further, however this improvement may come at the cost of a much more difficult closure of the equations.

References

[1] G. E. Moore, "Cramming more compononents onto integrated circuits", Electronics, Volume 38, Number 8, April 19, 1965.

[2] G.M. Whitesides, "The origins and the future of microfluidics," *Nature* 442.7101 (2006), 368-373.

[3] R.P. Feynman, "There's plenty of room at the bottom," *Engineering and Science*, 23.5 (1960), 22-36.

[4] D.W. Snoke, *Solid State Physics Essential Concepts*, Addison Wesley, 2009, pp.181-189.

[5] C. Kittel, *Introduction to Solid State Physics* (7th ed.), John Wiley & Sons, ISBN 0-471-11181, 1996.

[6] G.A. Bird, "Molecular gas dynamics." *NASA STI/Recon Technical Report A*, 76, (1976), 40225.

[7] J.P.M. Péraud,N.G. Hadjiconstantinou. "Efficient simulation of multidimensional phonon transport using energy-based variance-reduced Monte Carlo formulations." *Phys Rev B*, 84.20 (2011), 205331.

[8] R. Peierls, "Zur kinetischen Theorie der Wärmeleitung in Kristallen", Ann. Phys. 3 (1929) 1055.4

[9] W. Dreyer, H. Struchtrup, "Heat Pulse Experiments Revisted", Continuum Mech. Thermodyn. 5 (1993) 3-50.

[10] H. Grad, "On the kinetic theory of rarefied gases," Commun. Pure Appl. Math, 2 (1949) 331-407

[11] J.E. Jones, "On the Determination of Molecular Fields," Proc. R. Soc. Lond. A 106.738 (1924), 463-477.

[12] D.W. Snoke, *Solid State Physics Essential Concepts*, Addison Wesley, 2009, pp.124-125.

[13] D.W. Snoke, *Solid State Physics Essential Concepts*, Addison Wesley, 2009, pp.126-129.

[14] D.W. Snoke, *Solid State Physics Essential Concepts*, Addison Wesley, 2009, pp.130-139.

[15] D.W. Snoke, *Solid State Physics Essential Concepts*, Addison Wesley, 2009, pp.71.

[16] I. Müller, T. Ruggeri, *Rational Extended Thermodynamics* (2nd ed.), Springer, ISBN 0-387-98373-2, 1998.

[17] Y.A. Çengel, M.A Boles, *Therodynamics An Engineering Approach* (5th ed.), McGraw Hill, ISBN 0-07-288495-9, 2006, pp. 347.

[18] I. Müller, *Thermodynamics*, Pitman Publishing, ISBN 0-273-08577-8, 1985, pp. 156

[19] D.W. Snoke, *Solid State Physics Essential Concepts*, Addison Wesley, 2009, pp. 214-219.

[20] P.L. Bhatnagar, E.P. Gross, M. Krook, "A Model for Collision Processes in Gases. I. Small Amplitude Processes in Charged and Neutral One-Component Systems," Phys. Rev. 94: 511-525, (1954).

[21] J. Callaway, "Model for Lattice Thermal Conductivity at Low Temperatures", Phys. Rev. 113 (1959) 1046

[22] H.D. Young, R.A. Freedman, *University Physics with Modern Physics*, Addison-Wesley, 2008, pp. 486-489.

[23] H. Struchtrup, P. Taheri, "Macroscopic transport models for rarefied gas flows: a brief review," IMA Journal of Applied Mathematics, 76 (2011) 672-697

[24] J.A. Johnson, A.A. Maznev, J. Cuffe, J.K. Eilason, A.J. Minnich, T. Kehoe, C.M. Sotomayor Torres, G. Chen, K.A. Nelson, "Direct Measurement of Room Temperature Non-diffusive Thermal Transport Over Micron Distance in a Silicon Membrane," arXiv:1204.4735v1 [cond-mat.mtrl-sci]

[25] J.S. Blakemore, *Solid State Physics,* Cambridge University Press, Cambridge, 1985.

[26] Ioffe Physical Tehcnical Institute, "Thermal Properties of Silicon." www.ioffe.ru/SVA/NSM/Semicond/Si/thermal.html, Last visited 2012

[27] Y.S. Ju, K.E. Goodson, "Phonon scattering in silicon films with thickness of order 100 nm," *Appl. Phys. Lett.*, 74 (1999) 3005-3007.

[28] P. Debye, "Zur theorie der spezifischen wärmen." *Annalen der Physik* 39.4, 1912, 789.

[29] H. Struchtrup, *Macroscopic Transport Equations for Rarefied Gas Flows*, Springer, ISBN 978-3-540-24542-1, 2005.

[30] R. Freund, N. Nachtigal, QMR: A quasi-minimal residual method for non-Hermitian linear systems, Numer. Math. **60**, 315-339 (1991).

[31] A. Rana, M. Torrilhon, H. Struchtrup, "Heat transfer in micro devices packaged in partial vacuum." *J. Physics: Conference Series*, 362, 012034 , 2012.

[32] A. Rana, M. Torrilhon, H. Struchtrup, "A robust numerical method for the R13 equations of rarefied gas dynamics: Application to lid driven cavity." submitted (2012).

Appendix

A The Group Velocity

In order to localize the wavelike behavior of lattice vibrations into phonons, it is necessary to determine a phonon's velocity. This is done by determining the energy of the system and then calculating the velocity at which the energy propagates. For simplicity we consider a continuous system where the general solution is a superposition of plane waves

$$u\left(x,t\right)=\int A\left(k\right)e^{i(kx-\omega t)}dk \quad . \tag{A.1}$$

The energy, in general, is proportional to the product of the wave times its complex conjugate, summed over all k [22]:

$$E=\int\int_{-\infty}^{\infty}A(k)A^{*}(k')e^{-i(\omega(k)t-kx)}e^{i\left(w\left(k'\right)t-k'x\right)}dkdk' \quad , \tag{A.2}$$

where k' is simply a second variable of integration since k must be summed twice. The first step we take is to define a new variable so that k' is expressed as a difference of k.

$$\kappa=k'-k \quad . \tag{A.3}$$

Equation (A.2) can be rearranged such that

$$E=\int\int_{-\infty}^{\infty}A(k)A^{*}(k+\kappa)e^{i\left(\frac{\omega(k+\kappa)+\omega(k)}{\kappa}t-x\right)\kappa}dkd\kappa \quad . \tag{A.4}$$

Consider the energy of the signal in a small but finite space element Δx. It is important to not let Δx get too small. In essence a "coarse grain" of the wave solution must be used. The finite size of Δx can be viewed as the size of the wave packet or the radius of a phonon. The energy in such a wave packet is

$$e=\frac{1}{\Delta x}\int_{x-\frac{\Delta x}{2}}^{x+\frac{\Delta x}{2}}\int\int_{-\infty}^{\infty}A(k)A^{*}(k+\kappa)e^{i\left(\frac{\omega(k+\kappa)+\omega(k)}{\kappa}t-x\right)\kappa}dkd\kappa dx \quad . \tag{A.5}$$

Integrating the function in x yields

$$e=\int\int_{-\infty}^{\infty}A(k)A^{*}(k+\kappa)e^{i\left(\frac{\omega(k+\kappa)+\omega(k)}{\kappa}t-x\right)\kappa}\frac{\sin\frac{\kappa\Delta x}{2}}{\frac{\kappa\Delta x}{2}}dkd\kappa \ . \tag{A.6}$$

This is simply equation (A.4) scaled by $\frac{1}{\kappa}\sin\kappa\frac{\Delta x}{2}$. This scaling function is shown in Figure **??**. This scaling function shows that as the absolute value of κ gets large, equation (A.4) becomes more and more insignificant.

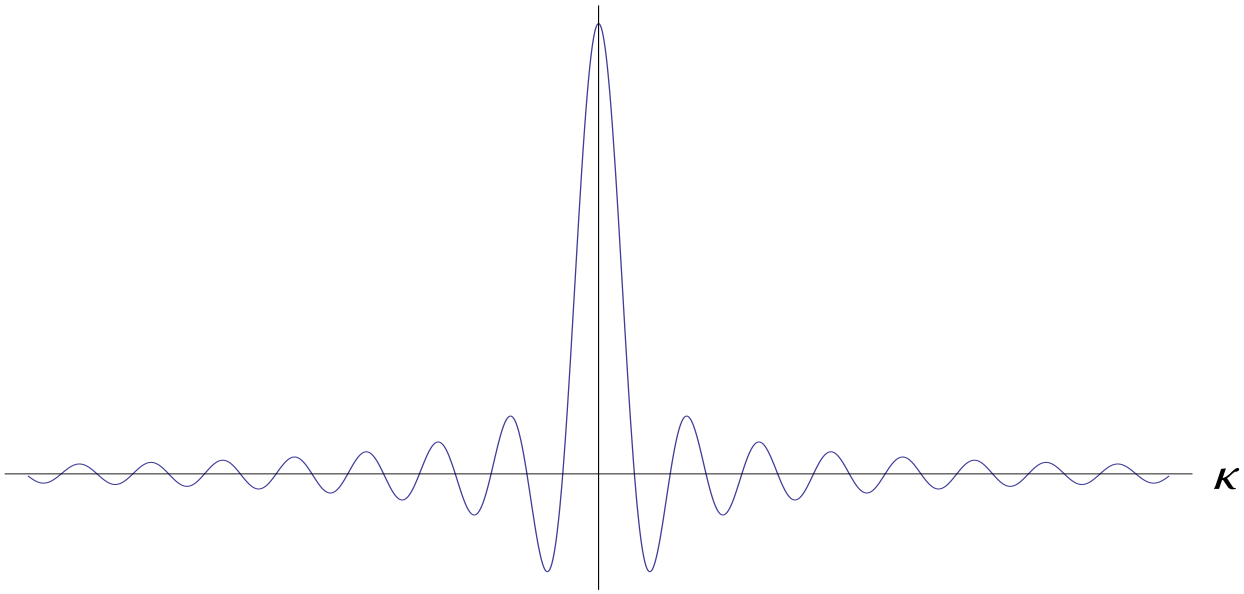

A plot showing the scaling function $\frac{1}{\kappa}\sin\kappa\frac{\Delta x}{2}$. As κ goes away from zero, the function diminishes significantly.

The effect of this scaling functon is that the energy in the wave packet only has to be integrated over small κ. The velocity of this energy packet, is the term multiplied by t in the argument of the exponential function

$$v = \frac{\omega\left(k+\kappa\right)+\omega\left(k\right)}{\kappa} \quad . \tag{A.7}$$

Notice that taking the limit as κ goes to zero in equation (A.7) and the definition of the derivative leads to the group velocity of the wave

$$v = v_g = \frac{\partial\omega}{\partial k} \quad . \tag{A.8}$$

Thus the energy wave packet travels with the derivative of the dispersion relation. This relation comes at a cost though, because as Δx gets smaller and smaller, κ must be integrated over larger and larger bounds to still accurately describe the energy of the wave packet. As κ becomes larger, it is more and more inaccurate to approximate equation (A.7) with equation (A.8). As a result of this derivation, a phonon is a particle that is localized within Δx and moves with the group velocity. Since Δx must be a "coarse grain" of the wave it is impossible to perfectly localize the phonon without sacrificing the knowledge of its velocity and vice versa.

B The Expanded Moment Equations in Cartesian Coordinates

The expanded 25 moment equations in cartesion coordinates are presented. The equations can be reduced to the 16 moment equations by making $R_{\langle ijkl\rangle} = 0$. They can be further reduced to the 9 moment equations by also making $M_{\langle ijk\rangle} = 0$.

Energy balance:

$$\frac{\partial \hat{E}}{\partial \hat{t}} + \left(\frac{\partial \hat{p}_x}{\partial \hat{x}} + \frac{\partial \hat{p}_y}{\partial \hat{y}} + \frac{\partial \hat{p}_z}{\partial \hat{z}} \right) = 0 \tag{B.1}$$

Momentum balance:

$$\frac{\partial \hat{p}_x}{\partial \hat{t}} + \frac{1}{3}\frac{\partial \hat{E}}{\partial \hat{x}} + \frac{\partial \hat{N}_{\langle xx\rangle}}{\partial \hat{x}} + \frac{\partial \hat{N}_{\langle xy\rangle}}{\partial \hat{y}} + \frac{\partial \hat{N}_{\langle xz\rangle}}{\partial \hat{z}} = -\frac{1}{Kn_R}\hat{p}_x \tag{B.2}$$

$$\frac{\partial \hat{p}_y}{\partial \hat{t}} + \frac{1}{3}\frac{\partial \hat{E}}{\partial \hat{y}} + \frac{\partial \hat{N}_{\langle xy\rangle}}{\partial \hat{x}} + \frac{\partial \hat{N}_{\langle yy\rangle}}{\partial \hat{y}} + \frac{\partial \hat{N}_{\langle yz\rangle}}{\partial \hat{z}} = -\frac{1}{Kn_R}\hat{p}_y \tag{B.3}$$

$$\frac{\partial \hat{p}_z}{\partial \hat{t}} + \frac{1}{3}\frac{\partial \hat{E}}{\partial \hat{z}} + \frac{\partial \hat{N}_{\langle xz\rangle}}{\partial \hat{x}} + \frac{\partial \hat{N}_{\langle yz\rangle}}{\partial \hat{y}} - \frac{\partial \hat{N}_{\langle xx\rangle}}{\partial \hat{z}} - \frac{\partial \hat{N}_{\langle yy\rangle}}{\partial \hat{z}} = -\frac{1}{Kn_R}\hat{p}_z \tag{B.4}$$

$\hat{N}_{\langle ij\rangle}$ balance:

$$\frac{\partial \hat{N}_{\langle xx\rangle}}{\partial \hat{t}} + \frac{2}{15}\left(2\frac{\partial \hat{p}_x}{\partial \hat{x}} - \frac{\partial \hat{p}_y}{\partial \hat{y}} - \frac{\partial \hat{p}_z}{\partial \hat{z}}\right) + \frac{\partial \hat{M}_{\langle xxx\rangle}}{\partial \hat{x}} + \frac{\partial \hat{M}_{\langle xxy\rangle}}{\partial \hat{y}} + \frac{\partial \hat{M}_{\langle xxz\rangle}}{\partial \hat{z}} = -\frac{1}{Kn}\hat{N}_{\langle xx\rangle} \tag{B.5}$$

$$\frac{\partial \hat{N}_{\langle xy\rangle}}{\partial \hat{t}} + \frac{1}{5}\left(\frac{\partial \hat{p}_x}{\partial \hat{y}} + \frac{\partial \hat{p}_y}{\partial \hat{x}}\right) + \frac{\partial \hat{M}_{\langle xxy\rangle}}{\partial \hat{x}} + \frac{\partial \hat{M}_{\langle xyy\rangle}}{\partial \hat{y}} + \frac{\partial \hat{M}_{\langle xyz\rangle}}{\partial \hat{z}} = -\frac{1}{Kn}\hat{N}_{\langle xy\rangle} \tag{B.6}$$

$$\frac{\partial \hat{N}_{\langle xz\rangle}}{\partial \hat{t}} + \frac{1}{5}\left(\frac{\partial \hat{p}_x}{\partial \hat{z}} + \frac{\partial \hat{p}_z}{\partial \hat{x}}\right) + \frac{\partial \hat{M}_{\langle xxz\rangle}}{\partial \hat{x}} + \frac{\partial \hat{M}_{\langle xyz\rangle}}{\partial \hat{y}} - \frac{\partial \hat{M}_{\langle xxx\rangle}}{\partial \hat{z}} - \frac{\partial \hat{M}_{\langle xyy\rangle}}{\partial \hat{z}} = -\frac{1}{Kn}\hat{N}_{\langle xz\rangle} \tag{B.7}$$

$$\frac{\partial \hat{N}_{\langle yy\rangle}}{\partial \hat{t}} + \frac{2}{15}\left(2\frac{\partial \hat{p}_y}{\partial \hat{y}} - \frac{\partial \hat{p}_x}{\partial \hat{x}} - \frac{\partial \hat{p}_z}{\partial \hat{z}}\right) + \frac{\partial \hat{M}_{\langle xyy\rangle}}{\partial \hat{x}} + \frac{\partial \hat{M}_{\langle yyy\rangle}}{\partial \hat{y}} + \frac{\partial \hat{M}_{\langle yyz\rangle}}{\partial \hat{z}} = -\frac{1}{Kn}\hat{N}_{\langle yy\rangle} \tag{B.8}$$

$$\frac{\partial \hat{N}_{\langle yz\rangle}}{\partial \hat{t}} + \frac{1}{5}\left(\frac{\partial \hat{p}_y}{\partial \hat{z}} + \frac{\partial \hat{p}_z}{\partial \hat{y}}\right) + \frac{\partial \hat{M}_{\langle xyz\rangle}}{\partial \hat{x}} + \frac{\partial \hat{M}_{\langle yyz\rangle}}{\partial \hat{y}} - \frac{\partial \hat{M}_{\langle yxx\rangle}}{\partial \hat{z}} - \frac{\partial \hat{M}_{\langle yyy\rangle}}{\partial \hat{z}} = -\frac{1}{Kn}\hat{N}_{\langle yz\rangle} \tag{B.9}$$

$\hat{M}_{\langle ijk\rangle}$ balance:

$$\frac{\partial \hat{M}_{\langle xxx\rangle}}{\partial \hat{t}} + \frac{3}{7}\left(\frac{\partial \hat{N}_{\langle xx\rangle}}{\partial \hat{x}} - \frac{2}{5}\left(\frac{\partial \hat{N}_{\langle xx\rangle}}{\partial \hat{x}} + \frac{\partial \hat{N}_{\langle xy\rangle}}{\partial \hat{y}} + \frac{\partial \hat{N}_{\langle xz\rangle}}{\partial \hat{z}}\right)\right) + \frac{\partial \hat{R}_{\langle xxxx\rangle}}{\partial \hat{x}} + \frac{\partial \hat{R}_{\langle xxxy\rangle}}{\partial \hat{y}} + \frac{\partial \hat{R}_{\langle xxxz\rangle}}{\partial \hat{z}} = -\frac{1}{Kn}\hat{M}_{\langle xxx\rangle} \tag{B.10}$$

$$\frac{\partial \hat{M}_{\langle xxy\rangle}}{\partial \hat{t}} + \frac{3}{7}\left(\frac{2}{3}\frac{\partial \hat{N}_{\langle xy\rangle}}{\partial \hat{x}} + \frac{1}{3}\frac{\partial \hat{N}_{\langle xx\rangle}}{\partial \hat{y}} - \frac{2}{15}\left(\frac{\partial \hat{N}_{\langle xy\rangle}}{\partial \hat{x}} + \frac{\partial \hat{N}_{\langle yy\rangle}}{\partial \hat{y}} + \frac{\partial \hat{N}_{\langle yz\rangle}}{\partial \hat{z}}\right)\right) + \frac{\partial \hat{R}_{\langle xxxy\rangle}}{\partial \hat{x}} + \frac{\partial \hat{R}_{\langle xxyy\rangle}}{\partial \hat{y}} + \frac{\partial \hat{R}_{\langle xxyz\rangle}}{\partial \hat{z}} = -\frac{1}{Kn}\hat{M}_{\langle xxy\rangle} \quad \text{(B.11)}$$

$$\frac{\partial \hat{M}_{\langle xxz\rangle}}{\partial \hat{t}} + \frac{3}{7}\left(\frac{2}{3}\frac{\partial \hat{N}_{\langle xz\rangle}}{\partial \hat{x}} + \frac{1}{3}\frac{\partial \hat{N}_{\langle xx\rangle}}{\partial \hat{z}} - \frac{2}{15}\left(\frac{\partial \hat{N}_{\langle xz\rangle}}{\partial \hat{x}} + \frac{\partial \hat{N}_{\langle yz\rangle}}{\partial \hat{y}} - \frac{\partial \hat{N}_{\langle xx\rangle}}{\partial \hat{z}} - \frac{\partial \hat{N}_{\langle yy\rangle}}{\partial \hat{z}}\right)\right) + \frac{\partial \hat{R}_{\langle xxxz\rangle}}{\partial \hat{x}} + \frac{\partial \hat{R}_{\langle xxyz\rangle}}{\partial \hat{y}} - \frac{\partial \hat{R}_{\langle xxxx\rangle}}{\partial \hat{z}} - \frac{\partial \hat{R}_{\langle xxyy\rangle}}{\partial \hat{z}} = -\frac{1}{Kn}\hat{M}_{\langle xxz\rangle} \quad \text{(B.12)}$$

$$\frac{\partial \hat{M}_{\langle xyy\rangle}}{\partial \hat{t}} + \frac{3}{7}\left(\frac{2}{3}\frac{\partial \hat{N}_{\langle xy\rangle}}{\partial \hat{y}} + \frac{1}{3}\frac{\partial \hat{N}_{\langle yy\rangle}}{\partial \hat{x}} - \frac{2}{15}\left(\frac{\partial \hat{N}_{\langle xx\rangle}}{\partial \hat{x}} + \frac{\partial \hat{N}_{\langle xy\rangle}}{\partial \hat{y}} + \frac{\partial \hat{N}_{\langle xz\rangle}}{\partial \hat{z}}\right)\right) + \frac{\partial \hat{R}_{\langle xxyy\rangle}}{\partial \hat{x}} + \frac{\partial \hat{R}_{\langle xyyy\rangle}}{\partial \hat{y}} + \frac{\partial \hat{R}_{\langle xyyz\rangle}}{\partial \hat{z}} = -\frac{1}{Kn}\hat{M}_{\langle xyy\rangle} \quad \text{(B.13)}$$

$$\frac{\partial \hat{M}_{\langle xyz\rangle}}{\partial \hat{t}} + \frac{1}{7}\left(\frac{\partial \hat{N}_{\langle xy\rangle}}{\partial \hat{z}} + \frac{\partial \hat{N}_{\langle xz\rangle}}{\partial \hat{y}} + \frac{\partial \hat{N}_{\langle xy\rangle}}{\partial \hat{z}}\right) + \frac{\partial \hat{R}_{\langle xxyz\rangle}}{\partial \hat{x}} + \frac{\partial \hat{R}_{\langle xyyz\rangle}}{\partial \hat{y}} - \frac{\partial \hat{R}_{\langle xxxy\rangle}}{\partial \hat{z}} - \frac{\partial \hat{R}_{\langle xyyy\rangle}}{\partial \hat{z}} = -\frac{1}{Kn}\hat{M}_{\langle xyz\rangle} \quad \text{(B.14)}$$

$$\frac{\partial \hat{M}_{\langle yyy\rangle}}{\partial \hat{t}} + \frac{3}{7}\left(\frac{\partial \hat{N}_{\langle yy\rangle}}{\partial \hat{y}} - \frac{2}{5}\left(\frac{\partial \hat{N}_{\langle xy\rangle}}{\partial \hat{x}} + \frac{\partial \hat{N}_{\langle yy\rangle}}{\partial \hat{y}} + \frac{\partial \hat{N}_{\langle yz\rangle}}{\partial \hat{z}}\right)\right) + \frac{\partial \hat{R}_{\langle xyyy\rangle}}{\partial \hat{x}} + \frac{\partial \hat{R}_{\langle yyyy\rangle}}{\partial \hat{y}} + \frac{\partial \hat{R}_{\langle yyyz\rangle}}{\partial \hat{z}} = -\frac{1}{Kn}\hat{M}_{\langle yyy\rangle} \quad \text{(B.15)}$$

$$\frac{\partial \hat{M}_{\langle yyz\rangle}}{\partial \hat{t}} + \frac{3}{7}\left(\frac{2}{3}\frac{\partial \hat{N}_{\langle yz\rangle}}{\partial \hat{y}} + \frac{1}{3}\frac{\partial \hat{N}_{\langle yy\rangle}}{\partial \hat{z}} - \frac{2}{15}\left(\frac{\partial \hat{N}_{\langle xz\rangle}}{\partial \hat{x}} + \frac{\partial \hat{N}_{\langle yz\rangle}}{\partial \hat{y}} - \frac{\partial \hat{N}_{\langle xx\rangle}}{\partial \hat{z}} - \frac{\partial \hat{N}_{\langle yy\rangle}}{\partial \hat{z}}\right)\right) + \frac{\partial \hat{R}_{\langle xyyz\rangle}}{\partial \hat{x}} + \frac{\partial \hat{R}_{\langle yyyz\rangle}}{\partial \hat{y}} - \frac{\partial \hat{R}_{\langle xxyy\rangle}}{\partial \hat{z}} - \frac{\partial \hat{R}_{\langle yyyy\rangle}}{\partial \hat{z}} = -\frac{1}{Kn}\hat{M}_{\langle yyz\rangle} \quad \text{(B.16)}$$

$\hat{R}_{\langle ijkl\rangle}$ balance:

$$\frac{\partial \hat{R}_{\langle xxxx\rangle}}{\partial \hat{t}} + \frac{4}{9}\left(\frac{4}{7}\frac{\partial \hat{M}_{\langle xxx\rangle}}{\partial \hat{x}} - \frac{3}{7}\left(\frac{\partial \hat{M}_{\langle xxy\rangle}}{\partial \hat{y}} + \frac{\partial \hat{M}_{\langle xxz\rangle}}{\partial \hat{z}}\right)\right) = -\frac{1}{Kn}\hat{R}_{\langle xxxx\rangle} \quad \text{(B.17)}$$

$$\frac{\partial \hat{R}_{\langle xxxy\rangle}}{\partial \hat{t}} + \frac{4}{9}\left(\frac{15}{28}\frac{\partial \hat{M}_{\langle xxy\rangle}}{\partial \hat{x}} + \frac{1}{4}\frac{\partial \hat{M}_{\langle xxx\rangle}}{\partial \hat{y}} - \frac{3}{14}\left(\frac{\partial \hat{M}_{\langle xyy\rangle}}{\partial \hat{y}} + \frac{\partial \hat{M}_{\langle xyz\rangle}}{\partial \hat{z}}\right)\right) = -\frac{1}{Kn}\hat{R}_{\langle xxxy\rangle} \quad \text{(B.18)}$$

$$\frac{\partial \hat{R}_{\langle xxxz\rangle}}{\partial \hat{t}} + \frac{4}{9}\left(\frac{15}{28}\frac{\partial \hat{M}_{\langle xxz\rangle}}{\partial \hat{x}} + \frac{13}{28}\frac{\partial \hat{M}_{\langle xxx\rangle}}{\partial \hat{z}} - \frac{3}{14}\left(\frac{\partial \hat{M}_{\langle xyz\rangle}}{\partial \hat{y}} - \frac{\partial \hat{M}_{\langle xyy\rangle}}{\partial \hat{z}}\right)\right) = -\frac{1}{Kn}\hat{R}_{\langle xxxz\rangle} \quad \text{(B.19)}$$

$$\frac{\partial \hat{R}_{\langle xxyy\rangle}}{\partial \hat{t}} + \frac{4}{9}\left(\frac{3}{7}\frac{\partial \hat{M}_{\langle xyy\rangle}}{\partial \hat{x}} + \frac{3}{7}\frac{\partial \hat{M}_{\langle xxy\rangle}}{\partial \hat{y}} - \frac{1}{14}\left(\frac{\partial \hat{M}_{\langle xxx\rangle}}{\partial \hat{x}} + \frac{\partial \hat{M}_{\langle yyy\rangle}}{\partial \hat{y}} + \frac{\partial \hat{M}_{\langle xxz\rangle}}{\partial \hat{z}} + \frac{\partial \hat{M}_{\langle yyz\rangle}}{\partial \hat{z}}\right)\right) = -\frac{1}{Kn}\hat{R}_{\langle xxyy\rangle} \quad \text{(B.20)}$$

$$\frac{\partial \hat{R}_{\langle xxyz\rangle}}{\partial \hat{t}} + \frac{4}{9}\left(\frac{3}{7}\frac{\partial \hat{M}_{\langle xyz\rangle}}{\partial \hat{x}} + \frac{1}{4}\frac{\partial \hat{M}_{\langle xxz\rangle}}{\partial \hat{y}} + \frac{9}{28}\frac{\partial \hat{M}_{\langle xxy\rangle}}{\partial \hat{z}} - \frac{1}{14}\left(\frac{\partial \hat{M}_{\langle yyz\rangle}}{\partial \hat{y}} - \frac{\partial \hat{M}_{\langle yyy\rangle}}{\partial \hat{z}}\right)\right) = -\frac{1}{Kn}\hat{R}_{\langle xxyz\rangle} \quad \text{(B.21)}$$

$$\frac{\partial \hat{R}_{\langle xyyy\rangle}}{\partial \hat{t}} + \frac{4}{9}\left(\frac{15}{28}\frac{\partial \hat{M}_{\langle xyy\rangle}}{\partial \hat{y}} + \frac{1}{4}\frac{\partial \hat{M}_{\langle yyy\rangle}}{\partial \hat{x}} - \frac{3}{14}\left(\frac{\partial \hat{M}_{\langle xxy\rangle}}{\partial \hat{x}} + \frac{\partial \hat{M}_{\langle xyz\rangle}}{\partial \hat{z}}\right)\right) = -\frac{1}{Kn}\hat{R}_{\langle xyyy\rangle} \quad \text{(B.22)}$$

$$\frac{\partial \hat{R}_{\langle xyyz\rangle}}{\partial \hat{t}} + \frac{4}{9}\left(\frac{3}{7}\frac{\partial \hat{M}_{\langle xyz\rangle}}{\partial \hat{y}} + \frac{1}{4}\frac{\partial \hat{M}_{\langle yyz\rangle}}{\partial \hat{x}} + \frac{9}{28}\frac{\partial \hat{M}_{\langle xyy\rangle}}{\partial \hat{z}} - \frac{1}{14}\left(\frac{\partial \hat{M}_{\langle xxz\rangle}}{\partial \hat{x}} - \frac{\partial \hat{M}_{\langle xxx\rangle}}{\partial \hat{z}}\right)\right) = -\frac{1}{Kn}\hat{R}_{\langle xyyz\rangle} \quad \text{(B.23)}$$

$$\frac{\partial \hat{R}_{\langle yyyy\rangle}}{\partial \hat{t}} + \frac{4}{9}\left(\frac{4}{7}\frac{\partial \hat{M}_{\langle yyy\rangle}}{\partial \hat{y}} - \frac{3}{7}\left(\frac{\partial \hat{M}_{\langle xyy\rangle}}{\partial \hat{x}} + \frac{\partial \hat{M}_{\langle yyz\rangle}}{\partial \hat{z}}\right)\right) = -\frac{1}{Kn}\hat{R}_{\langle yyyy\rangle} \quad \text{(B.24)}$$

$$\frac{\partial \hat{R}_{\langle yyyz\rangle}}{\partial \hat{t}} + \frac{4}{9}\left(\frac{15}{28}\frac{\partial \hat{M}_{\langle yyz\rangle}}{\partial \hat{y}} + \frac{13}{28}\frac{\partial \hat{M}_{\langle yyy\rangle}}{\partial \hat{z}} - \frac{3}{14}\left(\frac{\partial \hat{M}_{\langle xyz\rangle}}{\partial \hat{x}} - \frac{\partial \hat{M}_{\langle xxy\rangle}}{\partial \hat{z}}\right)\right) = -\frac{1}{Kn}\hat{R}_{\langle yyyz\rangle} \quad \text{(B.25)}$$

C Two Dimensional Boundary Conditions for up to 25 Moments

The boundary conditions for x and y walls are presented

x-wall boundary conditions

$$64\hat{E}\pi^4(-1+\alpha) + 15\alpha(-1+\gamma)(896\hat{M}_{\langle xxx\rangle} + 256\hat{p}_x - 3150\hat{R}_{\langle xxxx\rangle} + 128\hat{p}_x\alpha\gamma + 105\hat{R}_{\langle xxxx\rangle}\alpha\gamma - 120\hat{N}_{\langle xx\rangle}(2+\alpha\gamma)) = 64\hat{E}_s\pi^4(-1+\alpha) \quad \text{(C.1)}$$

$$\alpha(-1+\gamma)(35\hat{M}_{\langle xxy\rangle}(-1+\alpha\gamma) - 4(8\hat{N}_{\langle xy\rangle} + 3\hat{p}_y + 8\hat{N}_{\langle xy\rangle}\alpha\gamma - 3\hat{p}_y\alpha\gamma)) = 0 \quad \text{(C.2)}$$

$$128\hat{E}\pi^4(-1+\alpha) + 3\alpha(-1+\gamma)(2816\hat{p}_x - 28875\hat{R}_{\langle xxxx\rangle} + 1536\hat{p}_x\alpha\gamma - 1575\hat{R}_{\langle xxxx\rangle}\alpha\gamma - 1200\hat{N}_{\langle xx\rangle}(1+2\alpha\gamma) + 1280\hat{M}_{\langle xxx\rangle}(9+2\alpha\gamma)) = 128\hat{E}_s\pi^4(-1+\alpha) \quad \text{(C.3)}$$

$$128\hat{E}\pi^4(-1+\alpha)+3\alpha(-1+\gamma)(8960\hat{M}_{\langle xxx\rangle}-2800\hat{N}_{\langle xx\rangle}+4000\hat{N}_{\langle yy\rangle}+2304\hat{p}_x-30975\hat{R}_{\langle xxxx\rangle}+69300\hat{R}_{\langle xxyy\rangle}-$$
$$800\hat{N}_{\langle xx\rangle}\alpha\gamma-1600\hat{N}_{\langle yy\rangle}\alpha\gamma+1024\hat{p}_x\alpha\gamma+525\hat{R}_{\langle xxxx\rangle}\alpha\gamma$$
$$-6300\hat{R}_{\langle xxyy\rangle}\alpha\gamma+1280\hat{M}_{\langle xyy\rangle}(-3+4\alpha\gamma))=128\hat{E}_s\pi^4(-1+\alpha) \quad \text{(C.4)}$$

$$\alpha(-1+\gamma)(735\hat{M}_{\langle xxy\rangle}(-1+\alpha\gamma)-16(24\hat{N}_{\langle xy\rangle}(1+\alpha\gamma)+7(\hat{p}_y+8\hat{R}_{\langle xxxy\rangle}-\hat{p}_y\alpha\gamma+8\hat{R}_{\langle xxxy\rangle}\alpha\gamma)))=0 \quad \text{(C.5)}$$

$$\alpha(-1+\gamma)(735\hat{M}_{\langle xxy\rangle}(-1+\alpha\gamma)+2(245\hat{M}_{\langle yyy\rangle}(-1+\alpha\gamma)$$
$$-8(48\hat{N}_{\langle xy\rangle}(1+\alpha\gamma)+7(\hat{p}_y(3-3\alpha\gamma)+16(\hat{R}_{\langle xyyy\rangle}+\hat{R}_{\langle xyyy\rangle}\alpha\gamma))))))=0 \quad \text{(C.6)}$$

y-wall boundary conditions

$$64\hat{E}\pi^4(-1+\alpha)+15\alpha(-1+\gamma)(896\hat{M}_{\langle yyy\rangle}+256\hat{p}_y-3150\hat{R}_{\langle yyyy\rangle}$$
$$+128\hat{p}_y\alpha\gamma+105\hat{R}_{\langle yyyy\rangle}\alpha\gamma-120\hat{N}_{\langle yy\rangle}(2+\alpha\gamma))=64\hat{E}_s\pi^4(-1+\alpha) \quad \text{(C.7)}$$

$$\alpha(-1+\gamma)(35\hat{M}_{\langle xyy\rangle}(-1+\alpha\gamma)-4(8\hat{N}_{\langle xy\rangle}+3\hat{p}_x+8\hat{N}_{\langle xy\rangle}\alpha\gamma-3\hat{p}_x\alpha\gamma))=0 \quad \text{(C.8)}$$

$$128\hat{E}\pi^4(-1+\alpha)+3\alpha(-1+\gamma)(2816\hat{p}_y-28875\hat{R}_{\langle yyyy\rangle}+1536\hat{p}_y\alpha\gamma$$
$$-1575\hat{R}_{\langle yyyy\rangle}\alpha\gamma-1200\hat{N}_{\langle yy\rangle}(1+2\alpha\gamma)+1280\hat{M}_{\langle yyy\rangle}(9+2\alpha\gamma))=128\hat{E}_s\pi^4(-1+\alpha) \quad \text{(C.9)}$$

$$128\hat{E}\pi^4(-1+\alpha)+3\alpha(-1+\gamma)(8960\hat{M}_{\langle yyy\rangle}+4000\hat{N}_{\langle xx\rangle}-2800\hat{N}_{\langle yy\rangle}+2304\hat{p}_y+69300\hat{R}_{\langle xxyy\rangle}$$
$$-30975\hat{R}_{\langle yyyy\rangle}-1600\hat{N}_{\langle xx\rangle}\alpha\gamma-800\hat{N}_{\langle yy\rangle}\alpha\gamma+1024\hat{p}_y\alpha\gamma-6300\hat{R}_{\langle xxyy\rangle}\alpha\gamma$$
$$+525\hat{R}_{\langle yyyy\rangle}\alpha\gamma+1280\hat{M}_{\langle xxy\rangle}(-3+4\alpha\gamma))=128\hat{E}_s\pi^4(-1+\alpha) \quad \text{(C.10)}$$

$$\alpha(-1+\gamma)(735\hat{M}_{\langle xyy\rangle}(-1+\alpha\gamma)-16(24\hat{N}_{\langle xy\rangle}(1+\alpha\gamma)+7(\hat{p}_x+8\hat{R}_{\langle xyyy\rangle}-\hat{p}_x\alpha\gamma+8\hat{R}_{\langle xyyy\rangle}\alpha\gamma)))=0 \quad \text{(C.11)}$$

$$\begin{aligned}\alpha(-1+\gamma)(490\hat{M}_{\langle xxx\rangle}(-1+\alpha\gamma)+735\hat{M}_{\langle xyy\rangle}(-1+\alpha\gamma)\\ -16(48\hat{N}_{\langle xy\rangle}(1+\alpha\gamma)+7(\hat{p}_x(3-3\alpha\gamma)+16(\hat{R}_{\langle xxxy\rangle}+\hat{R}_{\langle xxxy\rangle}\alpha\gamma))))=0\end{aligned} \quad \text{(C.12)}$$

D Numerical Coefficient Matrices

The following are the coefficient matrices used in the numerical scheme presented in Section 7.4.

$$\mathcal{A}=\begin{bmatrix} 0 & 1 & 0 & 0 & 0 & 0 \\ \frac{1}{3} & 0 & 0 & 1 & 0 & 0 \\ 0 & 0 & 0 & 0 & 1 & 0 \\ 0 & \frac{4}{15} & 0 & 0 & 0 & 0 \\ 0 & 0 & \frac{1}{5} & 0 & 0 & 0 \\ 0 & -\frac{2}{15} & 0 & 0 & 0 & 0 \end{bmatrix} \quad \text{(D.1)}$$

$$\mathcal{B}=\begin{bmatrix} 0 & 0 & 1 & 0 & 0 & 0 \\ 0 & 0 & 0 & 0 & 1 & 0 \\ \frac{1}{3} & 0 & 0 & 0 & 0 & 1 \\ 0 & 0 & -\frac{2}{15} & 0 & 0 & 0 \\ 0 & \frac{1}{5} & 0 & 0 & 0 & 0 \\ 0 & 0 & \frac{4}{15} & 0 & 0 & 0 \end{bmatrix} \quad \text{(D.2)}$$

$$\mathcal{P} = \begin{bmatrix} 0 & 0 & 0 & 0 & 0 & 0 \\ 0 & \frac{1}{KnR} & 0 & 0 & 0 & 0 \\ 0 & 0 & \frac{1}{KnR} & 0 & 0 & 0 \\ 0 & 0 & 0 & \frac{1}{Kn} & 0 & 0 \\ 0 & 0 & 0 & 0 & \frac{1}{Kn} & 0 \\ 0 & 0 & 0 & 0 & 0 & \frac{1}{Kn} \end{bmatrix}$$

The coefficient matrices $\mathcal{X}$ and $\mathcal{X}^d$ are for an adiabatic wall. In Section 7.4 $\mathcal{X}^+$implies $n_x = 1$ and $\mathcal{X}^-$ implies $n_x = -1$.

$$\mathcal{X} = \begin{bmatrix} 1 & 0 & 0 & 0 & 0 & 0 \\ 0 & 0 & 0 & 0 & 0 & 0 \\ 0 & 0 & 1 & 0 & 0 & 0 \\ 0 & 0 & 0 & 1 & 0 & 0 \\ 0 & 0 & \frac{3n_x(-1+\alpha\gamma)}{8+8\alpha\gamma} & 0 & 0 & 0 \\ 0 & 0 & 0 & 0 & 0 & 1 \end{bmatrix} \tag{D.3}$$

$$\mathcal{X}^d = \begin{bmatrix} 0 \\ 0 \\ 0 \\ 0 \\ 0 \\ 0 \end{bmatrix} \tag{D.4}$$

The coefficient matrices $\mathcal{Y}$ and $\mathcal{Y}^d$ are for a wall with a controlled surface energy, $\hat{E}_s$

$$\mathcal{Y} = \begin{bmatrix} 1 & 0 & 0 & 0 & 0 & 0 \\ 0 & 1 & 0 & 0 & 0 & 0 \\ -\frac{n_y\pi^4(-1+\alpha)}{30\alpha(-1+\gamma)(2+\alpha\gamma)} & 0 & 0 & 0 & 0 & \frac{15n_y}{16} \\ 0 & 0 & 0 & 1 & 0 & 0 \\ 0 & \frac{3n_y(-1+\alpha\gamma)}{8+8\alpha\gamma} & 0 & 0 & 0 & 0 \\ 0 & 0 & 0 & 0 & 0 & 1 \end{bmatrix} \tag{D.5}$$

$$\mathcal{Y}^d = \begin{bmatrix} 0 \\ 0 \\ \frac{\hat{E}_s n_y\pi^4(-1+\alpha)}{30\alpha(-1+\gamma)(2+\alpha\gamma)} \\ 0 \\ 0 \\ 0 \end{bmatrix} \tag{D.6}$$